

Potential ecosystem effects of large upscaling of offshore wind in the North Sea

Bottom-up approach



Potential ecosystem effects of large upscaling of offshore wind in the North Sea

Bottom-up approach

Author(s)

ir. F.Zijl

Ir S.C. Laan

ir. A. Emmanouil

dr. ir.T. van Kessel

ir V.T.M. van Zelst

dr. L.M. Vilmin

dr. L.A. van Duren

Potential ecosystem effects of large upscaling of offshore wind in the North Sea

Bottom-up approach

Client	Rijkswaterstaat Water, Verkeer en Leefomgeving
Contact	dr. I. van Splunder
Keywords	Offshore wind, environmental impact, ecosystem effects, numerical models, hydrodynamics, fine sediment, water quality and ecology

Document control

Version	1.1
Date	22-04-2021
Project nr.	11203731-004
Document ID	11203731-004-ZKS-0015
Pages	96
Classification	
Status	final

Author(s)

	ir. F.Zijl	
	Ir S.C. Laan	
	ir. A. Emmanouil	
	dr. ir.T. van Kessel	
	ir V.T.M. van Zelst	
	dr. L.M. Vilmin	
	dr. L.A. van Duren	

Doc. version	Author	Reviewer	Approver	Publish
2.0	ir. F.Zijl	prof.dr. P.M.J. Herman	dr.ir. A.G. Segeren	
	Ir S.C. Laan			
	ir. A. Emmanouil			
	dr. ir.T. van Kessel			
	ir V.T.M. van Zelst			
	dr. L.M. Vilmin			
	dr. L.A. van Duren			

Summary

An initial explorative study has indicated that a future large-scale increase of offshore wind farms may have ecosystem effects that are at present either not occurring or are not relevant at the scale of an ecosystem. Such changes in the physical functioning of the North Sea may influence the foundation of the food web: primary production, which in turn will have consequences for all higher trophic levels. This study presents a first attempt to quantify the physical and ecological effects, using a new suite of ecosystem models, to assess which processes are relevant in which parts of the North Sea (a bottom up approach). Another part of the wider project assesses the best methodologies to ascertain in the near future what the consequences are of these changes on species of high conservation status (top-down approach).

The model results indicate that upscaling of offshore wind in the North Sea may indeed have significant effects on fundamental ecosystem processes. This research has been carried out with a new modelling suite. These models are currently in a testing phase. However, despite large uncertainties, the results are clear and significant enough to warrant follow-up research. We identified 5 regions in the North Sea that have different physical characteristics and react differently to the implementation of large numbers of wind turbines. These are: 1) the Central German Bight, where opposing effects are seen from changes in stratification and increases in fine sediment concentrations in the upper layers, 2) the UK coast and western parts of the Dutch continental shelf, which see in general limited effects, primarily due to increased SPM concentrations, 3) the Central Southern North Sea which sees very large effects due to relaxation of stratification, increases in primary production and a delay in the onset of primary production, 4) the Holland Coast and Rhine region of freshwater influence (ROFI) where we see some influence on salinity stratification and negative effects due to increases in fine sediment concentrations in the top layers and 5) the German Danish coastal areas that have unclear effects and are in many respects similar to the UK coastal areas.

Several parts of the modelling suite (particularly the fine sediment module and the water quality and ecological module) still have shortcomings that will be addressed in follow up projects. At this point in time, these models are research tools. The modelling results should at present not be used at face value, i.e. as predictions of what will happen in the future. However, the models definitely have the potential to be developed into future policy support tools.

Contents

	Summary	4
1	Introduction	9
1.1	General context – the WOZEP programme	9
1.2	Combined approach (Top-down and bottom-up)	9
1.2.1	Top-down approach	9
1.2.2	Bottom-up approach	9
1.2.3	Synthesis	10
1.3	Locations and spatial focus	10
1.4	Report lay-out	11
2	Scenario description	12
2.2	Rationale	12
2.2.1	Distribution	12
2.2.2	North Sea and adjacent waters	12
2.2.3	Physically diverse environments	13
2.2.4	International shipping lanes	13
2.2.5	N2000 areas	13
2.2.6	IJmuiden Ver	13
2.2.7	Factors <i>not</i> taken into account	13
2.3	Within farm lay-out	14
2.4	Scenario choice	14
3	Hydrodynamic model	16
3.1	Model setup	16
3.1.1	Introduction 3D DCSM-FM	16
3.1.2	Computational grid, bathymetry and bottom roughness	16
3.1.3	Open boundaries	17
3.1.4	Meteorological forcing	17
3.1.5	Mass flux	18
3.1.6	Freshwater discharges	18
3.1.7	Computational performance	18
3.1.8	Parameterization of wind farms	19
3.2	Model validation	19
3.2.1	Water levels	19
3.2.2	Temperature (stratification)	20
3.2.3	Residual transport through the English Channel	20
3.3	Results	21
3.3.1	General	21
3.3.2	Reference (no OWFs)	21
3.3.3	2020 Scenario (current farms)	24
3.3.4	Future hypothetical scenario	28
3.3.5	Comparison of temperature stratification	31
3.4	Discussion	33

3.4.1	Conclusions regarding the hydrodynamic model	33
3.4.2	Recommendations	34
4	Wave model	35
4.1	Approach	35
4.2	Model set-up	36
4.2.1	Model domains	36
4.2.2	Bathymetry	36
4.2.3	Boundary and input conditions	37
4.2.4	Reflecting/transmitting boundaries	37
4.2.5	Wind input	37
4.2.6	Hydrodynamics input	37
4.2.7	Numerical aspects and physical processes	38
4.3	Results and discussion	38
5	Fine sediment model	41
5.1	Fine sediment model set-up	41
5.1.1	Bottom shear stress by currents and waves	41
5.1.2	Sediment fractions	41
5.1.3	Initial conditions bottom layers	42
5.1.4	Initial conditions water column	42
5.1.5	Boundary conditions	42
5.2	Fine sediment model validation	43
5.2.1	Comparison with MWTL stations	44
5.2.2	Comparison with CEFAS smart buoys	45
5.2.3	Spatial distribution of monthly average SPM	47
5.3	Results and discussion	48
5.3.1	Results based on year-average hydrodynamic forcing	49
5.3.2	Large-scale effects	52
5.3.3	Seasonality	52
5.3.4	Longshore SPM fluxes	54
5.4	Conclusions	55
6	Water quality and ecological model	56
6.1	Model set-up	56
6.1.1	Introduction 3D DCSM-FM Water Quality	56
6.1.2	Simulated variables and processes	56
6.1.3	Open boundaries	58
6.1.4	Freshwater discharges	59
6.1.5	Other forcings	59
6.1.6	Simulated period and initial state	60
6.1.7	Representation of the effect of windfarms	60
6.1.8	Summary of ecological runs	61
6.1.9	Computational performance	62
6.2	Model validation	62
6.2.1	Time series comparison	62
6.2.2	Seasonal means of inorganic nutrients and chlorophyll a	68
6.3	Results	68
6.3.1	Effect of changes in hydrodynamics	69

6.3.2	Effect of mussel growth on pillars	74
6.3.3	Combined effects of changes in hydrodynamics and sediment dynamics	74
6.4	Discussion	75
6.4.1	First results on the ecological effects of OWFs	75
6.4.2	Future model improvements	76
7	Conclusions	78
7.1	Model performance	78
7.1.1	Coupling	78
7.1.2	Resolution and calculation times	78
7.1.3	Validation	78
7.1.4	Missing processes	79
7.2	Effects of wind farms	79
7.2.1	Effects through changes in benthic – pelagic transport	79
7.2.2	Effects through changes in temperature and / or habitat	80
7.2.3	Effects through changes in competition in lower trophic levels	80
7.3	Locations sensitive to ecosystem effects	80
7.3.1	Central German Bight	81
7.3.2	UK Coast and western most areas of the Dutch continental shelf	81
7.3.3	Central Southern North Sea	81
7.3.4	Holland coast and Rhine ROFI	82
7.3.5	German and Danish Wadden coast	82
7.3.6	The Dogger Bank	82
8	References	83
9	Acknowledgements	85
A	Memo regarding scenario choice	86
A.1	Background	86
A.2	Scenario context	86
A.3	Arguments used to get to this design	86
A.3.1	Power generation.	86
A.3.2	Distribution	87
A.3.3	Specific for the Dutch wind farms	88
A.4	Within farm lay-out	89
A.5	Scenario choice	89
A.5.1	Factors not taken into account	92
A.6	References	92
B	Fine sediment model (appendix)	93
B.1	Sedimentation and erosion parameters	93
B.2	Location of CEFAS smart buoys	93
B.3	Location of transects	94
B.4	Spatial distribution SPM	95
B.5	References	96

1 Introduction

1.1 General context – the WOZEP programme

The WOZEP programme (Wind Op Zee Ecologisch Programma) is an integrated research programme to reduce the knowledge gaps regarding the (possibly negative) environmental effects of offshore wind farms (OWFs) on the North Sea. A number of topics concentrate on the direct impacts on priority species such as birds and bats (collision risks), habitat loss of seabirds, effects of noise (specifically during construction) on marine mammals and effects of electromagnetic fields from infield cables on benthos and fish. A recent scoping study indicated that there may also be effects of offshore wind on the functioning of the ecosystem and knock-on effects on the marine food web, through indirect (physical and ecological) processes (Boon et al., 2018). This study indicated that the possible upscaling in offshore wind for 2030 and even more so for 2050 in the southern North Sea is likely to have an impact on its functioning in fundamental ways. Large-scale extraction of wind energy from the lower part of the atmosphere affects local wind patterns, wave generation, tidal amplitudes, stratification of the water column, dynamics of suspended particles and bedload transport of sediment. Furthermore, the infrastructure will provide hard substrate, not only on the bed (in the form of scour protection) but also providing attachment opportunities for biota in the upper layers of the water column. Such changes to the physical functioning of the North Sea may have significant consequences for the ecological functioning, such as changes to the total amount and the timing of primary production, food availability of filter feeders and higher trophic levels, and habitat suitability for many species.

The scoping study did not attempt to quantify the potential effects, but did identify that particularly the effect of destratification (already measured in two German offshore wind farms (Floeter et al., 2017) and effects of fine sediment dynamics on primary production are likely to occur and should be prioritised in future research.

This current project is the first attempt to quantify potential changes in the ecosystem through a coupled set of physical and ecological models and assess the impact of these changes for several priority species (birds and marine mammals).

1.2 Combined approach (Top-down and bottom-up)

This project will follow a three-tier approach:

1.2.1 Top-down approach

This part of the research estimates the vulnerability of the most policy-relevant species (birds, marine mammals and if possible, elasmobranchs) for changes in environmental conditions that can be caused by large-scale development scenarios for off shore wind. This part also aims to deliver the most appropriate methodologies to better quantify such effects.

1.2.2 Bottom-up approach

This part of the project uses numerical models to assess changes in hydrodynamics, sediment dynamics, light attenuation, primary production and secondary production. The hydrodynamic modelling focuses on potential changes in tidal flow, stratification and mixing of a number of scenarios. The scenarios include:

- a reference scenario without any wind farms
- a “2020” scenario with the currently present wind farms

- a hypothetical future scenario with a large upscaling of offshore wind farms in the southern North Sea. Details and rationale for the choice of scenario can be found in Chapter 2.

The hydrodynamic model forms the basis for the subsequent model simulations with a fine sediment model and a water quality and ecological model to assess changes in productivity (primary and secondary).

1.2.3 Synthesis

In the latter part of the research the two approaches are combined and from this, priorities for further research will be determined. A separate report will provide recommendations on an approach to fill the most pressing knowledge gaps. This recommendations report will be based on the joint position paper by Deltares, NIOZ and Wageningen Marine Research (Herman et al., 2019).

1.3 Locations and spatial focus

This study is predominantly focussed on the southern part of the greater North Sea. This part of the North Sea includes areas such as the Dogger Bank (a relatively shallow area in the central North Sea), the Cleaver Bank (an area characterised by stones and gravel), the Oyster Grounds (an area of the North Sea that used to be characterised by extensive flat oyster beds. The system is bordered by the Wadden Sea (a Dutch, German and Danish N2000 area and international World Heritage Site) and several other areas that differ in physical characteristics and ecology (*Figure 1.1*).

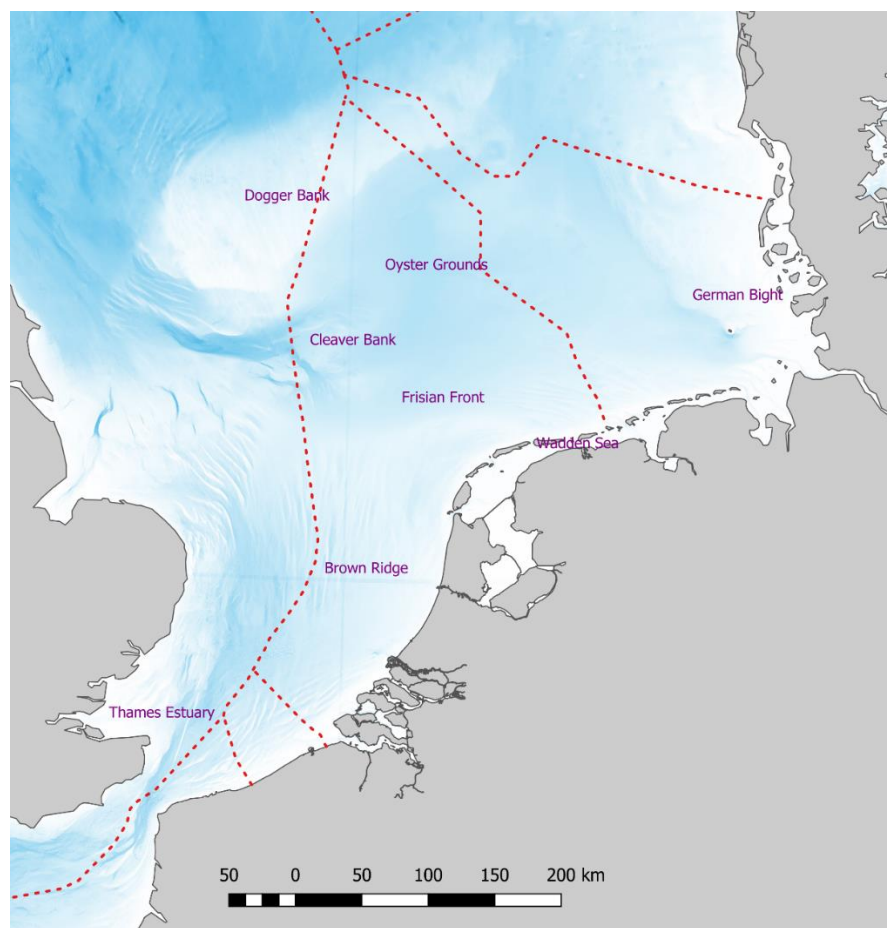


Figure 1.1 Map of the southern North Sea with some relevant areas indicated that are referred to in the rest of this report.

1.4 Report lay-out

Chapter 2 describes the rationale and the lay-out of the upscaling scenario, central to this study. Chapter 3 describes and discusses results of the hydrodynamic model. Chapter 4 describes the fine sediment model. Chapter 5 details the water quality and ecological model. Chapter 6 is a general integrated discussion of the three modules and conclusions regarding the effects.

2 Scenario description

2.1 Background and context

Based on the discussion during the project meeting on the 24th of February 2020, as well as internal discussions, we have constructed a large upscaling scenario. This is a scenario based on currently available targets of the offshore wind industry for 2050, distributed over available space in such a way that we can learn as much as possible from it. Note: this is a purely *theoretical* scenario for research purposes, not a proposal for a realistic future scenario. Below follows an abbreviated description of the arguments that lead to this choice. A full description can be found in Appendix A.

Some other user factors have been taken into account (locations of N2000 areas and shipping routes), but only because it was possible to do this, without compromising the primary goal: understanding the sensitivity of various parts of the North Sea for changes caused by the introduction of large-scale offshore wind energy.

2.2 Rationale

2.2.1 Distribution

We have used the national targets for 2050 obtained from “WindEurope” as a basis. These were presented during a special session at the EU parliament, regarding the future of fisheries in conjunction with offshore wind on the 22nd of January 2020. For the Netherlands the approximate target is currently 60 GW. In our scenario we have opted for a yield of 8 MW/km², requiring a total of 7500 km² in the Dutch EEZ. This is a compromise between what is technically feasible and what is optimal for the wind industry.

Most of the currently designated wind farm areas appear to have a ballpark size of around 600 km². Making contiguous windfarm areas too large would diminish their energy yield (Deutsche WindGuard, 2018). We have therefore chosen to opt for maximum cluster sizes in the order of magnitude of 400 km². With larger cluster sizes we assume the high yields of 8 MW/km² are physically not achievable. In order to reduce complexity and create a large number of clusters we have also opted for cluster sizes that are not much smaller than this.

2.2.2 North Sea and adjacent waters

Many countries have already defined search areas for wind energy. For the UK, Ireland, Denmark and Norway these search areas exceed the requirement. Wind farm clusters have been located in those search areas.

For countries such as the UK, France and Denmark with search areas in the North Sea as well as in other waters we have divided the wind farm clusters according to the ratios of designated search areas in the various waters.

For Germany we had to make a choice for areas as the currently available search areas are insufficient to achieve 36 GW. We have opted for a northern location. This was a previous search areas (Nordschillgrund) which has disappeared from the most recent maps. However, in the German EEZ there are not many alternatives.

2.2.3 Physically diverse environments

As this project will focus on wind farm effects on stratification and destratification, we have distributed hypothetical wind farms over the various stratification regimes, based on the map of Van Leeuwen et al. (2015). We need to bear in mind though, that these regimes are based on models and may differ from reality. They also may differ from our model.

We have furthermore deliberately placed some wind farms on known 'frontal' areas, such as the Frisian front system. Frontal systems are known to be a location very rich in benthic biomass and biodiversity (Neumann et al., 2016). They are also physically different from other areas and may therefore respond differently to the presence of wind turbines.

2.2.4 International shipping lanes

We have taken into account the location of the international shipping lanes and the traffic separation system (TTS) as defined by the International Maritime Organisation (IMO). These routes are based on international agreements and are unlikely to change drastically in the next few decades. However, potential new shipping lanes catering for routes via the Arctic area have not been taken into account. The existing shipping lanes are predominantly located south of the Gemini wind farms. As future farms are likely to be planned in the northern section of the Dutch EEZ, the impact on the layout of the scaled-up scenario is limited.

2.2.5 N2000 areas

Based on policies and the current draft of the North Sea agreement, we have decided to avoid The N2000 areas as well as the two additional areas "Central Oyster Grounds" and "Brown Ridge". These are likely to get some level of protected status and are unlikely to be re-designated for windfarms. Excluding these areas does not compromise our options for choosing hydrodynamically diverse areas. By not using these areas we hope to avoid misinterpretations of these maps, when the results of our study are made public.

2.2.6 IJmuiden Ver

In keeping with not building on the Brown Ridge area, we have shifted the current lay-out of "IJmuiden Ver" northward to fall outside the Brown Ridge area. Verbal comments from EZK and LNV indicated that this was likely. The shape of this area is likely to change in future, with this shift. However, at the time of taking decisions regarding the upscaling scenario, we had no indication how. Therefore, the shape was left unchanged.

2.2.7 Factors *not* taken into account

There are many other functions that will influence the future choices of farm locations. In our current lay-out we have ignored the demands of:

- Military zones
- Sand mining areas
- Important fishing grounds that in future may be kept free from wind farm development
- Important fly-ways for migrating birds
- Important areas for seals

We are aware that these issues may all play a role in future scenarios. It is therefore imperative that these scenario maps are not taken as realistic scenarios.

The other issue that has not been taken into account but should be addressed in future is the presence of land-based wind farms. On the larger North Sea scale, energy extraction from wind at sea, is likely to start interacting with wind extraction on land. The cumulative effects may be non-linear.

2.3 Within farm lay-out

For the wind farms already operational, under construction or in an advanced planning phase we use the in situ or the currently planned lay-out. For future farms the exact dimensions are unknown, but we have decided to set the turbine size (and the related distance between the turbines) at 12 MW for all future farms. Our current in-farm lay-out for present, planned and future farms is shown in Table 2.1.

Table 2.1: Proposed lay-out for operational, planned and future wind farms.

	Stem density (piles/km ²)	Stem diameter (m)
Operational	3.15	5
Under construction	0.85	8
Future	0.67	12

2.4 Scenario choice

Figure 2.1 shows the chosen lay-out, based on the arguments set out above. The focus of this project is on the Dutch EEZ, but we have included a number of wind farms in the Baltic, the Northern North Sea, around Ireland and the Atlantic. We have the targets for these countries available and we currently do not know how far effects of the installation of offshore wind farms extend.

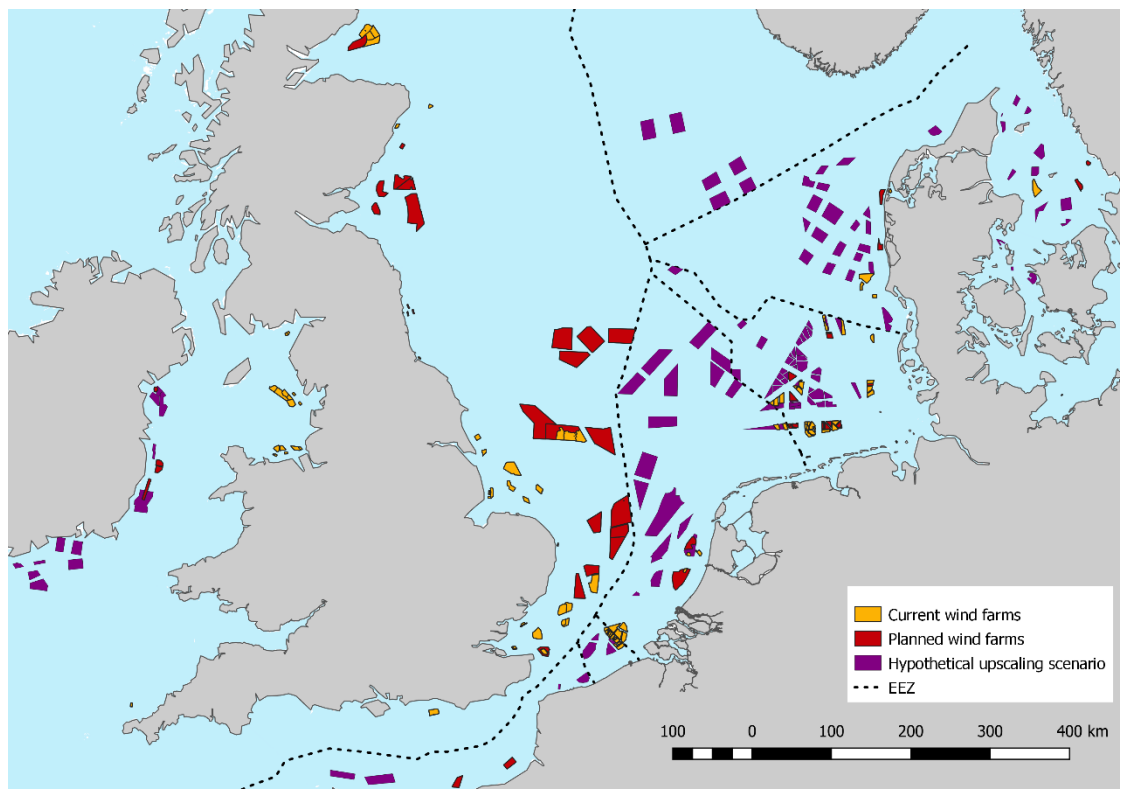


Figure 2.1: Current proposed layout for the large upscaling scenario.

Further details regarding the distribution of the future wind farms over physically important areas (e.g. different stratification regimes and frontal areas), as well as in relation to ecologically relevant areas are detailed in Appendix A.

3 Hydrodynamic model

3.1 Model setup

3.1.1 Introduction 3D DCSM-FM

For the hydrodynamic modelling, the 3D Dutch Continental Shelf Model – Flexible Mesh (3D DCSM-FM) is used, which was developed in recent years as part of Deltares' strategic research. The main purpose of 3D DCSM-FM is to have a versatile model that can be used for all manner of studies and research on the Northwest European Continental Shelf, including the North Sea and adjacent shallow seas, such as the Wadden Sea. It aims to combine state-of-the-art capabilities with respect to modelling of water levels (tide and surge) as well as (residual) transport phenomena. The latter is crucial for application in water quality and ecological modelling. By combining this, the model is ideally suited for this study.

This new model is the successor of the 3D southern North Sea model ZUNO-DD. 3D DCSM-FM is based on 2D DCSM-FM 0.5nm, which has been developed for the Dutch Ministry of Infrastructure and Water Management (Zijl and Groenenboom, 2019) and will be used for operational forecasting of water levels. The model includes 20 equidistant layers of the water column.

3.1.2 Computational grid, bathymetry and bottom roughness

3D DCSM-FM covers the Northwest European Continental Shelf, specifically the area between 15°W to 13°E and 43°N to 64°N. The network consists of approximately 630,000 grid cells. Compared to a structured grid approach, the new flexible mesh has coarser grid cells near the open boundaries and in deep waters, whereas the resolution increases toward the shallower waters. This gives a better match with the spatial scales of the locally relevant physical processes. Cells in deep oceanic waters have a resolution of 1/10° in longitudinal direction and 1/15° in latitudinal direction, which corresponds to approximately 4 by 4 nautical miles (nm). Along all coasts and in the southern North Sea cell sizes decrease to 0.5 by 0.5 nm, which corresponds to approximately 900 m.

A sigma-layer approach is used for the vertical schematization of the model. This implies that a fixed number of layers, with a thickness dependent on local water depth, is present. This results in a high vertical resolution in shallow areas. A total of 20 layers with a uniform thickness of 5% of the water column is applied.

The model bathymetry is based on the gridded dataset by the European Marine Observation and Data Network (EMODnet), a consortium of organizations collecting and distributing European marine data from different sources. For large parts of the Dutch waters, bathymetric information from the detailed baseline database by the Dutch government is used.

For the bed friction, a spatially varying Manning roughness coefficient is used. During the model calibration, using OpenDA-DUD, these values were adjusted to obtain an optimal water level representation. For the calibration of the bed roughness the model was run in 2D mode for the entire year of 2017, using more than 200 tide gauge stations shelf-wide.

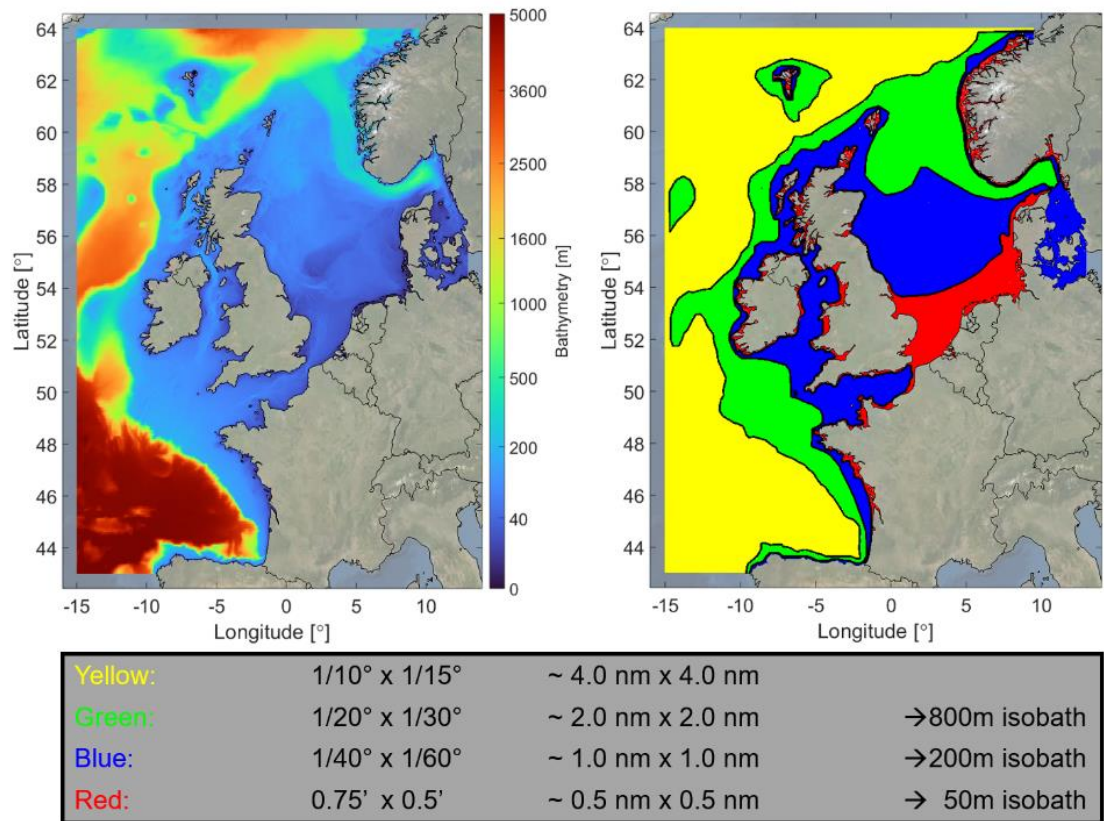


Figure 3.1 Bathymetry and grid cell sizes in 3D DCSM-FM.

3.1.3 Open boundaries

Water levels

At the northern, western and southern open boundaries of 3D DCSM-FM, water level boundaries are applied. At these locations, astronomical water levels are imposed, derived from a harmonic expansion of the amplitudes and phase lags of 31 tidal constituents. These constituents are retrieved from the global tide model FES2012. The surge at the open boundaries is approximated by addition of an inverse barometer correction (IBC) to the astronomical water levels. This correction is a time- and space-dependent function of the local atmospheric pressure. To account for steric effects, the daily mean water levels from CMEMS are used.

Salinity and temperature

At the lateral open boundaries, temperature and salinity are derived from CMEMS. These daily values at 50 non-uniformly spaced vertical levels are interpolated by Delft3D Flexible Mesh to the right horizontal location and model layers. The spatially varying salinity and temperature in the model are initialized by nudging 3D DCSM-FM with the data from the same source.

3.1.4 Meteorological forcing

For this study 3D DCSM-FM has been coupled to ECMWF's ERA5 reanalysis dataset. The forcing parameters used are described below.

Momentum flux

To account for the air-sea momentum flux time- and space-varying wind speeds (at 10 m height) and atmospheric pressure (at mean sea level (MSL)) are applied. With respect to air-sea momentum exchange, the aim is to be consistent with the Atmospheric Boundary Layer (ABL) model that is used in the meteorological model applied. For coupling to ERA5 this implies using a Charnock formulation and specifying a time-and space-varying Charnock coefficient. In computing the wind shear stress, which represents the momentum exchange between air and water, the wind speed relative to the flow velocity at the water surface is used. While this implies less consistency with the ABL approximation in the meteorological model, this was proven to be beneficial to the quality with which water levels are represented (Zijl, 2016).

Heat flux

Horizontal and vertical spatial differences in water temperature affect the transport of water through their impact on the water density. Heating of surface water and shallow waters cause temperature gradients that can generate horizontal flow. It can also lead to temperature stratification with accompanying damping of turbulence and hence a reduction in vertical mixing. To include these effects, the transport of temperature is modelled. For its main driver, exchange of heat with the atmosphere, a heat flux model is used. The temporally and spatially varying turbulent exchange of heat through the air-water interface is computed based on air temperatures (at 2 m), cloud cover, dew point temperature and wind speed from the ERA5 meteorological reanalysis. To account for the radiative heat fluxes the surface net solar (short-wave) radiation and the surface downwelling long wave radiation have been imposed, while the surface upwelling long-wave radiation is computed based on the modelled sea surface temperature. The incoming solar radiation is distributed over the water column, depending on the water transparency prescribed with a Secchi depth. In the hydrodynamic model a constant, uniform value of 4 m has been applied, except at the Wadden Sea, where this value is set to 1 m.

3.1.5 Mass flux

To account for the mass-flux through the air-sea interface time- and space varying fields of evaporation and precipitation have been applied.

3.1.6 Freshwater discharges

Freshwater discharges in the 3D DCSM-FM domain are prescribed as depth-averaged, climatological monthly means based on data from E-HYPE (the E-HYPE model calculates water balance, dynamics of hydrological variables and daily discharge for the continental Europe). These discharges include varying water temperatures. The seven most important discharges in the Netherlands and three most important German rivers are replaced by gauged discharges with an hourly or daily interval.

3.1.7 Computational performance

After starting from an external solution (CMEMS) with respect to temperature and salinity, a spin-up period of one year, forced by realistic meteorological and river discharge values, is applied to reach a dynamic equilibrium. Computations are performed on Deltares' h6 Linux-cluster using 5 nodes with 4 cores each. With a maximum timestep of 100 s, this results in a computation time of approximately 15 minutes per simulation-day (3.5 days per simulation-year). These computational times are for the hydrodynamics-only model. Together with the D-WAQ module, computational times are a factor 3-4 longer.

3.1.8 Parameterization of wind farms

With a grid size of at least 900m, the piles of the OWFs are too small to explicitly include in the model schematization. Therefore, a sub-grid approach is used. In this approach, a quadratic sink term is included in the horizontal momentum equations. The energy extracted from the main flow in this manner is at the same time reintroduced as a source term in the equation for turbulent kinetic energy (k).

The locations of the offshore wind farms are specified in the hydrodynamic model by means of a polygon along its boundaries. In each computational cell within this polygon the appropriate sink and source terms are computed considering the pile density (number of piles per unit of area) and mean pile diameter. As presented in Table 2.1, different values for turbine density and pile diameter are used for areas that are operational, under construction or planned.

Since the surface forcing applied does not yet include the impact of OWFs on the meteorological conditions, this has been included in a simplified manner through a 10% reduction of the 10 metre wind speeds (U_{10}). Other meteorological forcing parameters, such as air temperature and relative humidity, are left unchanged. Wake effects and directional changes of the wind are not considered.

The impact of the OWFs is assessed through the comparison of a multi-year scenario computation with a baseline computation. For the modelled period the environmental forcing conditions of years 2007 and 2008 have been selected, with 2006 used for spin-up. The selection of the period was based on several considerations including data availability, the inter-annual variability in temperature stratification in the central North Sea and residual transport through the English Channel.

3.2 Model validation

3.2.1 Water levels

The quality of the water level representation in the year 2014 has been determined in terms of the root-mean-square error (RMSE) and presented in Table 3.1. For these Dutch coastal stations, the average total water level RMSE is 6.9 cm. This result is significantly better than that of the previous generation 3D ZUNO-DD model of the southern North Sea (25.6 cm) and due to improvements in both tide and surge.

Table 3.1 Comparison of water level representation (RMSE, determined for 08-01-2014 to 01-01-2015) between ZUNO-DD and 3D DCSM-FM (0.5 nm), for tide, surge and total water level signal.

Station	RMSE tide (cm)			RMSE surge (cm)			RMSE water level (cm)		
	ZUNO-DD	0.5nm	%	ZUNO-DD	0.5nm	%	ZUNO-DD	0.5nm	%
Cadzand	30.5	5.0	-84%	13.1	4.2	-68%	33.2	6.6	-80%
Westkapelle	27.0	5.8	-79%	12.7	4.1	-68%	29.9	7.1	-76%
Haringvliet 10	21.1	4.5	-79%	11.9	4.5	-62%	24.3	6.3	-74%
Hoek van Holland	17.1	5.4	-68%	11.8	4.9	-58%	20.7	7.3	-65%
Scheveningen	19.5	4.9	-75%	12.0	4.6	-62%	22.9	6.7	-71%
IJmuiden Buitenhaven	18.7	5.7	-70%	12.2	5.0	-59%	22.4	7.6	-66%
Average	22.3	5.2	-77%	12.3	4.6	-63%	25.6	6.9	-73%

3.2.2 Temperature (stratification)

A comparison of the observed and modelled sea surface temperature shows an average RMSE of around 0.4 – 0.5 °C in the southern North Sea. The results for offshore measurement location Europlatform are shown in Figure 3.2. Crucially, the model shows a good representation of inter-annual variation in seasonal temperature stratification (cf. Figure 3.3). This variation is of importance to correctly predict oxygen profiles in subsequent water quality simulations.

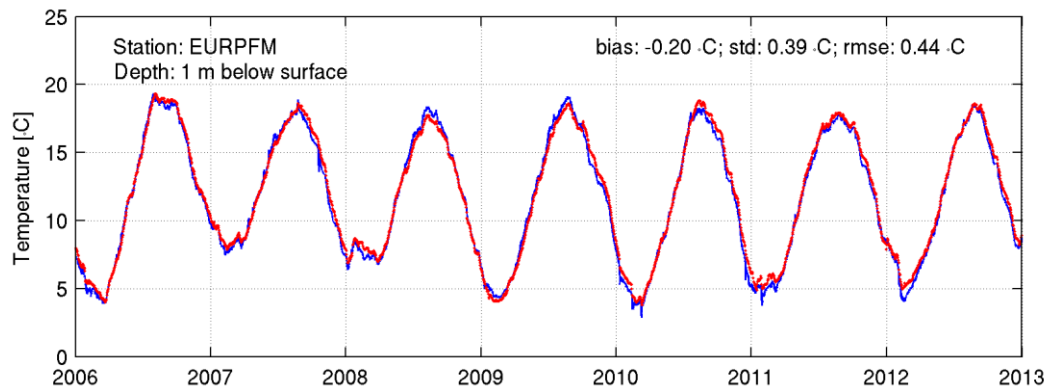


Figure 3.2 Time series of measured (red) and modelled (blue) surface temperature at offshore measurement location Europlatform.

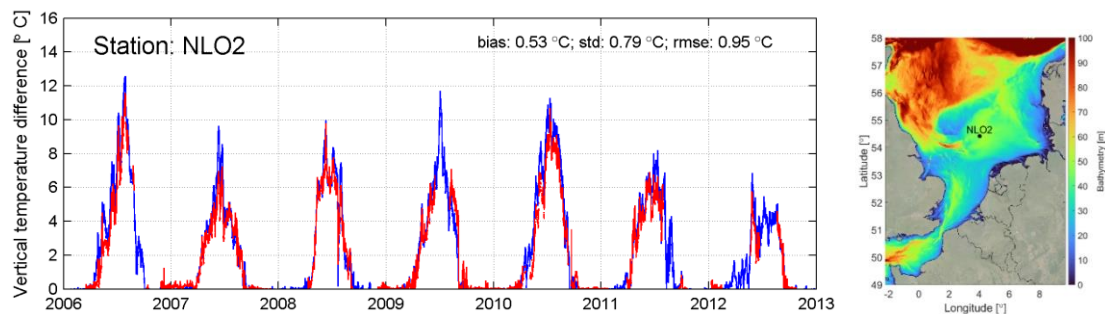


Figure 3.3 Time series of measured (red) and modelled (blue) vertical stratification at station NLO2.

3.2.3 Residual transport through the English Channel

In the previous generation 3D ZUNO-DD model, tilting of the southern boundary was needed to achieve a correct representation of residual transport through the English Channel. 3D DCSM-FM has a much larger model domain and thus there is no open boundary in the English Channel. This results in a good representation of this residual transport without the need to artificially adjust the open boundaries, due to a better representation of mainly barotropic phenomena. Model results show a considerable inter-annual variation in residual transport (cf. Figure 3.4).

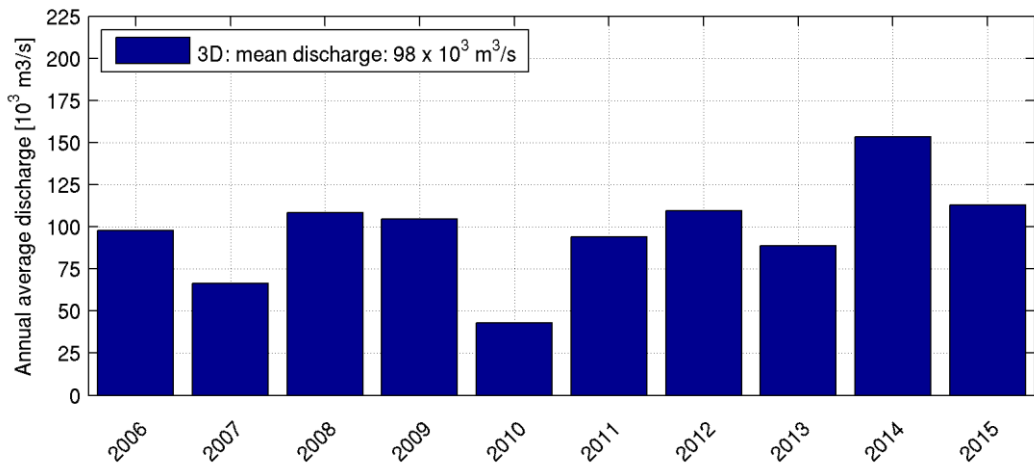


Figure 3.4 Annual average discharge through the English Channel computed with 3D DCSM-FM.

3.3 Results

3.3.1 General

The hydrodynamic impact of the OWFs will be assessed and presented in the following sections with respect to impact on:

- Sea surface temperature
- Temperature stratification
- Salinity stratification
- M2 tidal amplitude and phase
- Residual currents
- Age of water

3.3.2 Reference (no OWFs)

In the reference scenario, the effect of offshore wind farms is neglected entirely, including that of the already present wind farms. The results of this scenario give an overview of the occurring spatial patterns in the North Sea.

Temperature and salinity

Below, the reference situation is presented in terms of the mean annual sea surface temperature and salinity in 2007 as well as the stratification thereof. In these figures the amount of stratification is determined by subtracting the annual mean value in the top model layer from that in the bottom model layer.

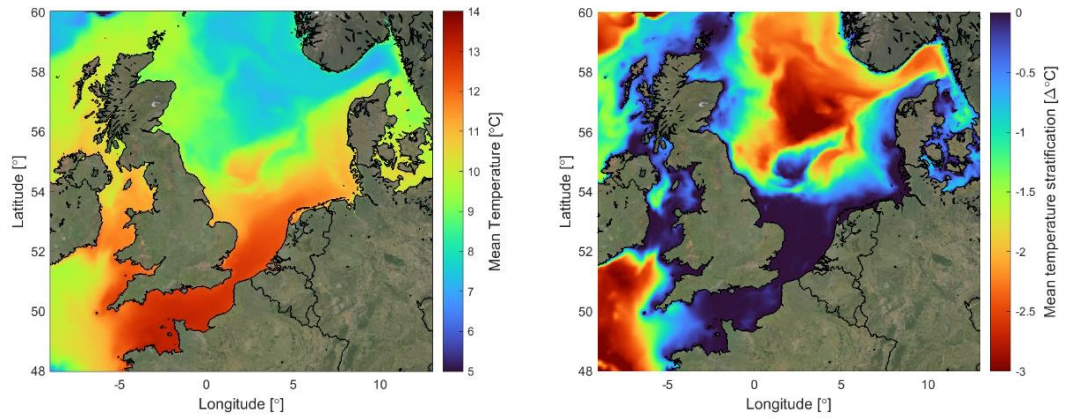


Figure 3.5 Annual mean of sea surface temperature (left) and vertical temperature difference (right) in 2007.

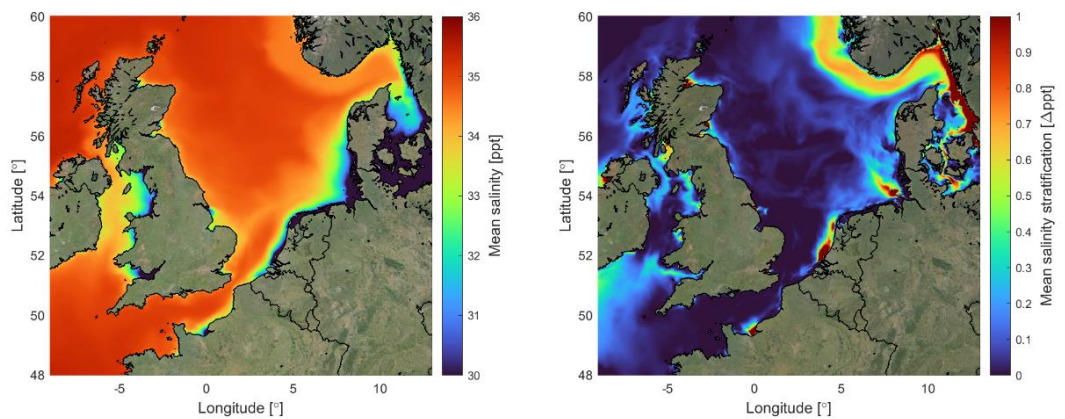


Figure 3.6 Annual mean of sea surface salinity (left) and vertical salinity difference (right) in 2007.

The overall pattern of the stratification is in line with the expected spatial variation (Van Leeuwen et al., 2015). A permanently mixed area is present in the most southern part of the North Sea, between the United Kingdom and the Netherlands. The central North Sea shows a large area with temperature stratification. As expected, temperature stratification (and to some extent salinity stratification) is distinctly reduced in the shallower waters of the Dogger Bank, while mean surface temperatures are higher. Along the coast, temperature stratification is weaker due to vigorous tidal mixing, but the effect of the ROFIs attaching to the coast is clearly visible in the salinity stratification.

Residual current patterns

In Figure 3.7 the magnitude of the annual mean (residual) currents at the surface and bottom are presented for the year 2007. These show the residual circulation at the surface roughly following a counter-clockwise pattern, with residual current at the bottom much lower than at the surface. As expected, the residual transport through the English Channel is in the direction of the North Sea.

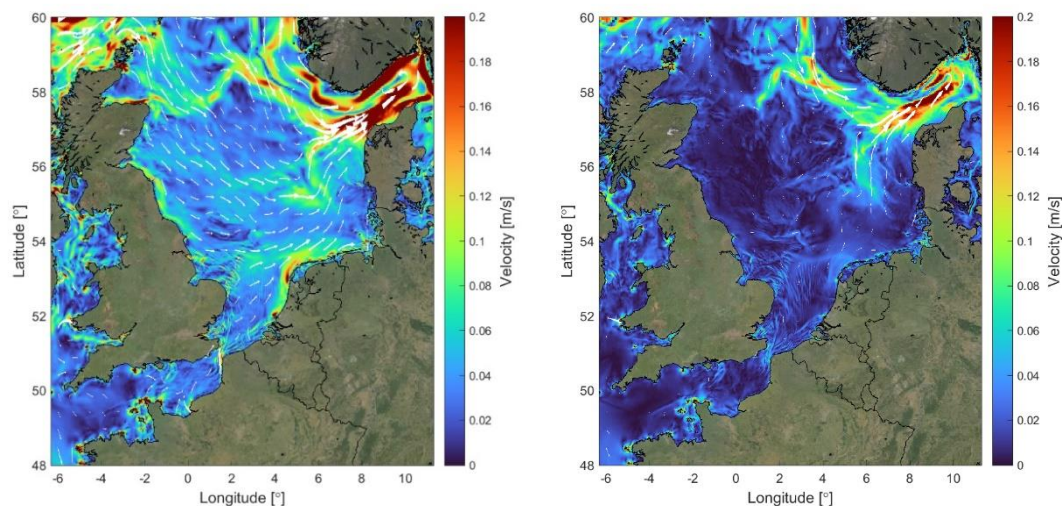


Figure 3.7: Annual mean velocity magnitude (2007) at the surface (left) and bottom (right) model layers.

M2 tide

The semidiurnal lunar M2 tide is the main tidal constituent in most parts of the North Sea. The computed amplitude and phase thereof are presented in Figure 3.8. These figures show the M2 tide behaving as a Kelvin wave, traveling in counter clock-wise direction through the North Sea and with generally higher amplitudes along the coast. Also clearly visible are the two complete amphidromic systems present in the North Sea, one at a latitude of 52.5° and the other further east near 55-56° latitude. In addition, there is a degenerate amphidromic system near the southern coast of Norway.

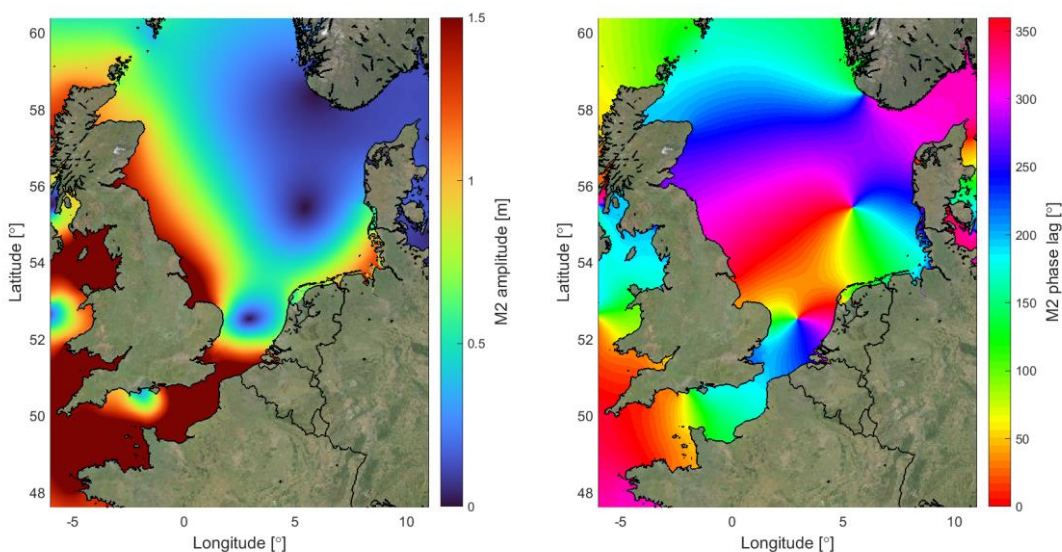


Figure 3.8 Computed M2 amplitude (left) and phase (right).

Age of water

To gain a more 'integrated' understanding on the impact of OWFs on larger scale transport patterns and residence times, the age of water was computed with the aid of two tracers added to the model: one conservative and the other with a constant decay rate. The age of a water particle is defined here to be the time elapsed since the particle under consideration entered the North Sea through one of its rivers.

In Figure 3.9 the age of water at the surface and bottom is presented for a random day in 2008. This shows ages of up to a few weeks to months along the coasts, increasing towards the central parts of the North Sea. Vertical differences in age are much smaller than horizontal differences.

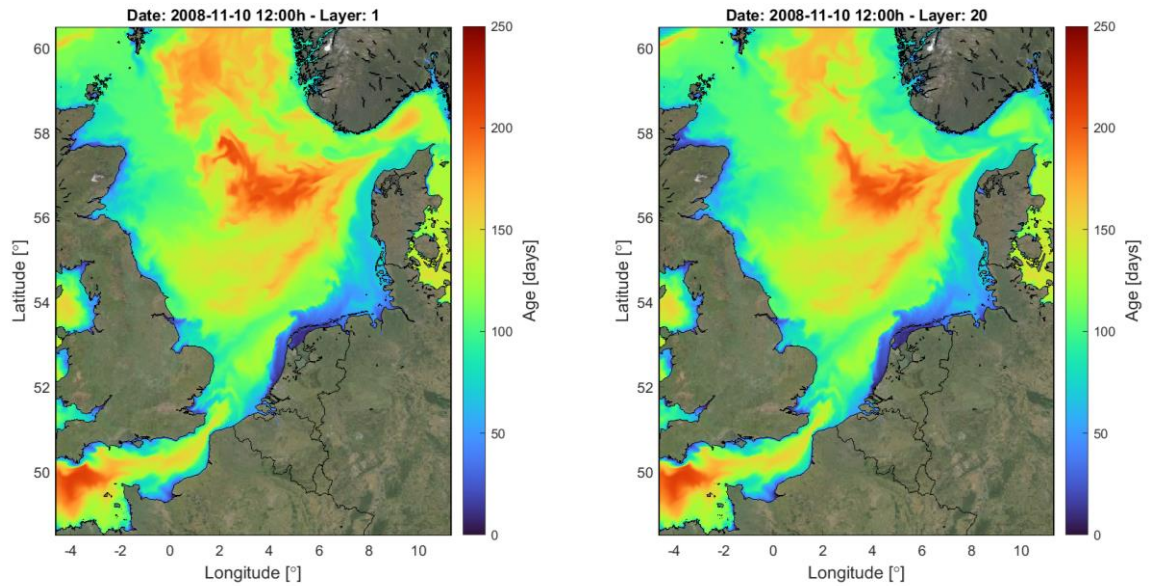


Figure 3.9: Age of water since discharged from river – bottom (left) and top layer (right).

3.3.3 2020 Scenario (current farms)

In this section the results of the 2020 current wind farms scenario are presented.

Temperature and salinity

In Figure 3.10 the change in the annual mean of the sea surface temperature and sea surface salinity is presented. This shows that the presence of the OWFs has limited impact on these parameters. In most areas the change is less than 0.1 °C and 0.1 psu. The largest changes can be observed in the OWFs north of The Netherlands. There, the sea surface temperature decreases by slightly more than 0.1 °C.

In Figure 3.11 the change in the annual mean of the vertical temperature difference is shown. There, a larger impact is present than in the surface values, which implies that the lower part of the water column is more affected, due to enhanced vertical mixing. The largest differences are again present in the OWFs north of The Netherlands, with decreases in mean vertical temperature difference of up to 0.5 °C. In a relative sense, the change in temperature stratification can be more than 50% in some areas.

In Figure 3.12 the change in the annual mean of the vertical salinity difference is shown. The largest differences are again present in the OWFs north of The Netherlands, with decreases in mean vertical salinity difference of up to 0.1 psu. This does not seem much, but in a relative sense, this implies a reduction in salinity stratification of more than 50% in some areas.

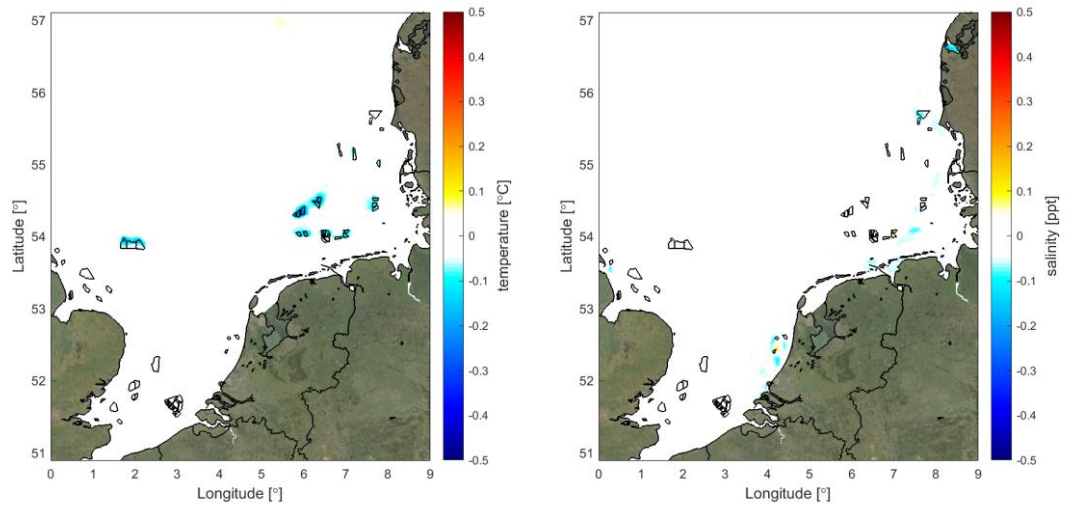


Figure 3.10 Change in annual mean of sea surface temperature (left) and sea surface salinity (right) – 2020 scenario.

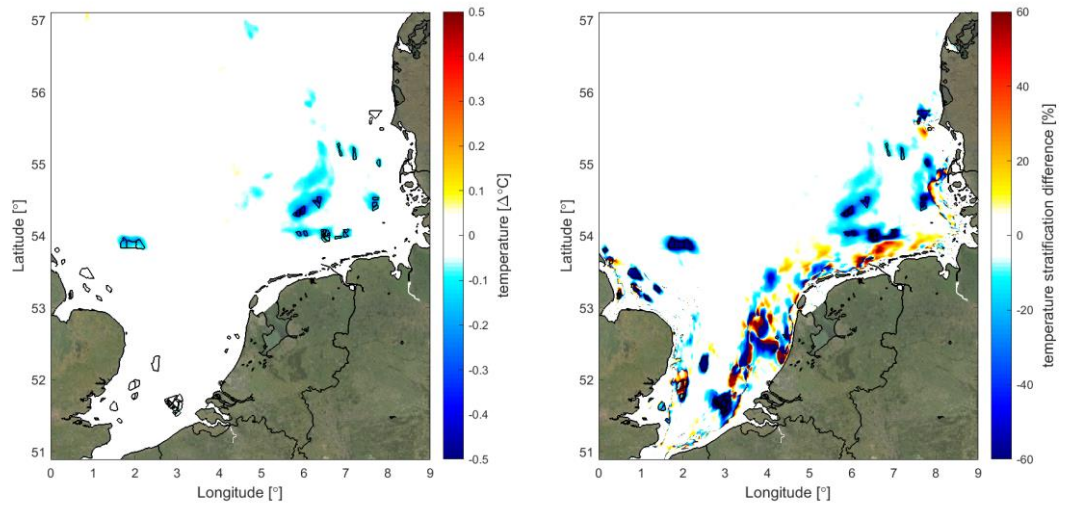


Figure 3.11 Absolute change (left) and relative change (right) in annual mean of vertical temperature difference (2020 scenario).

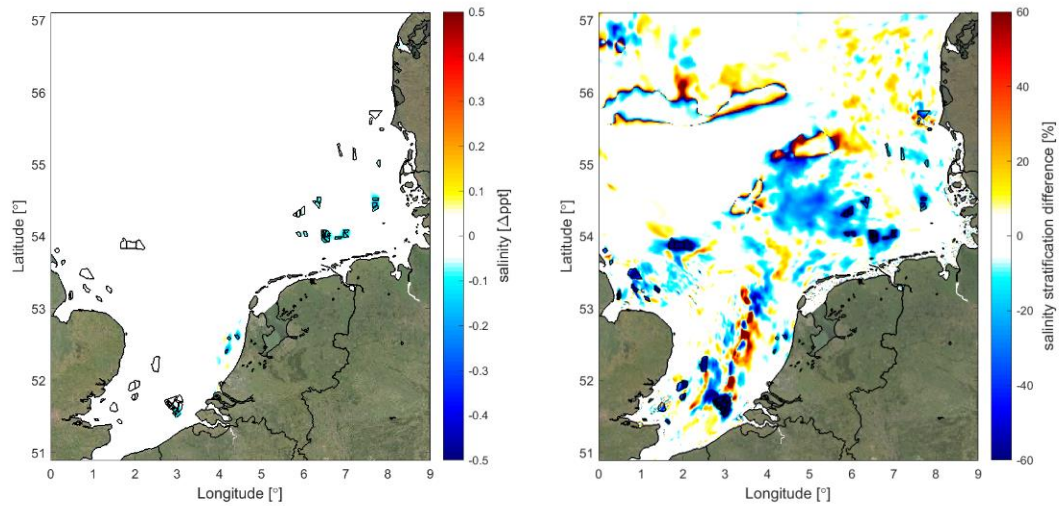


Figure 3.12 Absolute change (left) and relative change (right) in annual mean of vertical salinity difference (2020 scenario).

Currents

In Figure 3.13 the change in the magnitude as well as in the vector difference of the annual mean (residual) currents at the surface is presented for the year 2007. These figures show reductions of residual currents by up to 0.02 m/s at the surface, primarily inside the OWFs. Outside the OWFs both increases and decreases of up to 0.005 m/s in magnitude occur. This more scattered pattern suggests that while local changes are present, the general circulation pattern on a North Sea wide scale is hardly affected.

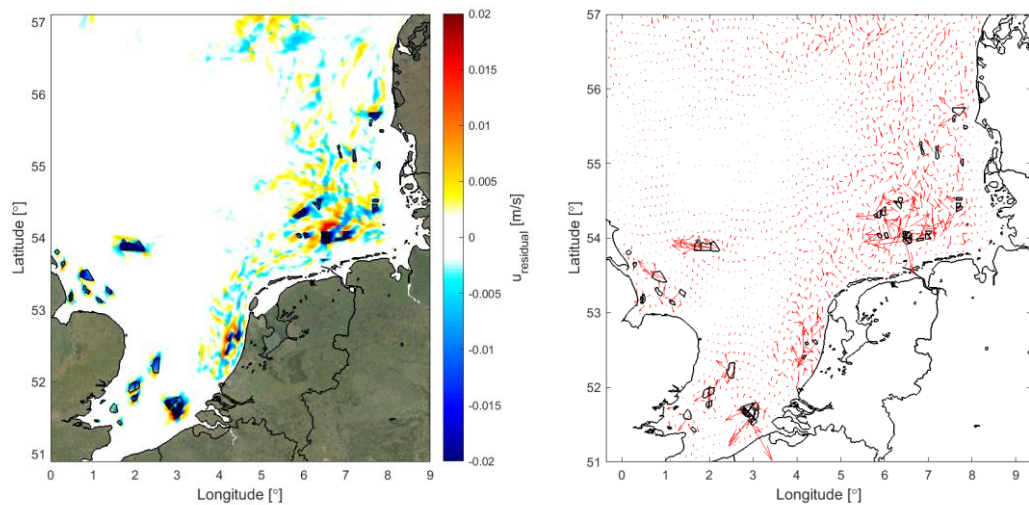


Figure 3.13: Absolute change in annual residual velocity in top layer (2007) – magnitude (left) and vectors (right).

M2 tide

In Figure 3.14 the spatial pattern of the change in M2 tidal amplitude and phase lag is shown. In most parts of the North Sea the impact on the amplitude is negligible with a magnitude of less than 1 mm. In the southern part of the Dutch waters and in the German Bight, a reduction in amplitude of up to 2 mm is present.

The largest impact on the phase lag is present around the amphidromic points. Note however that the resulting impact on tidal water levels is limited there because of the accompanying small amplitudes there. Further away from the amphidromic points the largest impact on the M2 phase is present near the Thames Estuary, where an increase of around 0.2° is present. Both a decrease in amplitude and an increase in phase are consistent with the increased dissipations through the drag introduced by the piles in the OWFs.

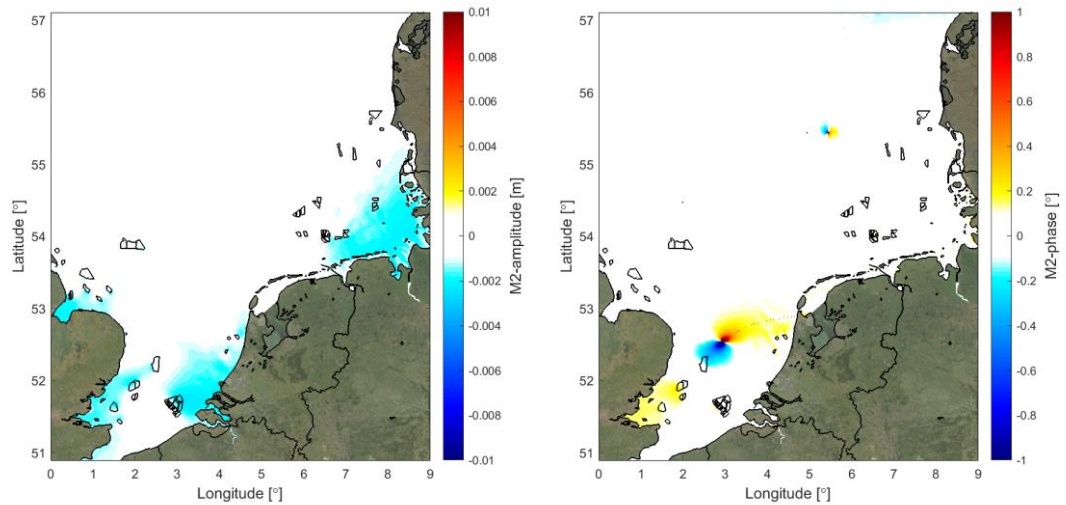


Figure 3.14: Change in M2-tide (2007) – amplitude (left) and phase lag (right).

Age of water

In Figure 3.15 the change in the age of water due to the presence of OWFs is presented. This shows that in most parts of the North Sea the impact is less than a couple of days. The largest changes occur where gradients in age were present in the reference scenario. This indicates that while local changes in residual transport exist, these do not seem to lead to changing basin-scale horizontal transport patterns.

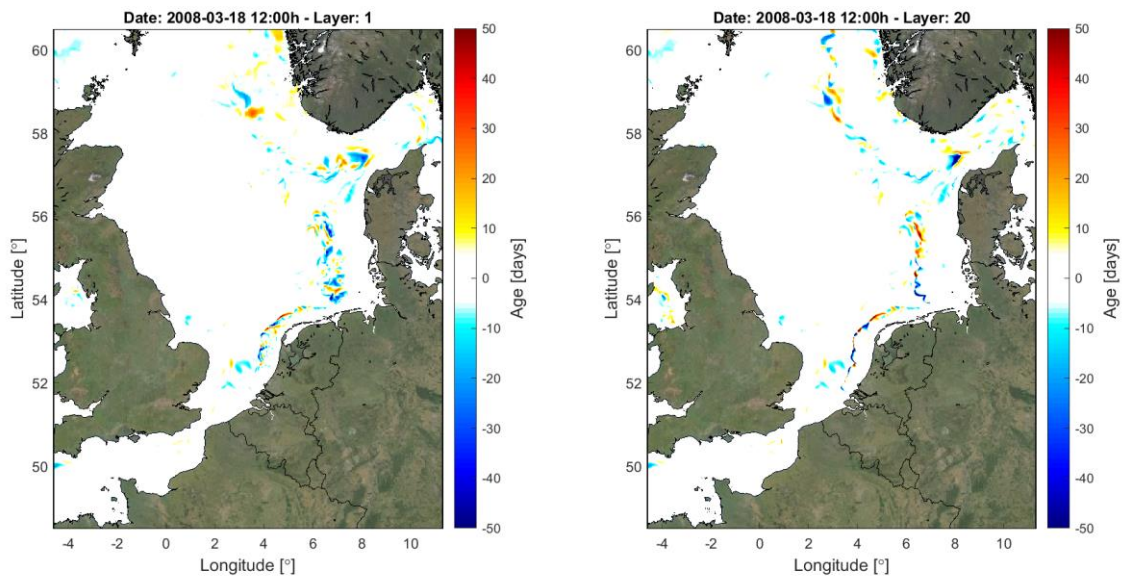


Figure 3.15 Change in age of water since discharged from river – bottom (left) and top layer (right).

3.3.4 Future hypothetical scenario

In this section the results of the future hypothetical wind farms scenario are presented.

Temperature and salinity

In Figure 3.16 the change in the annual mean of the sea surface temperature and sea surface salinity is presented. The largest changes in surface temperature can be observed in and around the band of 54° – 55° latitude, with decreases of up to 0.5 °C, but also some increases in temperature. The largest impact on sea surface salinity can be found in the region of the Rhine ROFI.

In Figure 3.17 the change in the annual mean of the vertical temperature difference is shown. There, a larger impact than in the surface values is present, which implies that the lower part of the water column is more affected, due to enhanced vertical mixing. The largest differences are again present in the OWFs in and around the band of 54° – 55° latitude, with decreases in mean vertical temperature difference of more than to 0.5 °C in large areas. In a relative sense, the change in temperature stratification can be more than 60% in many of the OWFs.

In Figure 3.18 the change in the annual mean of the vertical salinity difference is shown. The largest differences are present in the OWFs north of The Netherlands and in the Rhine ROFI, with decreases in mean vertical salinity difference of up to 0.5 psu in the latter area. In a relative sense, this implies a reduction in salinity stratification of more than 60% in some areas.

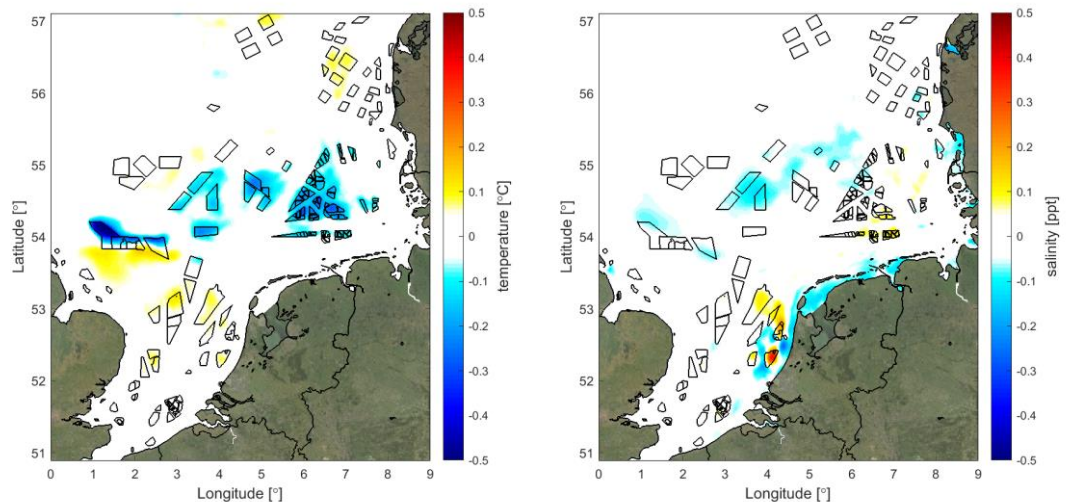


Figure 3.16 Change in annual mean of sea surface temperature (left) and sea surface salinity (right) – future hypothetical scenario.

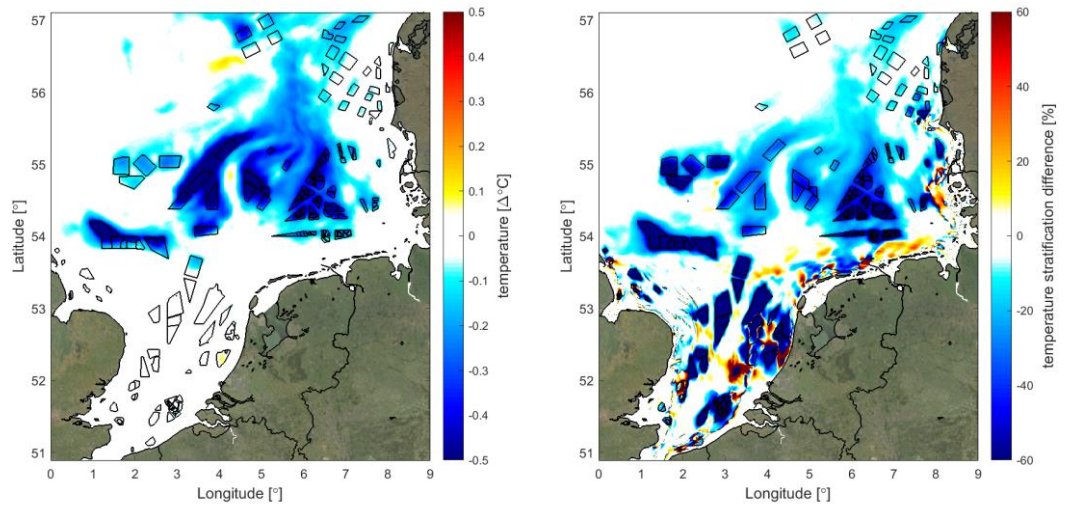


Figure 3.17 Absolute change (left) and relative change (right) in annual mean of vertical temperature difference (future hypothetical scenario).

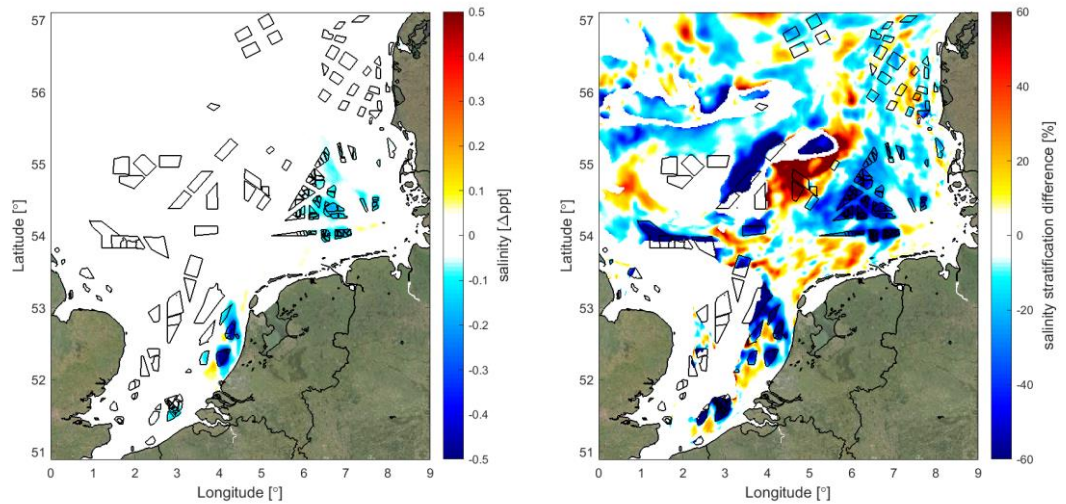


Figure 3.18 Absolute change (left) and relative change (right) in annual mean of vertical salinity difference (future hypothetical scenario).

Currents

In Figure 3.19 the change in the magnitude as well as in the vector difference of the annual mean (residual) currents at the surface is presented. These figures show reductions of residual currents by more than 0.02 m/s at the surface, primarily inside the OWFs. Outside the OWFs both increases and decreases in magnitude occur, with some increases along the OWF areas of more than 0.02 m/s.

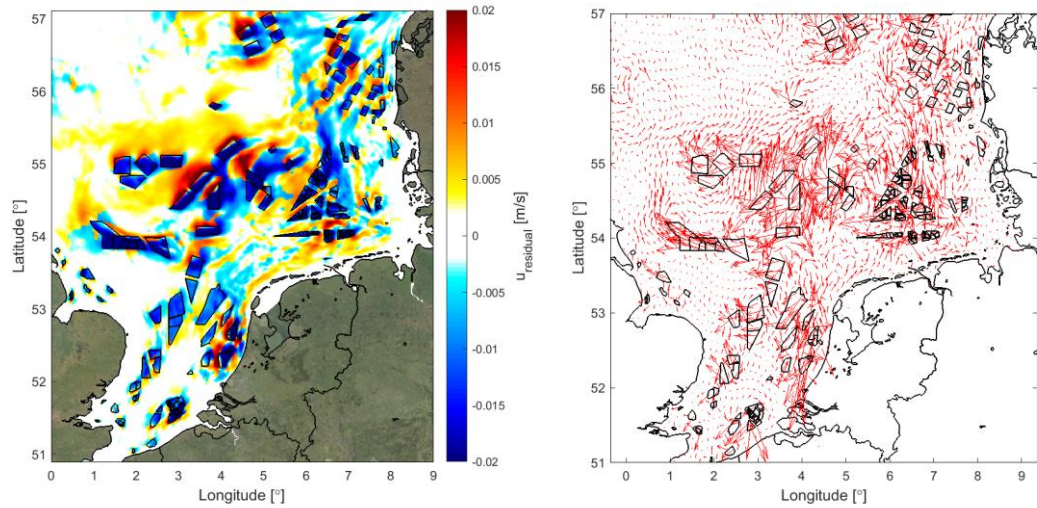


Figure 3.19: Absolute change in annual residual velocity in top layer (2007) – magnitude (left) and vectors (right).

M2 tide

In Figure 3.20 the spatial pattern of the change in M2 tidal amplitude and phase lag is shown. In most parts of the northern and central North Sea the impact on the amplitude is negligible with a magnitude of less than 1 cm. In the southern North Sea, primarily along the Belgian, Dutch and German coast, a more significant reduction in amplitude of up to 1 cm is present. The largest impact on the phase lag is present around the amphidromic points. Note however that the resulting impact on tidal water levels is limited there because of the accompanying small amplitudes there.

Further away from the amphidromic points the largest increase in phase lag is present to the west of Texel and off the German and southern Danish coast, whereas south of Norway a decrease in M2 phase is present.

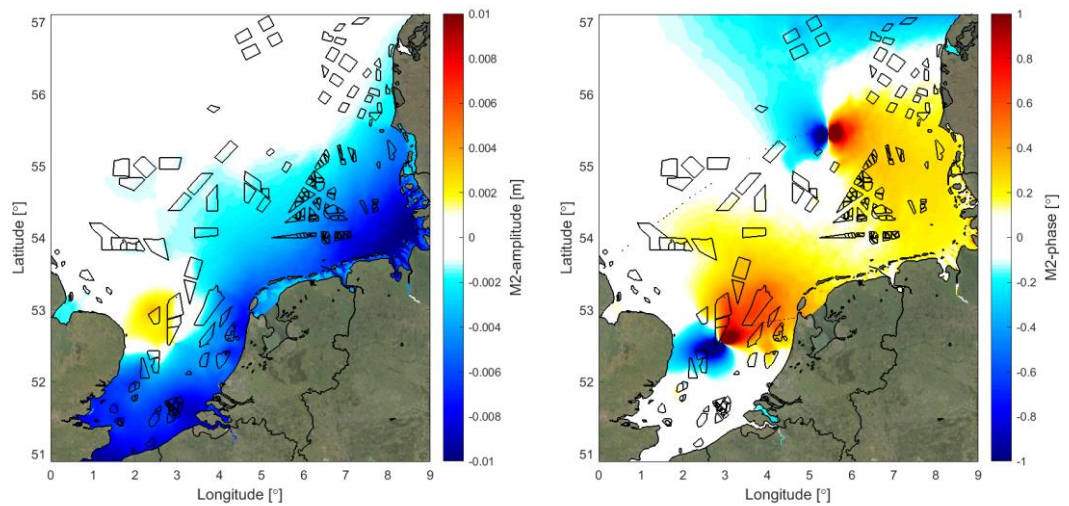


Figure 3.20: Change in M2-tide (2007) – amplitude (left) and phase lag (right).

Age of water

In Figure 3.21 the change in the age of water due to the presence of OWFs is presented. This shows that in most parts of the North Sea the impact is less than a couple of days. The largest changes occur where gradients in age were present in the reference scenario, for example at the location of fronts in the Rhine ROFI. This, and the fact that the sign of the change in age varies on relatively short spatial scales, indicates that while local changes in residual transport exist, these do not seem to lead to changing basin-scale horizontal transport patterns.

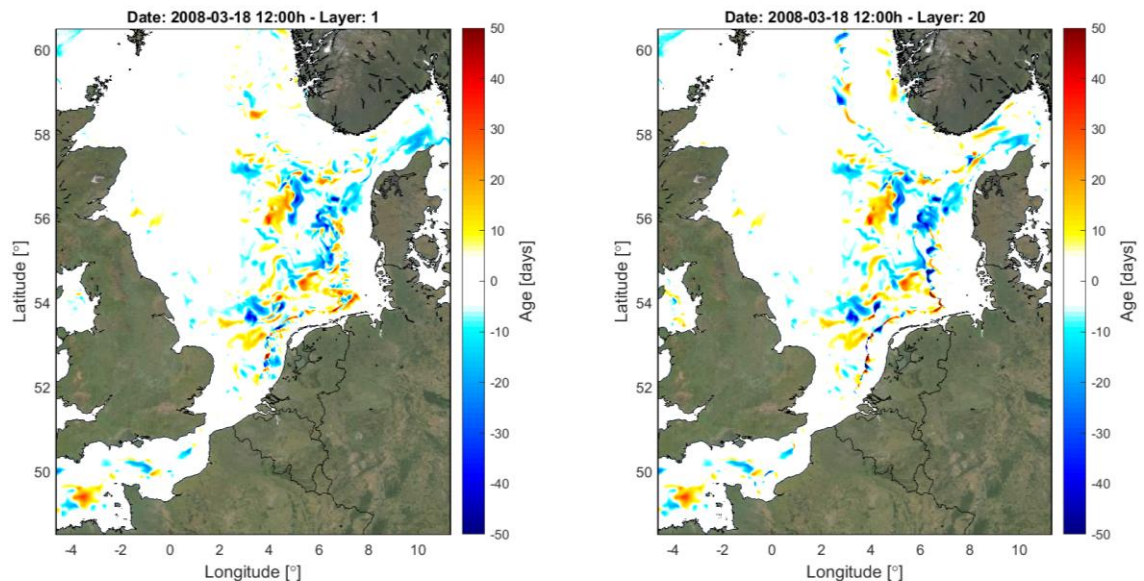


Figure 3.21: Absolute change in age of water since discharged from river – bottom (left) and top layer (right).

3.3.5 Comparison of temperature stratification

The timeseries in Figure 3.23 and Figure 3.24 show the amount of temperature stratification in 2007 and 2008 for the stations F3PFM and NLO2. Their locations, at the edge of offshore windfarms in the 2050 scenario, are given in Figure 3.22. In the legend the duration of the temperature stratification is shown, defined at the number of days for which the vertical temperature difference is above 0.5°C (plotted as a dashed line). Between the reference scenario and the 2020 scenario differences in the amount of stratification, temporal variation of stratification and the total duration of the stratification are small. This was expected, since in this scenario there were no OWFs nearby. However, the amount of stratification is smaller for the 2050 scenario. The duration of temperature stratification in 2007 is hardly affected in station NLO2, while a clear reduction is noticed in station F3PFM (from 156 to 120 days). In 2008 the duration of stratification is largely unaffected in both stations. At the other stations plotted in Figure 3.22, hardly any change in amount and duration of temperature stratification is noticeable, in both scenarios and in both years. In station NOORDWK70 and EURPFM this is because there is hardly any temperature stratification in the reference scenario. Stations AMSRA, AUKPFM, UKO5 and A12 are located in areas with seasonal temperature stratification but are further away from OWFs in the 2020 and 2050 scenario.

In the scenario computations, OWFs can have an impact on the hydrodynamic conditions through two mechanisms: the enhanced production of turbulent kinetic energy due to the presence of piles in the water column and through the reduction of wind speed due to the presence of the wind turbines in the atmospheric boundary layer. To be able to make a distinction between the impact of both mechanisms, additional scenario computations were made, where the reduction in wind speed within OWFs was turned off.

The results in Figure 3.23 and Figure 3.24 indicate that the presence of piles in the water column has more impact on stratification than the reduction of wind speed due to the presence of the turbines.

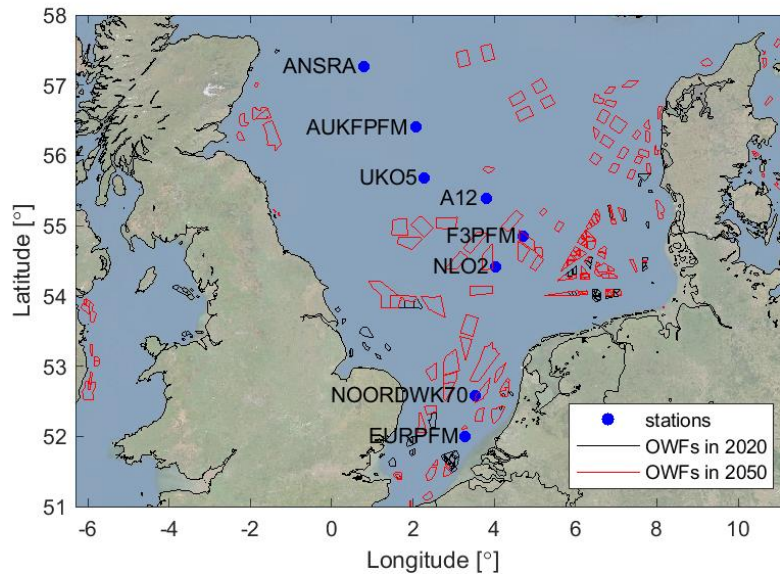


Figure 3.22 Locations of stations with plotted stratification and OWF scenarios.

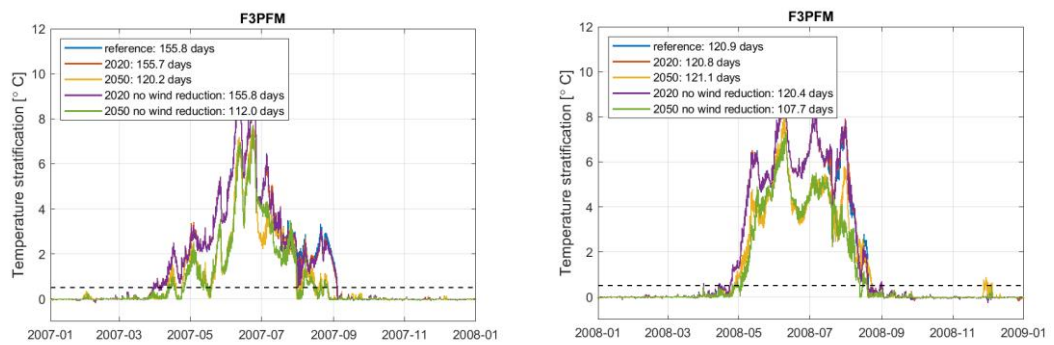


Figure 3.23 Temperature stratification at platform F3 for different modelled scenarios.

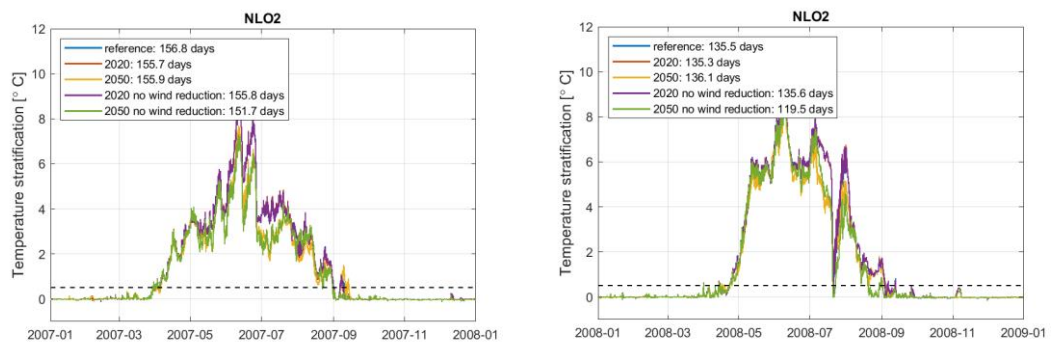


Figure 3.24 Temperature stratification at station NLO2 for different modelled scenarios.

3.4 Discussion

3.4.1 Conclusions regarding the hydrodynamic model

3D DCSM-FM shows a good representation of levels with an RMSE of the total water level around 7 cm at the Dutch coast. Sea surface temperatures in the model have an RMSE of around 0.5°C and temperature stratification in the central North Sea is well represented, including its seasonal and interannual variation. Furthermore, a good representation of the residual transport through the English Channel is found. Further validation of the hydrodynamic model has been performed in other projects (Zijl et al., 2020).

A reference scenario with the model, excluding all offshore windfarms, shows a spatial stratification pattern in line with expectations (Van Leeuwen et al., 2015). A permanently mixed area is present in the southern North Sea between the United Kingdom and the Netherlands. Residual currents show a circulation pattern in counter-clockwise direction with currents through the English Channel directed toward the North Sea. The M2 tide includes the expected two complete amphidromic points in the North Sea and a degenerate amphidromic point at the southern Norwegian coast. The age of the water since its discharge from rivers has been calculated. A high age is mainly present in the central North Sea. The vertical difference in age is smaller than the horizontal difference.

With respect to the impact of the OWFs, the following can be concluded:

- The two scenarios with offshore wind farms show similar results, but the magnitude of the effect of the wind farms is larger in the 2050 scenario. The 2020 scenario has a limited impact on annual mean surface salinity and surface temperature of often less than 0.1 psu and 0.1°C respectively. For the future hypothetical OWF2050 scenario surface temperature decreases with up to 0.5°C in some areas.
- The presence of OWFs also affects the annual mean of the vertical temperature difference to a larger extent than the surface values, due to enhanced vertical mixing. This implies that the lower part of the water column is more affected than the surface. In the OWF2020 scenario the largest differences are present in the OWFs north of The Netherlands, with decreases in mean vertical temperature difference and mean vertical salinity difference of up to 0.5 °C and 0.1 psu, respectively. In a relative sense, this implies a reduction in temperature and salinity stratification of more than 50% in some areas. In the OWF2050 scenario the largest differences are present in and around the band of 54° – 55° latitude in the case of temperature and in the OWFs north of The Netherlands and in the Rhine ROFI in the case of salinity. There, decreases in mean vertical temperature difference and mean vertical salinity difference occur of up to 0.5 °C and 0.5 psu, respectively. In a relative sense, the change in temperature and salinity stratification can be more than 60% in many of the OWFs.
- The magnitude of the annual mean (residual) surface currents decreases by up to 0.02 m/s in both scenarios, with the largest changes primarily occurring inside the OWFs. Outside the OWFs both increases and decreases in magnitude of up to 0.005 m/s and 0.02 m/s occur in the OWF2020 and OWF2050 scenario, respectively. However, on a larger scale the general circulation pattern of residual currents in the North Sea is hardly affected.
- This M2 tide shows a reduction of up to 2 mm or up to 1 cm for the 2020 scenario and the future hypothetical OWF2050 scenario respectively, with the largest impact on M2 amplitude present in the southern part of the Dutch waters and the German Bight. In the OWF2020 scenario the largest impact on M2 phase, away from the amphidromic points, occurs near the Thames Estuary, where an increase of around 0.2° is present. In the OWF2050 scenario the largest impact on M2 phase is present in larger areas to the west of Texel and off the German and southern Danish coast, with increases of up to 0.2° – 0.4°. Both a decrease in amplitude and an increase in phase are consistent with the increased dissipations through the drag introduced by the piles in the OWFs.

- The impact of OWFs in both scenarios on the age of water is less than a couple of days, with the largest changes occurring where gradients in age were present in the reference scenario. This, and the fact that the sign of the change in age varies on relatively short spatial scales, indicates that while local changes in residual transport exist, these do not seem to lead to changing basin-scale horizontal transport patterns.
- In locations where seasonal temperature stratification occurs, its magnitude can be affected by the presence of OWFs in the area. This effect is mainly seen inside and close to OWF. Stations further away are much less affected in both scenarios. In one location considered, the duration of temperature stratification is also be affected, although this effect is only present in 2007 and not in 2008.

3.4.2 Recommendations

A list of recommendations for the further general development of 3D DCSM-FM can be found in Zijl et al., 2020. Of specific relevance for this study is the recommendation to extend the validation against salinity- and temperature observations, in particular focusing on stratification. Currently, the model has been validated for temperature stratification at just one location (in the central North Sea).

A priority would be the validation of the parameterization of OWFs in the present application of this model. This is less straightforward than validating against measurements near OWFs, especially since the impact in the existing situation is limited compared to natural variability. Specific measurements just upstream, inside and downstream of OWFs would be useful. If these are not already available, a dedicated measurement campaign might be required.

Currently lacking in our hydrodynamic modelling framework is the coupling with a meteorological model. In the present approach, wake effects are ignored altogether and meteorological changes due to the presence of OWFS are limited to the OWF area itself. Also, the parameterization of the impact on U_{10} (wind speed at 10 metres above the water surface) is very rough (-10%). Impacts of OWFs on meteorological parameters influencing the exchange of heat with the atmosphere are also neglected (except for U_{10}), although there is evidence that this might be important. These parameters include net solar radiation (affected by changes in cloud cover), relative humidity, downwelling long wave radiation (also affected by cloud cover, and relative humidity) and air temperature. It is therefore recommended to explore the possibility to couple the hydrodynamic model directly to a meteorological model including the effect of OWFs on the relevant meteorology parameters.

4 Wave model

4.1 Approach

Numerical wave modelling has been performed using SWAN in order to capture the effects of waves on fine sediment. The wave numerical model in combination with the 3D hydrodynamic model presented in Chapter 3 provide the effective shear stresses near the bed and hence forcing for fine sediment modelling for the three considered scenarios of offshore wind farm development.

For the numerical modelling of waves, the third-generation shallow water wave model SWAN (Simulating WAVes Nearshore; <http://swanmodel.sourceforge.net/>) is used. More precisely, the ERA5 wind data have been used to force Deltares' Dutch Continental Shelf Model (DCSM) SWAN model. Moreover, the ERA5 wave data is applied at the model North Atlantic boundaries and the water levels and currents from the extensively calibrated 2D (depth-averaged) DCSM-FM are applied in the whole model domain. The DCSM-SWAN model is extensively calibrated against observations at various locations in the North Sea.

The effects of wind farms on waves for the considered scenarios are implicitly modelled by adjusting the wind forcing of the wave model. Similar to the hydrodynamic modelling approach, a 10% reduction of wind speeds is applied uniformly across the areas designated for future wind farm development (2020 and 2050 scenarios).

The approach followed for the wave modelling is presented in Figure 4.1 below.

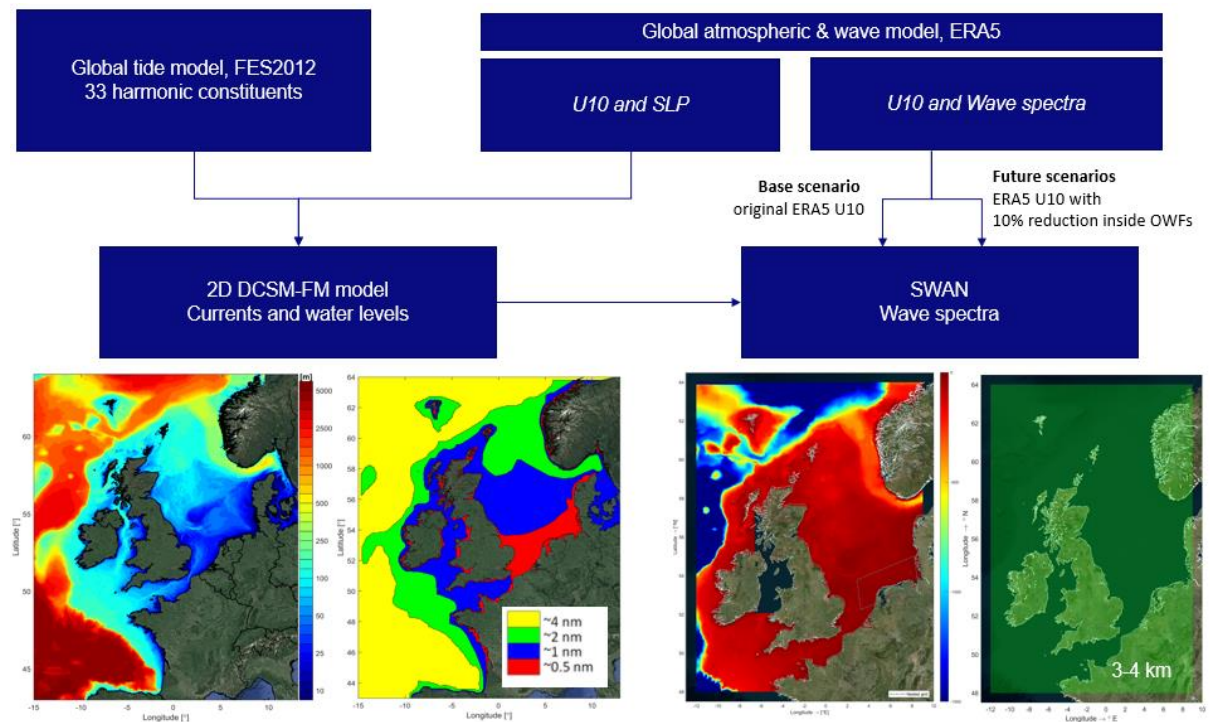


Figure 4.1 Wave modelling approach.

4.2 Model set-up

4.2.1 Model domains

SWAN requires the specification of three types of grids:

1. a computational grid which defines the 2D geographical space of the grid points;
2. a directional grid which defines the directional range (usually 360°) and resolution;
3. a frequency grid which defines the range and resolution of the grid in frequency space.

The DCSM-SWAN covers the region of interest with a spatial resolution of 1/20 degree (≈ 4.0 -2.4 km) in longitudinal (East-West) direction and of 1/30 degree (≈ 3.7 km) in lateral direction (North-South). Moreover, the directional grid in SWAN covers the full circle (360°). The number of directional bins is set to 45, resulting in a directional resolution of 8°. Finally, the spectral grid of the numerical model covers a frequency range from 0.03 Hz to 0.6 Hz, allowing for representation of wave periods ranging from 1.67 s to 33.33 s. The distribution of the frequencies, f , is logarithmic with a constant relative resolution, $\Delta f/f$, close to 0.1. This results in 32 frequency bins.

4.2.2 Bathymetry

Similar to the 3D DCSM-FM model bathymetry, the DCSM-SWAN model bathymetry has been derived from a gridded bathymetric dataset (October 2016 version) from the European Marine Observation and Data Network (EMODnet). The resolution of the gridded EMODnet dataset is 1/8' x 1/8' (approx. 160 x 230 m). An overview of the DCSM-SWAN model bathymetry is presented in Figure 4.2. Note that although the Irish Sea is within the extent of the model's computational grid, the area is not modelled by locally excluding bathymetric information. This is done for computational efficiency. As a result, wave effects within this area are not captured by the model.

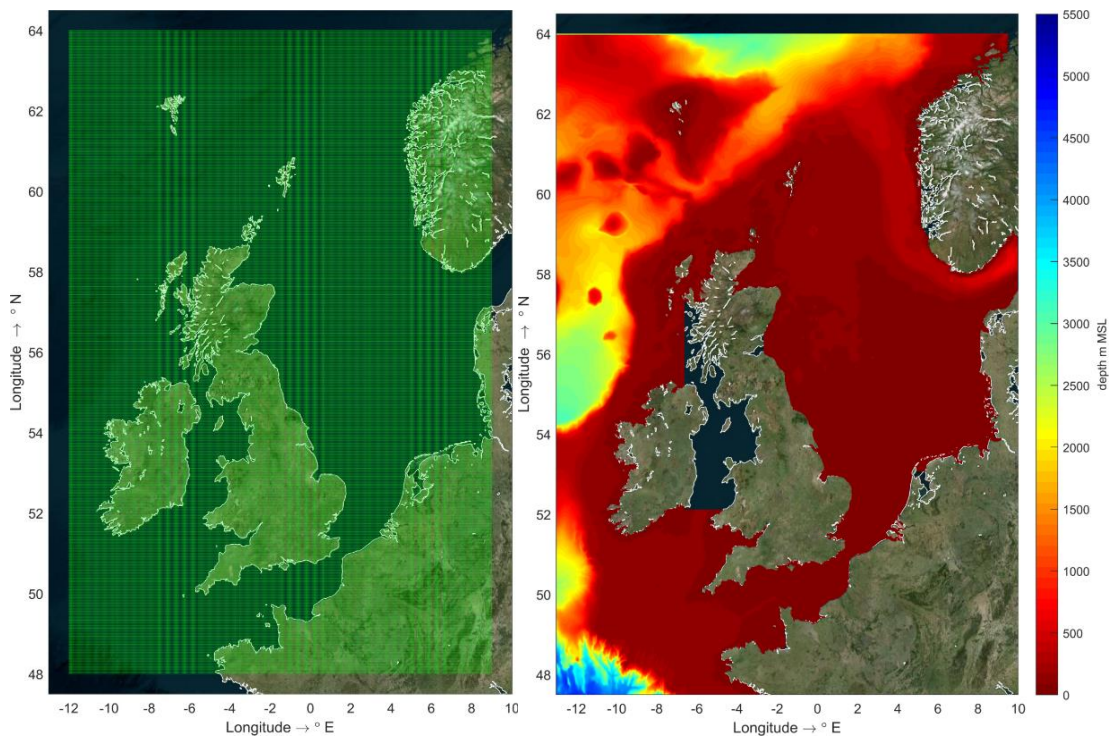


Figure 4.2 Grid and bathymetry in DCSM-SWAN wave model.

4.2.3 Boundary and input conditions

The wave model is run in non-stationary mode (i.e. taking evolution of the wave conditions in time into account) for the period from 2006 to 2017. The model uses a timestep of one hour, which is equal to the time step of the (ERA5) input wind fields. The first 48 hours simulated time are considered as the spin-up period of the model¹.

- The SWAN model was forced at the outer boundaries of the overall domain with parameterized wave spectra described by ERA5 time series of five wave parameters; (i) Significant wave height, H_s , (ii) Peak wave period, T_p , (iii) Mean wave direction (coming from), MWD, (iv) Directional spreading, σ or m and (v) Spectral shape, γ .
-
- The spectral shape, γ , was assumed to be constant for all computations, being a JONSWAP shape (Hasselmann et al., 1973) with a value of $\gamma = 3.3$. The exact value of γ prescribed along the boundary is not critical, since the model will automatically properly redistribute the wave energy in the frequency domain and in balance with the wind forcing. The amount of directional spreading present at the incoming boundaries was derived from the ERA5 time series for “wave spectral directional width”. For numerical reasons, this value was capped at a maximum of $\sigma = 37.5^\circ$ (one-sided directional spreading level from the mean direction). Also, for this boundary parameter, the exact value prescribed is not critical, since the model will automatically properly redistribute the wave energy over the different directions in the computed domain.

4.2.4 Reflecting/transmitting boundaries

No reflecting or transmitting boundaries were defined. All wave energy reaching an outer boundary or land boundary is assumed in the model to be fully absorbed at that location. At the sections bordering the Irish Sea waves propagate out of the computational domain uninfluenced (as if they move into the Irish Sea).

4.2.5 Wind input

The SWAN model domain was forced spatially using the ERA5 wind fields with no corrections on the wind speeds or directions for the base scenario. For the two future scenarios modelled, only the magnitude of 10 metre wind speeds (U_{10}) was reduced by 10% at all computational grid points inside the respective polygons of designated windfarm development. Wake effects and directional changes of the wind are not considered, similar to the approach followed in the hydrodynamic model (see Section 3.1.8).

4.2.6 Hydrodynamics input

The spatially varying hourly water level and depth-averaged current fields from the 2D DCSM-FM have been used as input to both SWAN wave modelling domains. This means that the wave model simulates how the spatially distributed water levels and currents (speeds and directions) influence the wave propagation and evolution. Regarding the modelling of the two future scenarios, the effect of changing water levels and currents due to the applied wind magnitude reductions was deemed negligible for wave propagation. Therefore, the hydrodynamic input to the wave simulations of all three scenarios is taken the same as in the base case scenario for modelling efficiency.

¹ The spin-up period is the modelling interval which is required for the model to start up and initialise. This includes allowing the wave energy from the boundary to distribute over the total modelling domain. A spin-up period of 48 hours (2 days) is typically used. Results for the spin-up period may not be reliable and are discarded.

4.2.7 Numerical aspects and physical processes

All physical processes relevant were activated in SWAN for the wave modelling in this study. These physical processes were modelled based on specific formulations and associated parameters, which are summarized in Table 4.1, together with the selected numerical settings.

Table 4.1 Summary of applied settings in the wave model for numerical aspects and physics parameters.

Model parameter	Applied setting
Mode	Non-stationary
Accuracy	Changes of less than 1% in H_s and $T_{m0,1}$ at 99% of the grid points relatively to the previous iterations, a maximal number of 60 iterations
Integration scheme	BSBT (Backward Space Backward Time)
Generation	3 rd generation including quadruplets (iquad=3 for currents activated and iquad=2 for hindcast modelling)
Wind drag	Wu (1982)
Bottom friction	JONSWAP formulation (Hasselmann et al., 1973) ($C_{JON} = 0.038 \text{ m}^2/\text{s}^3$, (Zijlema et al., 2012))
Depth-induced wave breaking	Default Battjes-Janssen formulation (Battjes and Janssen, 1978)
White-capping	Formulations by Rogers et al. (2003)

4.3 Results and discussion

The results of the wave model for the three scenarios modelled are presented in terms of instantaneous absolute and relative differences in significant wave height between the base and each of the two future scenarios in Figure 4.3 and Figure 4.4.

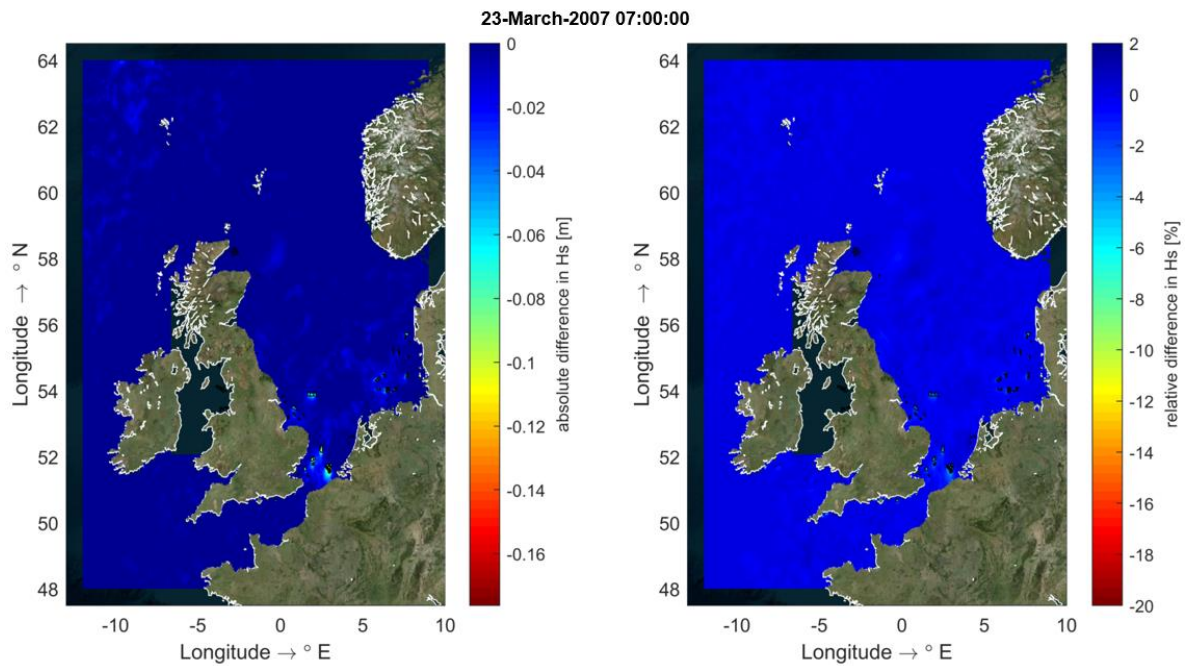


Figure 4.3 Absolute (left) and relative (right) differences in significant wave height (H_s) between the base and 2020 Scenario (with operational, and under construction OWFs in the North Sea) in 23rd March 2007, 07:00:00.

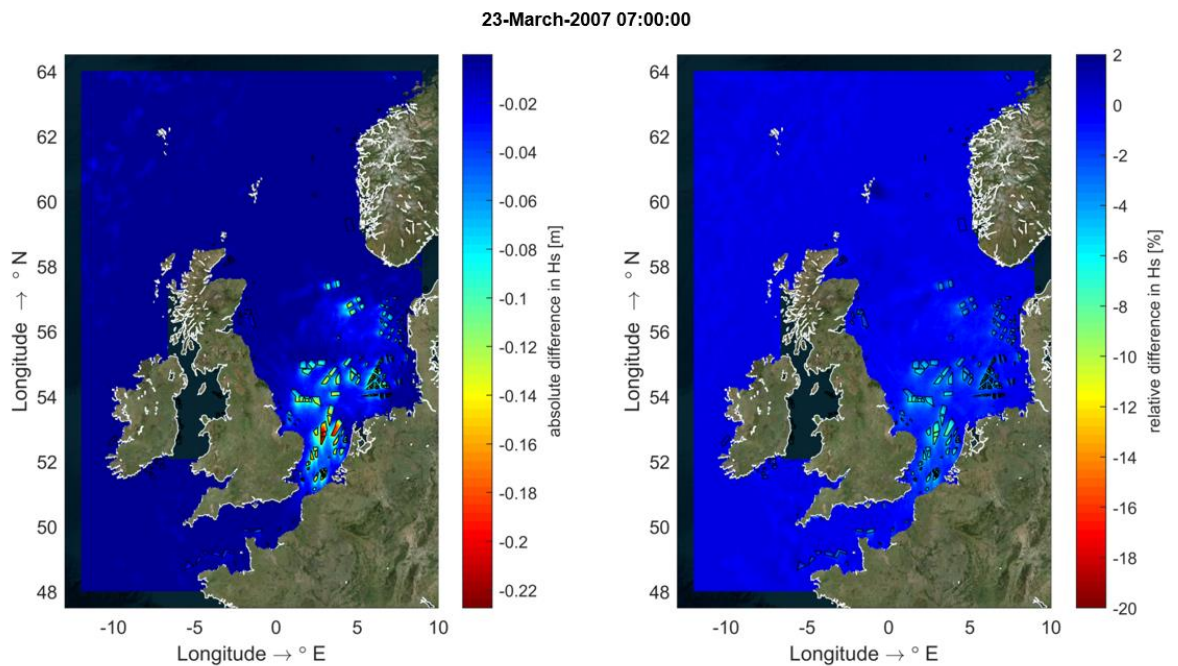


Figure 4.4 Absolute (left) and relative (right) differences in significant wave height (H_s) between the base and future hypothetical scenario (with operational, under construction and planned OWFs in the North Sea) in 23rd March 2007, 07:00:00.

The time of the simulation period for which results are presented is deemed representative for typical storm conditions in the North Sea and serves here as an example to discuss the results of the wave model. During such conditions, Figure 4.3 shows that only a moderate effect of the wind farms is predicted for the 2020 scenario on wave energy. This is explained by the relatively small areas of the windfarms within which wind magnitudes decrease.

Note that this is partly a limitation of the followed modelling approach, in which the spatial resolutions of the computational grid and of the input wind field are relatively coarse to effectively capture the effects of decreasing wind speeds for certain wind farms characterized by limited extents. However, in practice, it can also be expected that wind farms extending over limited areas have a limited effect on the wind field and in turn on wave energy generation in their vicinity compared to larger wind farms. Nevertheless, a close inspection of the wave model results indicates a limited and local effect of the reduced wind speeds on wave heights within the wind farms.

On the other hand, wave simulations of the hypothetical future scenario, which includes large wind farm development areas, demonstrate a much more significant effect on the predicted wave energy across the North Sea at the same instance of time. In fact, Figure 4.4 shows that the effects of the largest wind farms on wave energy are not only limited within the polygons but extend (decreasing) even further according to the local wave propagation direction. Obviously, this is a direct result of the local decrease in wind-induced wave energy generation eventually leading to less energy propagating away from the wind farm areas, given that no wake effects are resolved in the current modelling approach. For the presented conditions, wave heights reduce in the order of roughly 8% as a result of the 10% decrease in wind magnitudes 10 meters above the sea surface. The relative difference in predicted significant wave heights within the OWF polygons is in the same order of magnitude for all neighbouring wind farms where the pattern of decreasing wave heights is clearly observed. This is irrespective of the corresponding absolute decrease in wave energy and the size of the wind farms. However, the wake effects from the decreased local wave energy generation increase at the vicinity of larger wind farms or at areas where several wind farm developments are foreseen next to each other. Additionally, it is worth mentioning that the predicted effect of wind reduction on peak wave periods is negligible (not presented here).

Additional detailed analysis is required to provide insight into the cumulative effects of wind farm development specifically on wave energy in the North Sea. For the purposes of the present study, the wave model provides a basis for the fine sediment modelling and hence such an analysis is not deemed necessary. It is concluded that based on the wave model output (significant wave heights and peak periods), representative wave-induced near-bed shear stresses can be obtained for the three scenarios in the area of interest.

5 Fine sediment model

5.1 Fine sediment model set-up

The DELWAQ fine sediment module for the North Sea has been developed over the years to describe the natural fine sediment dynamics and human impacts hereon such as Maasvlakte-2 land reclamation and sand mining. It has been used for a number of environmental impact assessments in the Dutch coastal zone and is a logical candidate to assess the impact of wind farms on fine sediment dynamics and ecology. In previous impact studies the module has already been coupled to ecological models on light climate, nutrient transport and primary production.

The essence of the fine sediment module is that it considers three compartments, i.e. the water column (represented in 3D) and the bed represented by a fluff layer with a low threshold for resuspension and a buffer layer with a high threshold for resuspension. The buffer layer represents the sandy North Sea bed through which fine sediment may be mixed during calm periods and released during energetic periods. As much more fine sediment is present in the seabed than in the water column, the mean residence time of fine sediment is much longer than the residence time of seawater.

For this study a new fine sediment model is set-up that is online coupled with the hydrodynamic flow model and offline coupled with a SWAN wave model. The settings of the fine sediment model are largely based on the validated parameterization of the ZUNO-DD fine sediment model (the predecessor of DCSM). The model had to be recalibrated due to differences in hydrodynamic forcing and model domain. The fine sediment model is applied to compute the impact of existing wind farms on SPM dynamics inside and in the vicinity of the parks. This is done to gain confidence in the model on this aspect (as it is the first time the model is applied for impact assessment of wind farms). Secondly, the model is applied for scenarios including and excluding planned wind farms to assess the impact of these parks on SPM dynamics relative to the reference scenario (2007 situation without wind farms).

5.1.1 Bottom shear stress by currents and waves

The total bottom shear stress is an important parameter for fine sediment dynamics. Accounting for both is important to realistically model sediment resuspension during calm and more energetic conditions. The wave-induced bed shear stress is calculated using the formulation of Swart (1974) based on non-stationary fields of significant wave height (H_s) and peak wave period (T_p) provided by the wave model and a Nikuradse value of $1 \cdot 10^{-3}$ m. This value is set after comparison of the total bed shear stress values from the older ZUNO-DD model (as used e.g. in Maasvlakte 2 and MER Zandwinning studies) and DCSM model within the domain of the ZUNO-DD model. The total bed shear stress is determined by the sum of the bed shear stress contributions by waves and currents, hereby disregarding the direction of the current and waves.

5.1.2 Sediment fractions

The fine sediment model is set-up with three mud fractions (similar to ZUNO-DD). Inclusion of multiple fractions allows better representation of spatial patterns, tidal and seasonal variations and concentrations during more energetic conditions. The three mud fractions are characterized by their different sedimentation velocities (Table 5.1). These fractions do not interact in the water column, i.e. flocculation is not (yet) included in the model.

Notwithstanding, the average settling velocity in the model is variable, as different mud fractions have a different dispersion behaviour and the average composition is therefore variable. Additional erosion and sedimentation related parameters are included in Appendix B.1.

Table 5.1 Sedimentation velocities of mud fractions.

Mud fraction	Sedimentation velocity [mm/s]
IM1 (micro flocs)	0.125
IM2 (macro flocs)	1.000
IM3 (background concentration)	0.001

5.1.3 Initial conditions bottom layers

The size of the DCSM model domain does not allow a traditional modelling approach, where the initial simulation starts with a (near) empty bed and spins-up towards equilibrium by influx from sediment from the boundaries, because of the extensive computational costs. The model boundaries are situated in deep water (some segments at over 1 km depth), which makes it very unlikely that sediments entering at the boundaries end up in the area of interest, the North Sea. In this case, the initial sediment availability in the bed becomes of great importance, together with the sediment influx from the rivers.

The initial mud availability in the buffer layer (S2) is based on mud percentages by Bockelmann (2018). These percentages are converted to mass using a porosity of 0.4 and a layer thickness of 10 cm. This dataset does cover the entire area of interest but does not cover the full model domain of DCSM. For the remaining area, the mud percentage is derived using a regression model that is based on mud percentages of Bockelmann (2018) and nearest corresponding depths from DCSM. The distribution of the available mud mass in the buffer layer between the sediment fractions (

Table 5.1) is based on the fraction distribution in the bed of ZUNO-DD. Initially, the easily erodible so-called fluffy layer is empty, as the mass in the fluffy layer is relatively small compared to the buffer layer. Spin-up simulations are performed with a coarser model grid (4nm) to reduce computational times. In total 5 spin-up years were calculated, before any wind park scenarios were modelled.

5.1.4 Initial conditions water column

The initial sediment concentration in the water column is based on yearly average near surface concentrations derived from satellite imagery of the year 2007 (Silva, 2016). The distribution between the mud fractions is based on ZUNO-DD.

5.1.5 Boundary conditions

Sediment influx is prescribed at the open boundaries and at discharge points, e.g. rivers and sluices. The sediment concentration at the open boundaries is set at 0.1 mg/L for all mud fractions.

The model contains almost 1000 discharges. For the most relevant rivers and sluices the sediment concentration is prescribed based on ZUNO-DD and expert judgement (Table 5.2). For the remaining discharges the sediment concentration for fractions IM1 and IM2 is set to 5 mg/L.

Additional sediment loads are added to account for structural erosion at some parts of the coast within the area of interest (Table 5.3). The sediment load (in mass) is determined by multiplication of the sediment concentration with a constant discharge rate of 1 m³/s. The location and total added mass of the loads is equal to the settings of ZUNO-DD.

Table 5.2 Sediment concentrations per fraction (see Table 5.1) at discharges.

Name	IM1 [mg/L]	IM2 [mg/L]	IM3 [mg/L]
Meuse	4.6	4.6	0.0
Rhine	14.5	14.5	0.0
Scheldt	35	35	0.0
Den Oever	14	14	0.0
Kornwerderzand	14	14	0.0
IJmuiden	5	5	0.0
Clevering	10	10	0.0
Eems	10.8	10.8	0.0
Weser	19.7	19.7	0.0
Elbe	18.2	18.2	0.0
Humber	8.4	8.4	0.0
Tees	21.9	21.9	0.0
Seine	15.8	15.8	0.0
Loire	30.0	30.0	0.0
Gironde	20.0	20.0	0.0
Severn	10.0	10.0	0.0
Thames	10.0	10.0	0.0
Others	5.0	5.0	0.0

Table 5.3 Additional sediment loads.

Name	IM1 [mg/L]	IM2 [mg/L]	IM3 [mg/L]
Holderness	4.12E04	4.12E04	0.0
Norfolk	6.35E04	6.35E04	0.0
Suffolk	5.07E04	5.07E04	0.0
English Channel	3.17E04	3.17E04	0.0
Vlaamse Banken	3.17E04	3.17E04	0.0

5.2 Fine sediment model validation

As most applications so far have been within a short distance from the Dutch coastline, model validation has been focused on the first 10 km offshore. With projected wind farm reaching further out offshore, also model validation should focus more on offshore areas. Points of attention are the reproduction of the East Anglia plume, seasonal SPM dynamics and the observed correlation of inter-annual SPM variations on a large spatial scale. Because of the larger depth and the smaller influence of salinity gradients offshore, it is expected that ROFI dynamics and water-bed exchange are less dominant and the effect of temperature gradients and water column processes more important. Additional points of attention are the longshore sediment flux along the Dutch coast, the sediment residence time in the seabed (steered by the thickness of the buffer layer and the intensity of water-bed exchange) and the adaptation of the initial bed composition towards dynamic equilibrium.

The fine sediment model is calibrated using data from:

- MWTL stations (low frequency, multi-year)
- CEFAS smart buoys (high frequency, multi-year)
- CEFAS spatial multi-year monthly average near surface SPM (1998-2015)

The validation of the fine sediment model builds upon the validation of the hydrodynamic and wave models, as mixing, residual flows and current- and wave-induced bed shear stress are very important input parameters for the SPM model.

5.2.1 Comparison with MWTL stations

The MWTL stations are measurement locations where roughly 20 times a year near surface sediment concentrations are measured at set cross-shore distances. Also, data gathered in other years than 2007 are used for comparison, due to the limited amount of data gathered per year. Time series of two example locations are presented in Figure 5.1. The measurements indicate that the concentration in 2007 was slightly lower in comparison to the multi-year average. The average suspended sediment concentrations are reproduced to a satisfactory degree, although deviations can be observed. For example, periods of higher sediment concentrations at NOORDWK70 are underestimated. In addition, the lower values (5 percentile) at TERSLG100 seemed too low, while the higher values are too high (95 percentile). With exception of the underestimation of the lower values at TERSGL100/235, the model simulated SPM values within a factor 2 (Table 5.4).

Table 5.4 SPM comparison with MWTL stations.

MWTL Station	SPM 2004- 2017			SPM DCSM	
	N	50%ile	(5%ile / 95%ile)	50%ile	(5%ile/95%ile)
NOORDWK10	297	4.3	(2 / 15.6)	5.5	(2.5 / 18.8)
NOORDWK20	242	3.8	(1.6 / 16.3)	3.2	(1.3 / 12.2)
NOORDWK70	241	2.9	(1.4 / 14.5)	2.4	(1.5 / 4.9)
TERSLG100	175	1.9	(0.9 / 3.2)	1.3	(0.2 / 7.7)
TERSLG235	114	2	(1.1 / 6.8)	0.9	(0.1 / 5.6)

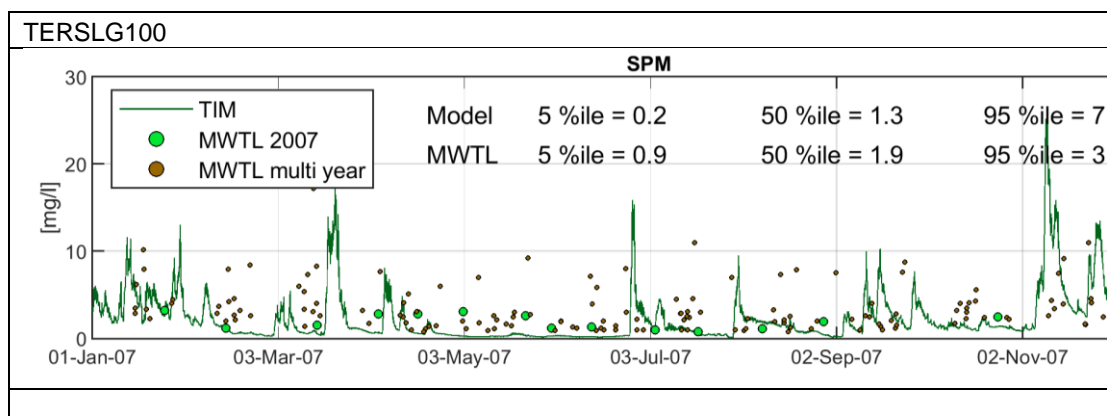
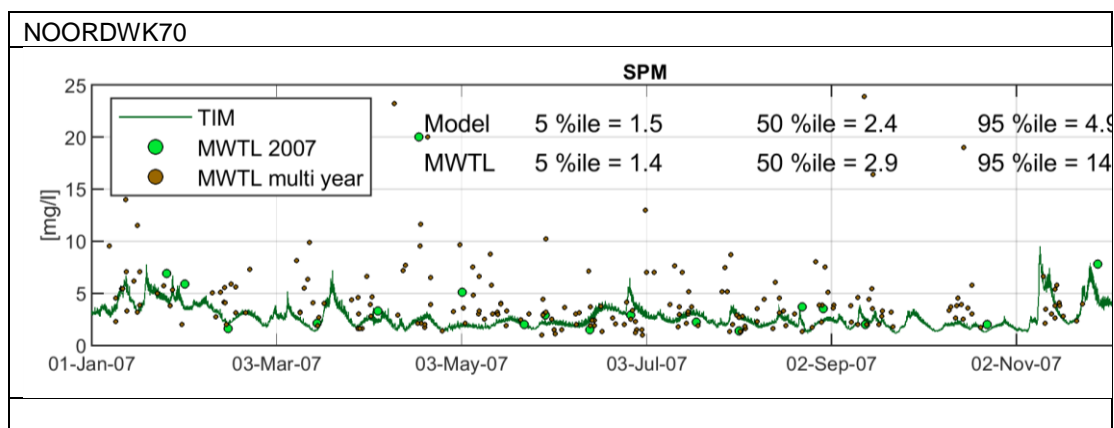


Figure 5.1 Time series of calculated near surface SPM and MWTL data 2007 (large green dots) and MWTL multi-year data (small brown dots). Top: NOORDWK70. Bottom: TERSLG100.

5.2.2 Comparison with CEFAS smart buoys

The Centre for Environment, Fisheries and Aquaculture Science (CEFAS) collects near surface SPM data at various locations in the coastal waters around the UK using smart buoys. Opposite to the MWTL measurements, the CEFAS smart buoys collect high frequency measurements. This allows for validation of modelled SPM values during more energetic conditions, that are normally not represented in the MWTL data. In Figure 5.2 the time series for 2007 are presented for two smart buoys locations (map of the locations can be found in Appendix B.2). These smart buoys are selected due to their location in the area of interest and the different hydrodynamic forcing at Oyster Ground and West Gabbard.

At Oyster Grounds the bed shear stress is relatively low during daily conditions. Therefore, at this location typical peaks in SPM can be observed during more energetic (wave) conditions. For the Oyster Grounds the timing and the pattern of the peaks is quite well represented, however the modelled magnitude often exceeds the measured values. During daily and low energetic conditions, the modelled SPM underestimates the near surface sediment concentration.

The hydrodynamic conditions, and thus the bed shear stresses, at West Gabbard are dominated by strong currents. This implies that a clear pattern of calm period and storm events is absent. The SPM signal at this location shows intra tidal variation and seasonal dynamics. Both effects are to some extent captured by the model and the yearly average SPM concentration matches to a satisfactory degree. However, the modelled SPM signal is somewhat flattened and thus less dynamic.

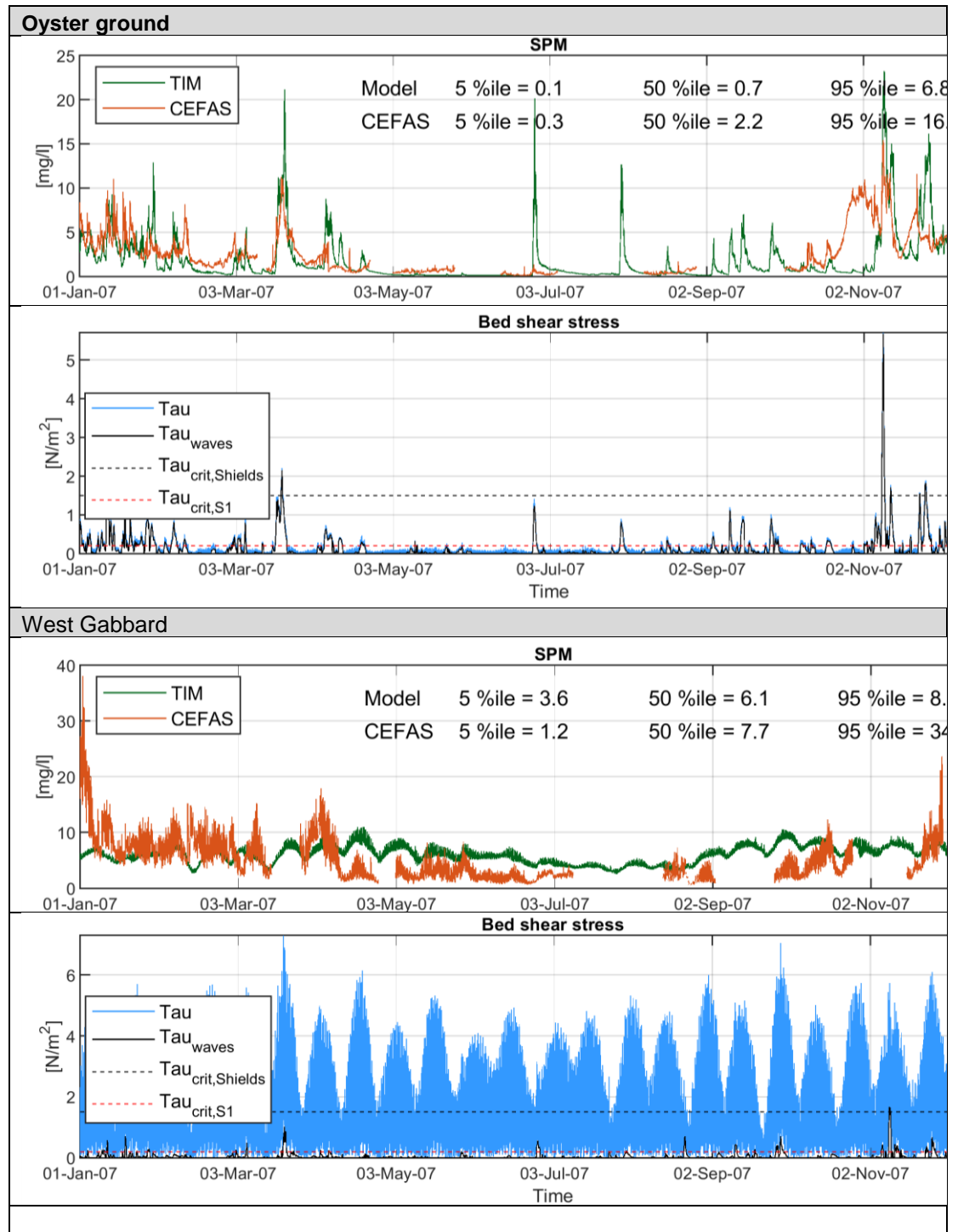


Figure 5.2 Time series of modelled near surface SPM compared with CEFAS smart buoy data at Oyster ground (Top) and West Gabbard (Bottom).

5.2.3 Spatial distribution of monthly average SPM

The modelled spatial distribution of near surface SPM is compared to CEFAS EO imagery (Silva, 2016) (Figure 5.3). In the North Sea the overall spatial patterns are quite well reproduced, especially in the summer (Figure 5.4), e.g. the East Anglia Plume. Areas associated with higher sediment concentrations such as Vlaamse Banken, mouth of the Scheldt, Suffolk and the Ems match quite well. Although the model reproduced the overall patterns, the magnitude of SPM is overall underestimated. Logically, this effect is more clearly observed in periods during which higher SPM values occur, e.g. in the winter months. In these periods an underestimation of over 10 mg/L is observed near the coast. Further offshore the bias decreased in absolute sense, however in relative sense the near surface SPM was underestimated with approximately a factor 2 – 3. An overview of the results for other selected months is attached in Appendix B.3. These observations indicate that the model represents the spatial patterns relatively well, but that the fine sediment model is not yet sufficiently calibrated to accurately simulate SPM values. For this reason, in the next chapter the impact of wind farms on fine sediment dynamics is expressed relative to the reference simulation.

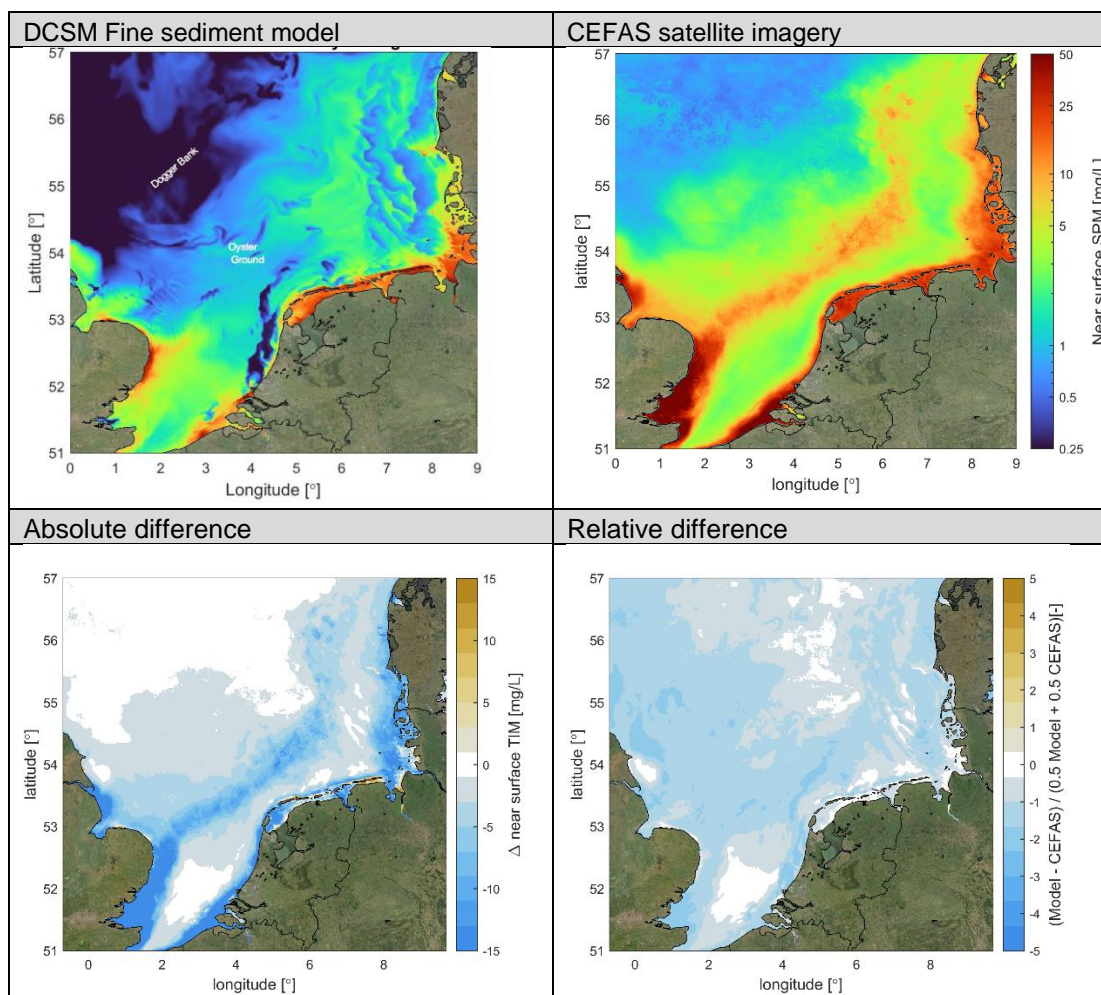


Figure 5.3 Modelled spatial distribution near surface SPM versus CEFAS EO data year 2007.

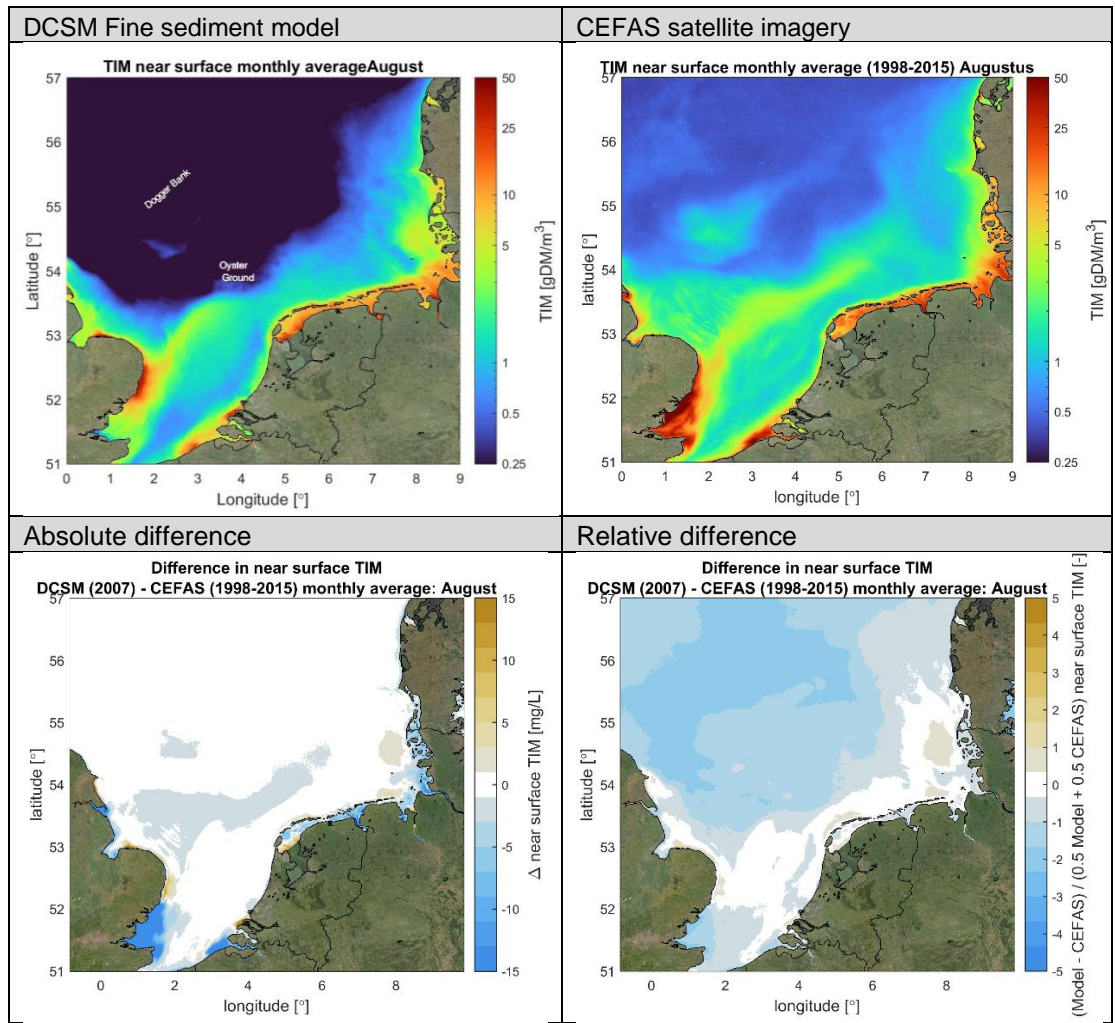


Figure 5.4 Modelled spatial distribution near surface SPM versus CEFAS EO data month August.

5.3 Results and discussion

In Chapter 4.2 of Boon et al. (2018) potential effects of wind farms on SPM dynamics were discussed. A qualitative description of the effects was given, but a quantitative description was not yet possible as results from numerical simulations were not yet available. Quantitative evaluation is not straightforward, as both mechanisms that may enhance and mechanisms that may reduce sea surface concentration (SSC) levels were identified, and it is not obvious which mechanisms will dominate. Fortunately, results from numerical simulations have become available, so quantitative assessment is now possible. Without repeating the analysis in Boon et al. (2018) herein, it is recapped that the main driving forces for changes in SSC are:

- changes in bed shear stress that may shift the balance between deposition and resuspension,
- changes in vertical mixing or settling velocity that may change the vertical gradient in SSC, and
- changes in residual flow that may change horizontal SPM transport and SSC levels in some regions.

These processes are schematised in Figure 5.5 (a copy of Figure 4.2 in Boon et al., 2018).

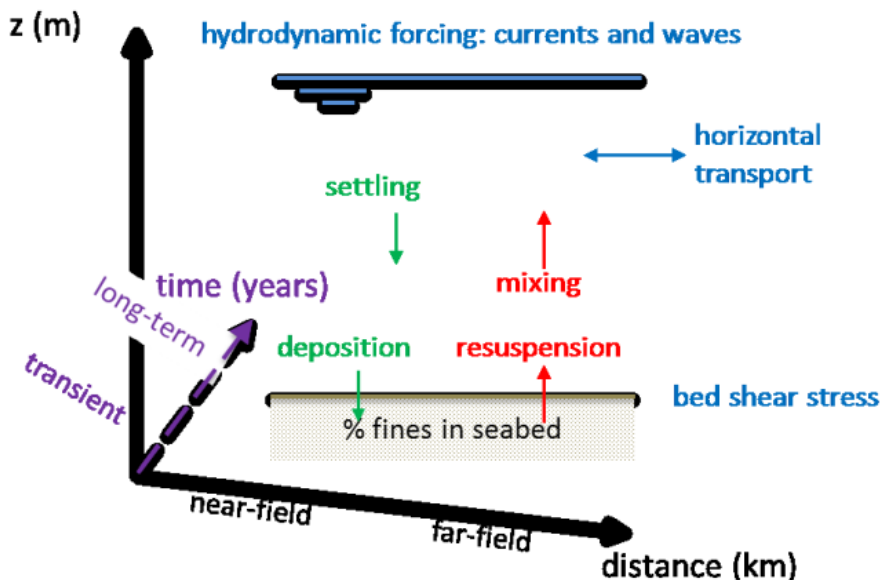


Figure 5.5: Illustration of processes important for fine sediment transport within space and time.

Based on the results from the numerical model, we will now discuss how these processes are affected by the construction of wind farms in a quantitative way. First, results based on average hydrodynamic forcing are discussed, both at the local scale of a single wind farm and at the large scale for the cumulative effect of multiple wind farms. Second, the sensitivity of the results on hydrodynamic forcing are discussed. Are the wind farm effects on SPM dynamics persistent, or are they larger in some conditions than in other conditions? This is examined for seasonal dynamics in temperature and salinity stratification, wave-induced resuspension and the influence of wind speeds and direction on residual transport. Third, the sensitivity of wind farm effect to location is discussed. At some locations the same wind farm may have a larger effect than at other locations, e.g. dependent on local water depth, tidal current velocity and mixing.

5.3.1 Results based on year-average hydrodynamic forcing

As the baseline scenario still shows a substantial bias (see discussion above), results are discussed in relative sense, i.e. the percentage change in SSC levels of the wind farm scenarios with respect to the baseline scenario. In addition to the baseline scenario, wind farm scenarios are simulated using 2020 (current) and 2050 (possible future) wind farm configurations. For these simulations the meteorological data, river run-offs etc. of the years 2007 and 2008 are used as basis (in line with the hydrodynamic model approach described in Chapter 3). Results are discussed for the hydrodynamic year 2007 only. Computations for 2008 were also made but are not shown herein, as relative impacts show only minor differences between 2007 and 2008.

Small-scale effects

Effects of wind farms on SSC may be caused by the combination of three effects:

- the amount of SSC may change
- the composition of SSC may change
- the vertical distribution of SSC may change

Bed shear stress determines deposition and resuspension. The balance between deposition and resuspension determines whether a wind farm acts as a net sediment sink or net sediment source. Vertical mixing is determined by a combination of bed shear stress, turbulence around the piles and wind stress at the water surface. The vertical distribution of SSC may change caused by changes in both vertical mixing and settling velocity (hence sediment composition).

To understand the changes in SSC, we first have to understand the changes in bed shear stress and vertical mixing. The latter were already discussed in the hydrodynamics section. Here it suffices to remind the reader that at most locations wind farms result in increased mixing and reduced temperature and salinity stratification. In principle the same is expected for SPM, with lower near-bed SSC and higher surface SSC if neither the amount nor the composition of SPM in the wind farm areas would change.

Regarding bed shear stress, Figure 5.6 shows that the average bed shear stress decreases along the Dutch, German and Danish coast, both within wind farms and around them. Therefore, although the vertical concentration gradients in the water column may become smaller, the local balance between deposition and resuspension will shift more towards deposition, hence reducing the SSC and increasing the availability of fines in and on the seabed. Near the bed, SSC will decrease for two reasons, i.e. both enhanced vertical mixing and reduced resuspension. Near the surface both effects act in opposite direction on SSC: enhanced mixing implies increased SSC, whereas reduced resuspension implies reduced SSC.

A lower bed shear stress can be explained by the friction around the wind turbine piles. A (small) part of the energy that without wind farms is dissipated by bed friction becomes dissipated by pile friction with wind farms. This results in slightly lower bed shear stress. The bed shear stress is not reduced everywhere. At some locations, the bed shear stress is increased inside wind farm areas. This is most prominent for the wind farms along the English and French coast. An explanation for higher bed shear stress is the possible steepening of the velocity profile within wind farms by enhanced turbulence and momentum transfer. This may result in steeper near-bed velocity gradients and hence higher bed shear stress. This effect is most prominent for wind farms in regions with limited stratification.

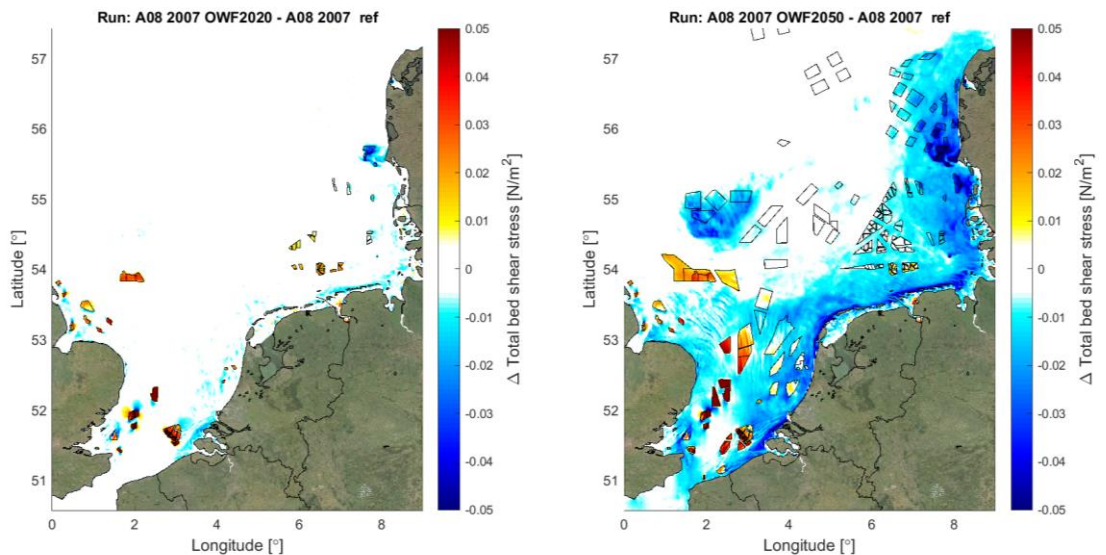


Figure 5.6: Change in year-average bed shear stress (2007) for scenarios OWF2020 (left) and OWF2050 (right) with respect to reference scenario.

With regard to SSC model results, surface SSC increases with about 10-20% at most locations within the wind farms (see Figure 5.7). This is in contrast with near-bed SSC, which decreases with 5-15% at most (but not all) locations (Figure 5.8). Sediment stratification therefore becomes weaker within the wind farms, due to additional mixing by turbulence generated around the piles. This is consistent with temperature and salinity stratification, which show a substantial decrease (see previous chapter on hydrodynamic results).

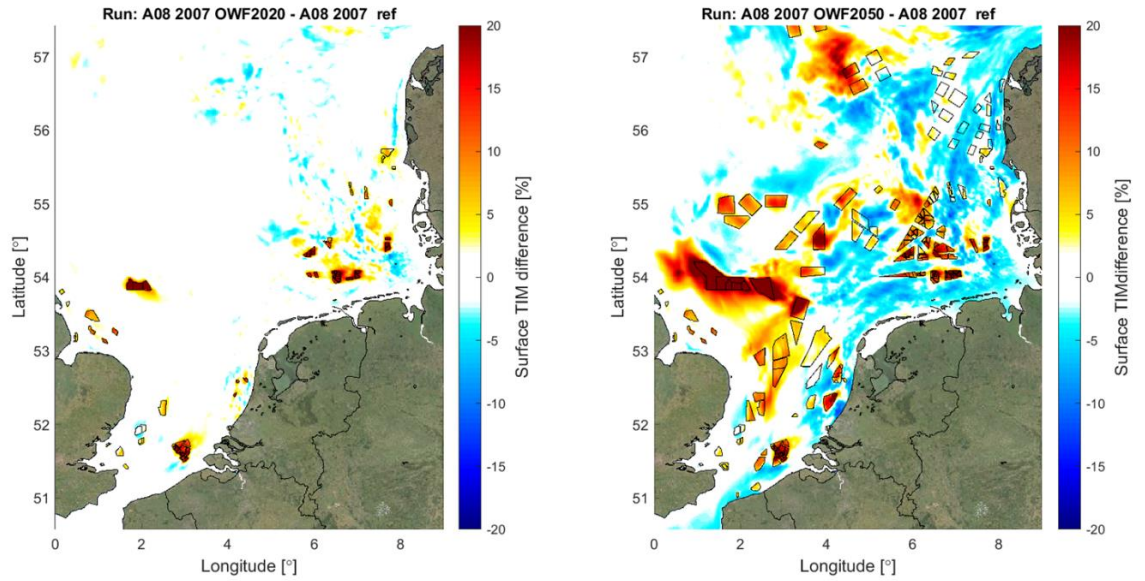


Figure 5.7: Change in year-average surface SSC (2007) for scenarios OWF 2020 (left) and OWF2050 (right) with respect to reference scenario. Resolution 0.5nm.

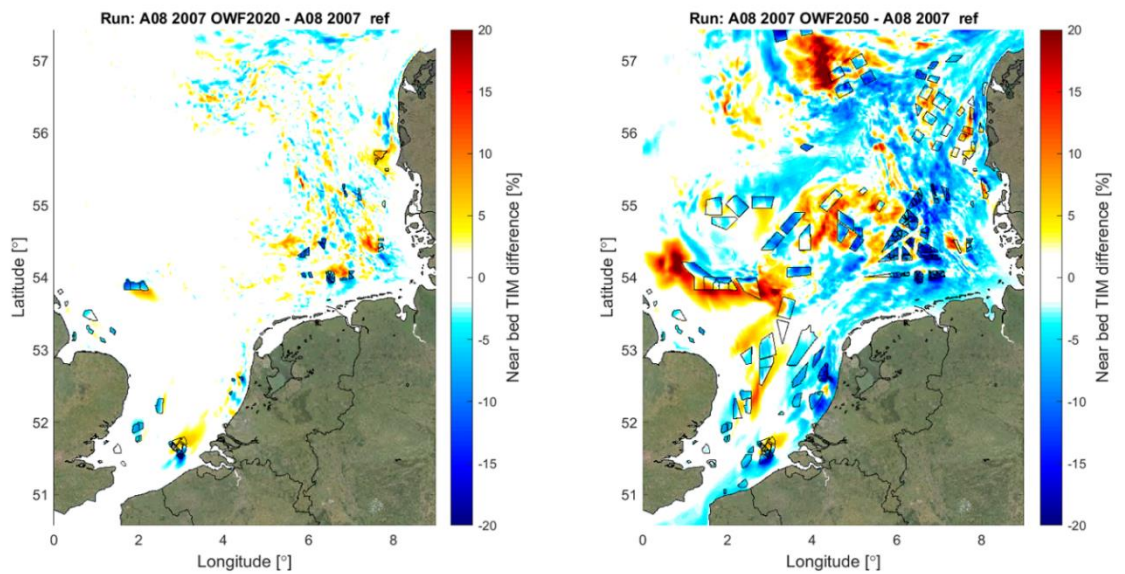


Figure 5.8: Change in year-average near-bed SSC (2007) for scenarios OWF 2020 (left) and OWF2050 (right) with respect to reference scenario. Resolution 0.5nm.

5.3.2 Large-scale effects

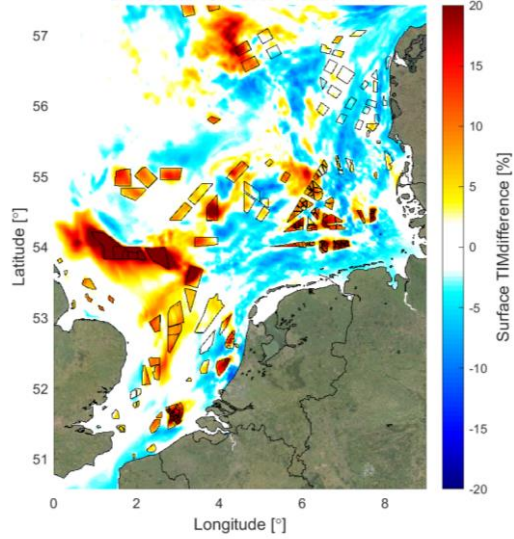
At the scale of the Dutch near-coastal zone a clear net effect occurs for the OWF2050 scenario. Near the surface, SSC decreases with about 5% outside wind farms, but increases with about 5% inside wind farms. More to the north and east the decrease outside wind farms becomes weaker, whereas the increase inside wind farms becomes more prominent (see right panel of Figure 5.7).

Near the bed the effects are different from those near the surface. A decrease in SSC of 5-10% is computed within the Dutch near-coastal zone and the German Bight, both inside and outside wind farms. More to the NE, this decrease becomes less prominent and also zones with 5-10% increase are computed (see right panel of Figure 5.8).

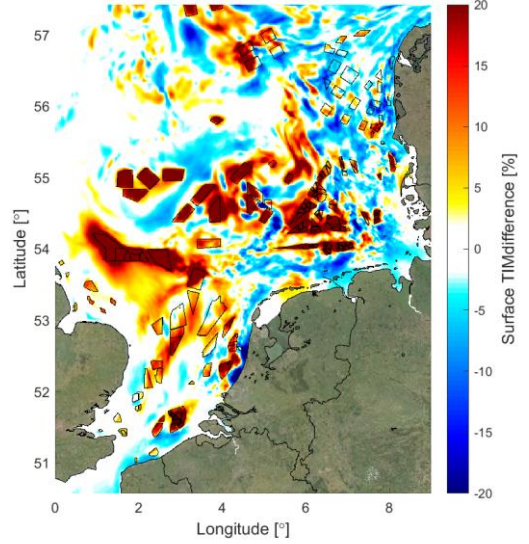
5.3.3 Seasonality

Figure 5.9 and Figure 5.10 show the seasonal-average effects for the near-surface and near-bed SSC. Effects on near-surface SSC show a distinct seasonality, with a larger increase in the summer period (March – June and notably June – September) within and in a large area around the wind farms in the Central North Sea. This is an area that experiences temperature stratification in summer. The seasonality in near-bed SSC changes is much weaker, notably in stratified areas. Note that these results are shown on the 4nm grid instead of the 0.5nm grid as for the year-average results.

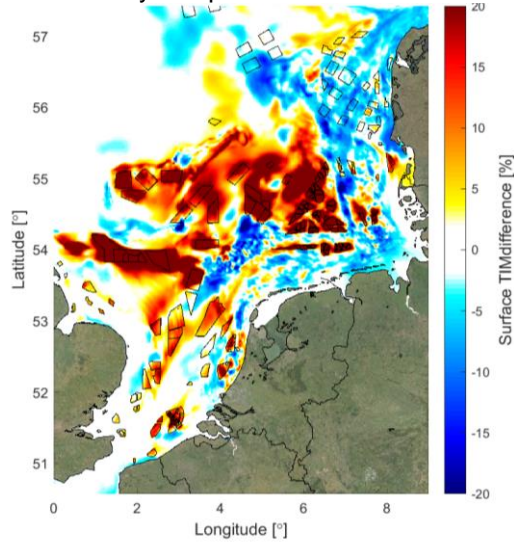
A. 2007 (full year)



B. 2007 March - June



C. 2007 July - September



D. 2007 September - December

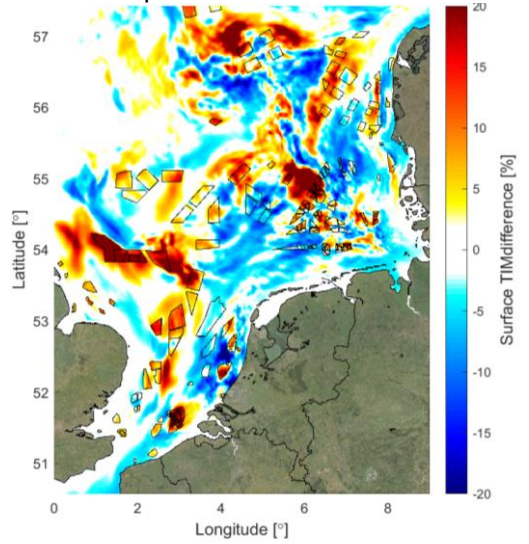


Figure 5.9 Change in seasonal-average surface SSC (2007) for scenario OWF 2020 with respect to reference scenario. a) full year 2007 b) March – June c) June – September d) September – December.

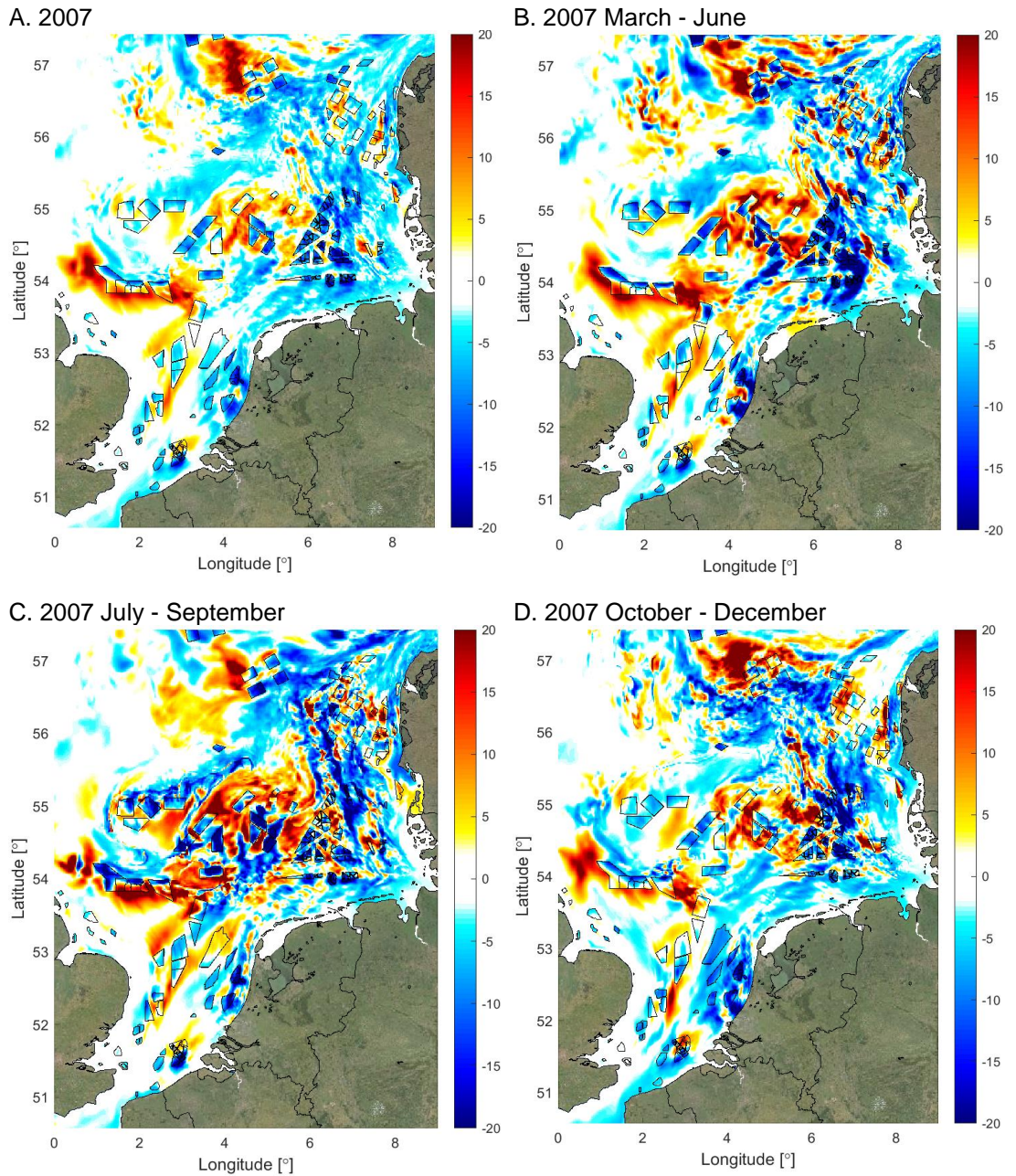


Figure 5.10 Change in seasonal-average near-bed SSC (2007) for scenario OWF 2020 with respect to reference scenario. a) full year 2007 b) March – June c) June – September d) September – December.

5.3.4 Longshore SPM fluxes

Figure 5.11 shows the relative changes in residual SPM flux through a number of transects perpendicular to the Dutch coastline. Changes for the OWF2020 scenario remain <1% for most transects. For the Walcheren transect a 2% reduction is computed. Changes for the OWF2050 are larger, with a 10% decrease of the residual flux through the Texel transect. This reduction is consistent with the computed reduction in nearshore SSC.

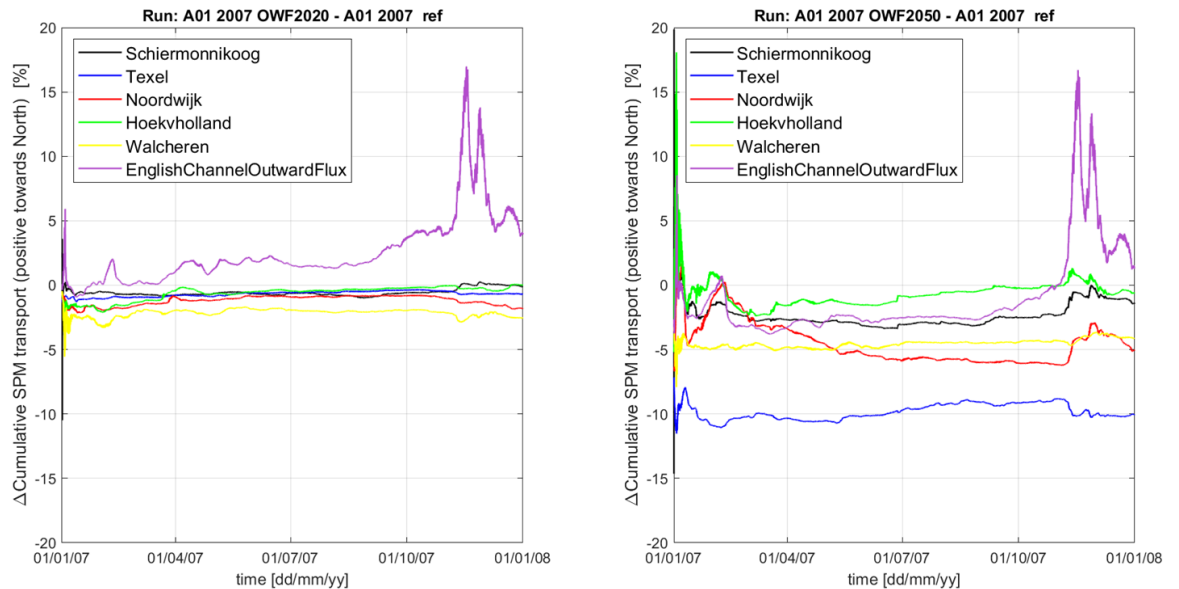


Figure 5.11: Longshore residual SPM fluxes at some cross-sections along the Dutch coast (2007) for scenarios OWF 2020 (left) and OWF2050 (right) with respect to reference scenario. Location of transects can be found in Appendix B.3.

5.4 Conclusions

Based on the comparison between scenarios OWF2020 and OWF2050 with respect to the reference scenario, the following conclusions are drawn:

- Changes in SSC are caused by both changes in bed shear stress and vertical mixing.
- Higher vertical mixing caused by wind farms reduces near-bed SSC and enhances surface SSC.
- Reduced bed shear stress caused by wind farms reduces both near-bed and surface SSC. The combined effect of both is a 10-20% increase in surface SSC within wind farms and a 5-15% decrease in near-bed SSC for scenario OWF2050.
- For scenario OWF2020 the changes are substantially smaller and more confined to the wind farm areas themselves.
- Scenario OWF2050 does show large-scale effects beyond the scale of individual wind farms. In the Dutch coastal zone and German Bight, SSC decreases with about 5% over a large area. Also, the longshore SSC flux is reduced with up to 10% near Texel, which may influence fine sediment transport towards the Wadden Sea.
- Effects of scenario OWF2050 on SSC are of the same order of magnitude as some present large-scale interventions such as MV2, sand mining and the release of dredged material. It is recommended to investigate the interaction between these effects.
- Effects in SSC in the Rhine ROFI or farther in northern or eastern direction differ. Within the ROFI, overall surface SSC decrease is computed, whereas farther NE, both areas with increasing and decreasing SSC occur.
- Although the computed effects on SSC are persistent over the year, effects on surface SSC are more prominent in summer than in winter. The effect on near-bed SSC varies less over the year.

These scenario results are used for ecological computations as discussed in the next chapter.

6 Water quality and ecological model

6.1 Model set-up

6.1.1 Introduction 3D DCSM-FM Water Quality

Water quality processes are simulated using the D-Water Quality module (successor of Delft3D-WAQ, a.k.a. DELWAQ). It is here fully integrated with D-Flow FM. This ensures a better consistency between simulated processes, the transport of water quality constituents for example being calculated within D-Flow FM, in the same way as that of water masses, salt and temperature. Furthermore, in its “integrated, simultaneously running” version, D-Water Quality benefits from computation developments from DFlow-FM, such as parallelization capabilities.

6.1.2 Simulated variables and processes

As its first fully-integrated application within 3D DCSM-FM, the D-Water Quality module was setup based on the processes and their parameterization in the GEM model (Blauw et al., 2009), which has been applied in earlier ecosystem projects focused on the North and Wadden seas, such as the “MER zandwinning Noordzee” project for Rijkwaterstaat (Deltares, 2017). The only change in setup with respect to the “MER zandwinning” model concerns the accumulation of particulate matter on the seabed. This is now modelled using a net sedimentation rate, while it used to be calculated as the result of sedimentation and re-suspension processes. This choice was made to avoid overestimating re-suspension at offshore locations, where the bottom shear stress in 3D DCSM-FM is higher than estimated by the “MER zandwinning” model. Accumulation processes should most likely be recalibrated once the sediment and water quality modules can be fully coupled. The substances included in the model are listed in Table 6.1.

Table 6.1: Description of simulated water quality state variables.

Model state variable	Description	Unit	Active*
OXY	Dissolved oxygen	mg/L	✓
NH4	Ammonium	mgN/L	✓
NO3	Nitrate	mgN/L	✓
PO4	Phosphate	mgP/L	✓
Si	Silica	mgSi/L	✓
Opal	Biogenic silica	mgSi/L	✓
POC	Particulate Organic Carbon	mgC/L	✓
PON	Particulate Organic Nitrogen	mgN/L	✓
POP	Particulate Organic Phosphorus	mgP/L	✓
DIAT_X, DINO_X, FLAG_X, Phae_X (X=E, N, P)	Diatoms, dinoflagellates, flagellates and <i>Phaeocystis</i> (energy-, nitrogen- and phosphorus-limited)	mgC/L	✓
DetCS	Detrital carbon in sediment layer	gC/m ²	
DetNS	Detrital nitrogen in sediment layer	gN/m ²	
DetPS	Detrital phosphorus in sediment layer	gP/m ²	
DetSiS	Detrital silica in sediment layer	gSi/m ²	
Mussel_V	Structural biomass of mussels	gC/m ²	
Mussel_E	Energy reserves of mussels	gC/m ²	
Mussel_R	Reproductive biomass of mussels	gC/m ²	
Ensis_V	Structural biomass of <i>Ensis</i>	gC/m ²	
Ensis_E	Energy reserves of <i>Ensis</i>	gC/m ²	
Ensis_R	Reproductive biomass of <i>Ensis</i>	gC/m ²	

* “Active substances” are those that can be transported by advection/diffusion processes

The water quality model simulates the cycles of major nutrients (nitrogen, phosphorus and silica, herein noted N, P and Si), organic carbon and dissolved oxygen (O₂). Simulated processes comprise (Figure 6.1):

- Phytoplankton photosynthesis and associated uptake of nutrients and O₂ production that depend on the light climate (extinction);
- Phytoplankton respiration and mortality resulting in the release of nutrients and the consumption of O₂;
- Metabolism of grazers (blue mussels and *Ensis*)
- Mineralization of organic matter in the water column and in the sediment and associated O₂ consumption;
- Dissolution of biogenic silica in the water column and in the sediment;
- Settling of organic matter and phytoplankton and burial of detrital organic matter;
- Nitrification;
- Denitrification in the water column and in the sediment;
- Atmospheric deposition of NH₄ and NO₃;
- Oxygen re-aeration at the water surface.

Process representations are selected from the D-Water Quality Process Library (Deltares, 2020).

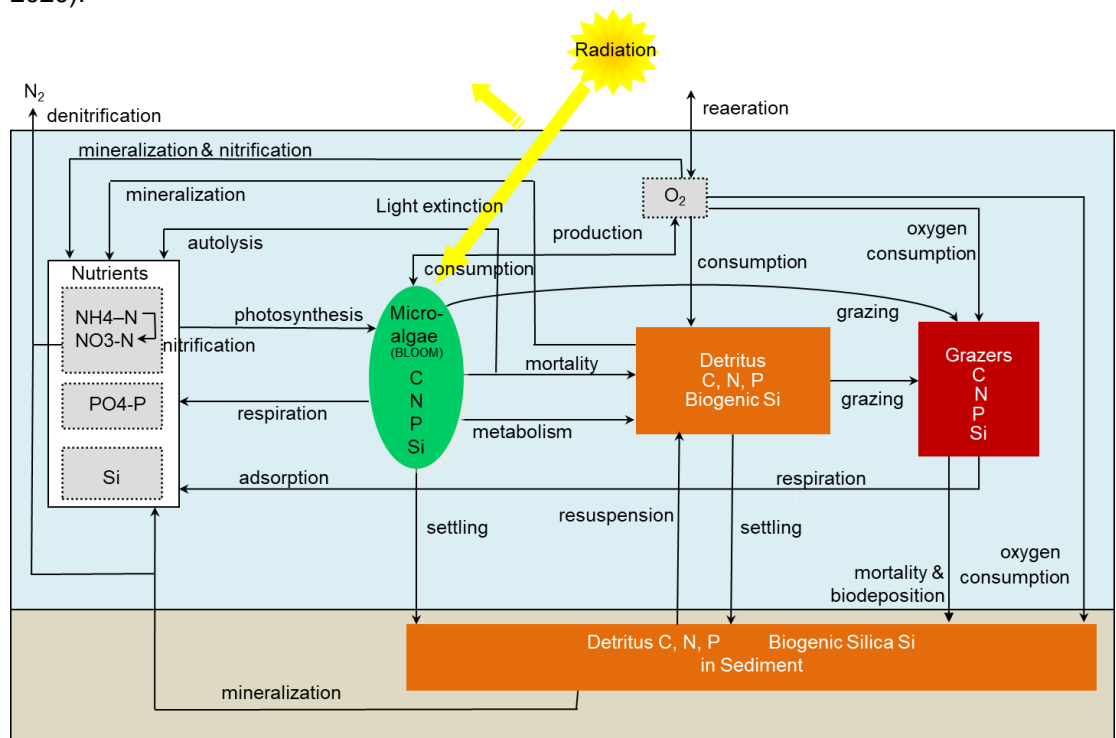


Figure 6.1 Scheme of variables and processes simulated within the WOZEP project.

Phytoplankton dynamics (primary production, respiration and mortality) are simulated using the BLOOM module (Los, 1988; 2008). BLOOM represents competition and adaptation of phytoplankton to nutrient or light-limiting conditions. Here, four species groups are simulated: marine diatoms, flagellates, dinoflagellates and *Phaeocystis*. For each of these groups, three ecotypes are defined to account for adaptation to changing environmental conditions:

- an energy type (“_E”), with relatively high growth rate, low mortality rate and high N:C and P:C ratio, and higher chlorophyll content;
- a nitrogen type (“_N”), with typically lower internal N:C ratio, lower maximum growth rate, higher mortality rate, higher settling velocity and lower chlorophyll-a content;
- a phosphorus type (“_P”), similar to the nitrogen type with typically lower internal P:C ratio.

BLOOM assumes that fast-growing phytoplankton (energy type) dominate in situations where light and nutrient resources are abundant, while slow-growing, efficient phytoplankton species become dominant when resources become limited (Blauw et al., 2009).

Species composition is calculated using linear programming to maximize the total net production of the whole phytoplankton community, depending on the prevailing conditions, and therefore does not require any initialization or boundary conditions for the simulated phytoplankton.

Grazer dynamics are simulated with the DEBGRZ module (Troost, 2010). DEBGRZ is based on the Dynamic Energy Budget (DEB) theory (Kooijman, 2010). The DEB theory describes the uptake and use of energy and nutrients and the consequences for physiological organization throughout an organism's life cycle. In the present model, DEBGRZ is used to model blue mussel banks in the Wadden Sea and *Ensis* in the North Sea, as done in the "MER zandwinning" project. For each of these species, biomass is divided into three pools: the structural biomass (Mussel_V and Ensis_V), energy reserves (Mussel_E and Ensis_E) and gonadal biomass (Mussel_R and Ensis_R), used for reproduction once the organisms reached their maturity. Mussels and *Ensis* are represented as whole populations, assuming their size distributions remain constant (V1-morph approach). The same module is used for the simulation of blue mussels on wind turbine pillars. This is described in more detail in 6.1.7 (p. 60).

As developments for the fine sediment modelling and ecological modelling were carried out simultaneously, these could not be fully coupled at this stage. To account for the effect of inorganic suspended sediments on light climate in the ecological model, we use the weekly sediment field from the "MER zandwinning" project (representative of the year 2007). The use of 3D time-varying forcing fields is not yet possible within D-Water Quality. Since primary production in the North Sea mostly occurs close to the water surface, top layer concentrations were applied to the entire water column.

All processes are calculated at a 10 min time step, except for those related to the BLOOM module that has a daily time step.

6.1.3 Open boundaries

Concentrations of the active water quality constituents at the open ocean boundaries are derived from the CMEMS monthly global ocean biogeochemistry hindcast product (GLOBAL_REANALYSIS_BIO_001_029). This product provides 3D biogeochemical fields at a ¼-degree horizontal resolution, and on 75 vertical levels. These fields include concentrations of dissolved oxygen (CMEMS_OXY), nitrate (CMEMS_NO3), orthophosphate (CMEMS_PO4), silica (CMEMS_Si) and carbon in phytoplankton (CMEMS_PHYC). CMEMS_PHYC is used as a proxy for the concentrations of different organic state variables (Table 6.2). NH4 concentrations at the boundary are set to zero. We assume that inorganic N mostly occurs as NO3 in the open ocean, and that the speciation between NH4 and NO3 in the study area is the result of biogeochemical processes.

Table 6.2: Equations used to convert CMEMS data to model state variables at the open boundaries.

Model state variable	Conversion from CMEMS data (CMEMS variables in $\mu\text{mol/L}$)
OXY	CMEMS_OXY \times 32/1000
NH4	0.
NO3	CMEMS_NO3 \times 14/1000
PO4	CMEMS_PO4 \times 31/1000
Si	CMEMS_Si \times 28/1000
Opal	CMEMS_PHYC \times (28/12) \times 0.5 \times 0.13 ^a
POC	CMEMS_PHYC \times 2 \times 12/1000 ^b
PON	POC \times (14/12) / 106 ^c
POP	POC \times (31/12) / 106 ^c
DIAT_X, DINO_X, FLAG_X, Phae_X (X=E, N, P)	0.

^a Using the C:Si ratio for diatoms from Brzezinski (1985) and assuming that half of the phytoplankton carbon biomass is constituted by diatoms.

^b Assuming a carbon detritus to algae ratio of 2.

^c Using the molar Redfield C:N:P ratio 106:16:1 (Redfield, 1934).

6.1.4 Freshwater discharges

As for the hydrodynamics, water quality constituents' concentrations in freshwater discharges are represented with monthly means of E-HYPE model outputs from the Swedish meteorological institute (SMHI), adjusted with country correction factors to be consistent with national measured total N and P loads. EHYPE provides concentrations of inorganic and organic N (IN and ON) and dissolved and particulate P (DP and PP). We assume that 10% of the IN is NH₄ and 90% is NO₃. O₂ is fixed to 8 mg/L, and Si to 2.6 mg/L in all river inflows.

The largest Dutch and German rivers are described using daily concentrations of NH₄, NO₃, PO₄, Si, total N (TN) and total P (TP) from Pätsch and Lenhart (2019). For these inflows, O₂ is fixed to 8 mg/L, PON is calculated as TN-(NH₄+NO₃), POP as TP-PO₄, and POC as 12. \times PON (see Table 6.2 for explanations).

6.1.5 Other forcings

Daily surface radiation

The BLOOM module, computed at a 24 h time step, uses daily radiation as an input, and can therefore not use the higher-frequency 3D radiation field from the hydrodynamics module. The daily solar surface radiation used for the simulation of light extinction in D-Water Quality is forced as spatially homogeneous time series, calculated from the hourly ERA5 field at the centre of the model domain (latitude = 52.5, longitude = 4.0).

Atmospheric deposition

Atmospheric deposition is included in the model as an extra source of dissolved IN. Deposition rate is forced using the 2017 total (wet+dry) deposition fields of reduced nitrogen for NH₄ and oxidized nitrogen for NO₃ from the Norwegian Meteorological Institute (MET Norway). These fields have a 0.1-degree horizontal resolution and were calculated using the EMEP MSC-W chemical transport model (EMEP, 2019; https://emep.int/mscw/mscw_moddata.html).

6.1.6 Simulated period and initial state

The ecological model is run for the year 2007. It is initialized using a one-year spin-up (2006). The 2006 spin-up run is initialized using 3D fields from CMEMS for active constituents (see Table 6.2), and 2D fields from the “MER zandwinning” model for non-transported variables (bottom detritus, mussels and *Ensis*).

For additional model testing, and due to time constraints, a coarse-grid version of the model (4 nautical mile resolution) was also applied, using the same settings as the fine-grid model described herein.

6.1.7 Representation of the effect of windfarms

Effect of changes in hydrodynamics

The changes in hydrodynamics due to the presence of OWFs (related to wind reduction and the presence of piles in the water column) is simulated as described earlier in section 3.1.8

Effect of mussel growth on wind turbine pillars

The effect of the presence of mussel biomass on wind turbine pillars is simulated using the DEBGRZ modules, with the same parameterization as for blue mussels on the coastal seafloor. Therefore, the integrated version of D-Water Quality was adapted to be able to simulate inactive substances (i.e., not affected by transport) at any location in the water column, and not only on the seafloor (i.e., as a 3D field instead of 2D).

According to Krone et al. (2013), who studied epifauna dynamics on pillars in the German Bight, attached mussel biomass shows very little inter-annual variability, but does vary seasonally. The lowest mussel density was observed in spring 2005, with 23 kg/m² of wet weight at 1 m-depth; a maximum density of 45 kg/m² was observed in summer 2007. No offshore sampling was carried out in winter due to weather conditions. In this study, mussels were observed until a depth of 5 m, and constituted less than 1% of the total epifauna biomass in deeper samples, dominated by *Jassa* and Anthozoa communities.

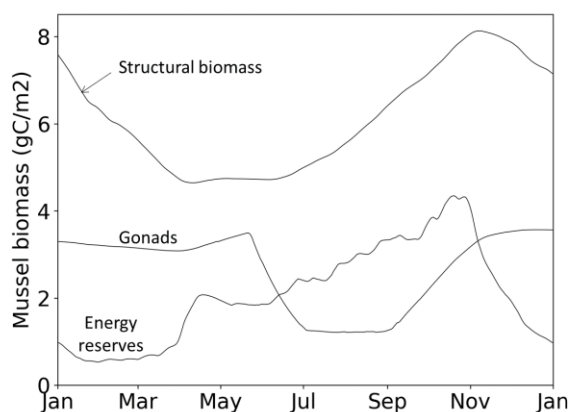


Figure 6.2 Example of simulated bed mussel biomass in one model grid cell of the Wadden Sea in 2007.

Based on this, in scenarios with mussel growth along wind turbine pillars, we assume that mussels are present along the top 5 m of the pillars. Moreover, in areas of the model, where bottom mussel biomass is at equilibrium at an inter-annual time scale (on the Wadden Sea bed), we note that mussel total biomass in winter is close to that simulated in summer (with lower energy reserves but higher gonadal biomass, see Figure 6.2). We therefore initialize these simulations with a biomass of 45 kg/m² of wet weight of total mussel biomass, divided as 10/16 of structural biomass, 5/16 of gonadal biomass and 1/16 of energy reserves.

Effect of disruptions in sediment dynamics

Tests were carried out with the coarse-grid model to have a first assessment of the combined effects of changes in hydrodynamics and sediment dynamics on primary production. Therefore, perturbation of the sea surface inorganic sediment field was calculated using the fine sediment model and applied to the sediment field forcing of the ecological model (Figure 6.3). The calculated 3D DCSM-FM sediment fields were transformed to weekly-means and interpolated to the “MER zandwinning” model grid. The perturbation factor for the OWF2020 and OWF2050 scenarios was calculated as the ratio of surface total inorganic matter concentration calculated in each of the respective OWF scenarios with respect to the surface concentration in the reference run.

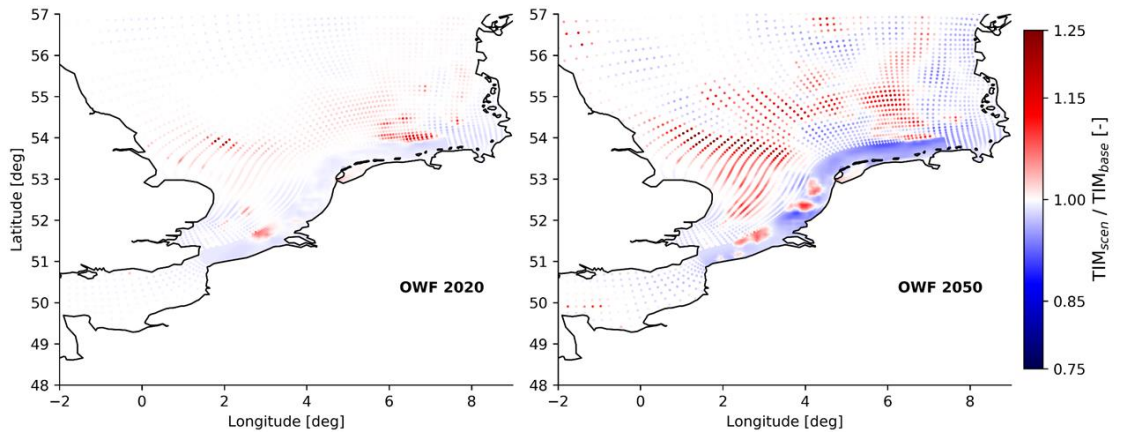


Figure 6.3 Perturbations of the sediment field used for the OWF2020 and OWF2050 scenarios. Red areas indicate where sea surface concentrations were increased in the OWF-2020 and OWF-2050 scenarios and blue indicates where sea surface SPM concentrations were decreased, relative to the reference scenario.

6.1.8 Summary of ecological runs

In total, on top of the 2007 reference simulation, four scenarios were run using the fine-grid ecological model to assess the potential effects of future OWFs on primary production. These simulate the effects of 1) changes in hydrodynamics alone, and 2) changes in hydrodynamics and mussel growth on pillars on primary production for the 2020 and 2050 OWF scenarios. These scenarios were run with the coarse-grid model as well for comparison. Additional runs were carried out with the coarse-grid model to analyze the effects of perturbations in the sediment field due to the presence of OWFs.

All runs are summarized in Table 6.3. Additional runs were carried out with the coarse grid to check reproducibility. This confirmed that two runs using the same restart file give the same results, both using the 2D and 3D options for inactive water quality substances. These are not presented here.

Table 6.3: Description of ecological scenario runs.

Scenario name	Model grid	Description
reference	Fine	No windfarms
OWF2020 hydro	Fine	Hydrodynamic changes due to 2020-scenario windfarms
OWF2020 hydro+mussels	Fine	Hydrodynamic changes + mussel growth on top 5 m of pillars in 2020-scenario windfarms
OWF2050 hydro	Fine	Hydrodynamic changes due to 2050-scenario windfarms
OWF2050 hydro+mussels	Fine	Hydrodynamic changes + mussel growth on top 5 m of pillars in 2050-scenario windfarms
C-reference	Coarse	No windfarms
C-OWF2020 hydro	Coarse	Same as "OWF2020 hydro"
C-OWF2020 hydro+mussels	Coarse	Same as "OWF2020 hydro+mussels"
C-OWF2050 hydro	Coarse	Same as "OWF2050 hydro"
C-OWF2050 hydro+mussels	Coarse	Same as "OWF2050 hydro+mussels"
C-OWF2020 hydro+sed	Coarse	Same as "OWF2020 hydro" with 2020-scenario sediment field perturbation
C-OWF2050 hydro+sed	Coarse	Same as "OWF2050 hydro" with 2050-scenario sediment field perturbation

6.1.9 Computational performance

The fine-grid model scenarios were run on the Cartesius cluster at SURFSara (The Netherlands) to speed up calculation times. Using 256 computation cores, a 1-year simulation took 62.5 to 70.6 hours to run. Additional scenarios were tested using the coarse-grid model. These were run on the Deltares h6 cluster, using 20 computational cores. With this setup, the water quality for one year was computed in 46.2-46.5 h.

6.2 Model validation

6.2.1 Time series comparison

Results from the reference simulation are compared with available monitoring data for the year 2007, to assess the model ability to capture temporal and spatial patterns in relevant water quality variables. This allows for identifying potential model drawbacks, which could induce uncertainties on scenario results. Concentrations of chlorophyll-a, NO₃, PO₄ and O₂ are compared to measurements at 15 Rijkswaterstaat monitoring locations (MWTL), along four transects (Figure 6.4, Table 6.4, <https://waterinfo.rws.nl>). We present here time series plots along the Noordwijk and Terschelling transects (Figure 6.5 and Figure 6.6).

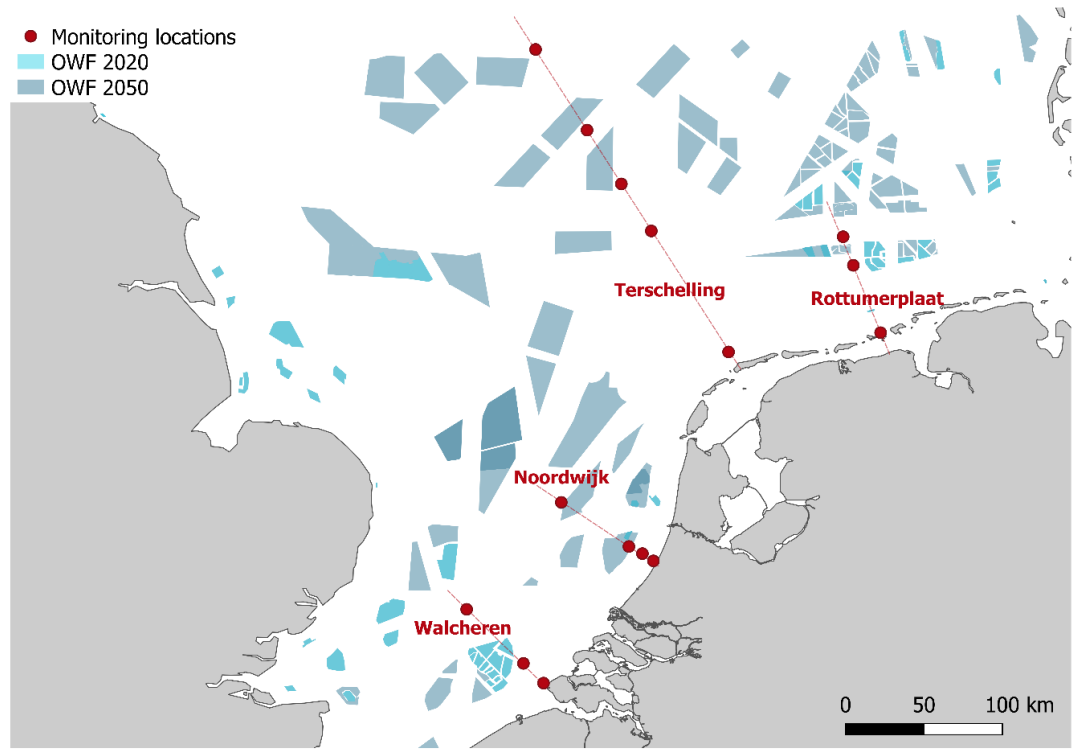


Figure 6.4 Location of the monitoring stations where model outputs are compared to measurements.

Table 6.4 Statistical comparison of measured and simulated time series for the year 2007. σ_{obs} =standard deviation of observations; σ_{sim} =standard deviation of model results at sampling dates; ρ =correlation.

Station Stat. criterion Unit	Chlorophyll-a					NO3					PO4					OXY				
	σ_{obs}	σ_{sim}	RMSE	Bias	ρ	σ_{obs}	σ_{sim}	RMSE	Bias	ρ	σ_{obs}	σ_{sim}	RMSE	Bias	ρ	σ_{obs}	σ_{sim}	RMSE	Bias	ρ
	$\mu\text{g/L}$	$\mu\text{g/L}$	$\mu\text{g/L}$	$\mu\text{g/L}$	-	mgN/L	mgN/L	mgN/L	mgN/L	-	mgP/L	mgP/L	mgP/L	mgP/L	-	mg/L	mg/L	mg/L	mg/L	-
Walcheren 2 km	11.3	2.7	12.5	-6.5	0.35	0.26	0.12	0.16	0.01	0.90	0.013	0.009	0.014	-0.012	0.91	2.24	1.02	1.82	-0.61	0.68
Walcheren 20 km	9.3	2.2	10.5	-6.5	0.59	0.11	0.05	0.13	0.08	0.42	0.011	0.005	0.009	-0.005	0.84	1.57	0.92	1.44	-0.77	0.63
Walcheren 70 km	1.1	0.9	1.8	-1.2	0.07	0.04	0.02	0.06	0.04	0.23	0.015	0.002	0.015	-0.002	0.42	0.87	0.75	0.82	-0.58	0.75
Noordwijk 2 km	13.7	6.9	11.6	-1.0	0.54	0.39	0.23	0.20	-0.06	0.93	0.015	0.012	0.012	-0.009	0.85	1.48	1.05	1.00	-0.29	0.77
Noordwijk 10 km	8.7	5.8	8.3	0.9	0.42	0.22	0.16	0.14	0.07	0.86	0.011	0.009	0.009	-0.005	0.76	1.84	1.28	1.11	-0.32	0.83
Noordwijk 20 km	5.7	5.3	5.5	0.3	0.50	0.16	0.12	0.13	0.07	0.73	0.010	0.008	0.008	-0.004	0.77	1.58	1.13	1.26	-0.69	0.74
Noordwijk 70 km	3.4	2.2	3.7	0.2	0.16	0.05	0.07	0.09	0.03	0.15	0.006	0.005	0.006	-0.003	0.53	1.50	0.80	1.15	-0.49	0.75
Terschelling 10 km	6.2	2.2	6.9	-2.2	0.04	0.19	0.11	0.12	0.02	0.81	0.012	0.008	0.011	-0.006	0.61	1.50	0.88	1.55	-0.83	0.49
Terschelling 100 km	1.3	1.6	1.7	0.0	0.30	0.03	0.03	0.02	-0.01	0.75	0.006	0.005	0.005	-0.004	0.98	0.88	0.84	0.83	-0.59	0.78
Terschelling 135 km	1.1	1.3	0.9	-0.2	0.73	0.03	0.03	0.02	0.00	0.73	0.007	0.005	0.006	-0.004	0.84	0.91	0.86	0.72	-0.48	0.81
Terschelling 175 km	0.9	1.6	1.1	0.1	0.73	0.03	0.04	0.01	0.00	0.92	0.006	0.006	0.004	-0.003	0.93	0.74	0.78	0.62	-0.55	0.93
Terschelling 235 km	1.1	2.1	1.3	0.6	0.91	0.03	0.04	0.01	0.00	0.98	0.006	0.006	0.005	-0.003	0.75	0.69	0.81	0.54	-0.38	0.88
Rottumerplaat 3 km	7.2	2.9	8.3	-5.7	0.56	0.35	0.22	0.17	-0.07	0.98	0.011	0.009	0.016	-0.013	0.60	1.44	0.84	1.26	-0.69	0.68
Rottumerplaat 50 km	1.3	1.8	2.7	1.3	-0.08	0.00	0.02	0.07	0.06	-0.37	0.001	0.002	0.004	-0.004	0.06	0.48	0.39	0.43	-0.19	0.63
Rottumerplaat 70 km	0.5	1.5	1.9	1.2	0.14	0.00	0.02	0.04	0.04	0.00	0.001	0.001	0.003	-0.003	0.16	0.25	0.33	0.32	-0.22	0.72

Note that the bad correlations between observations and simulations calculated at locations Rottumerplaat 50 km and 70 km are due to the fact that measurements are only available in the summer period. During this period, the measurements show that NO3 is totally depleted, while it isn't in the model.

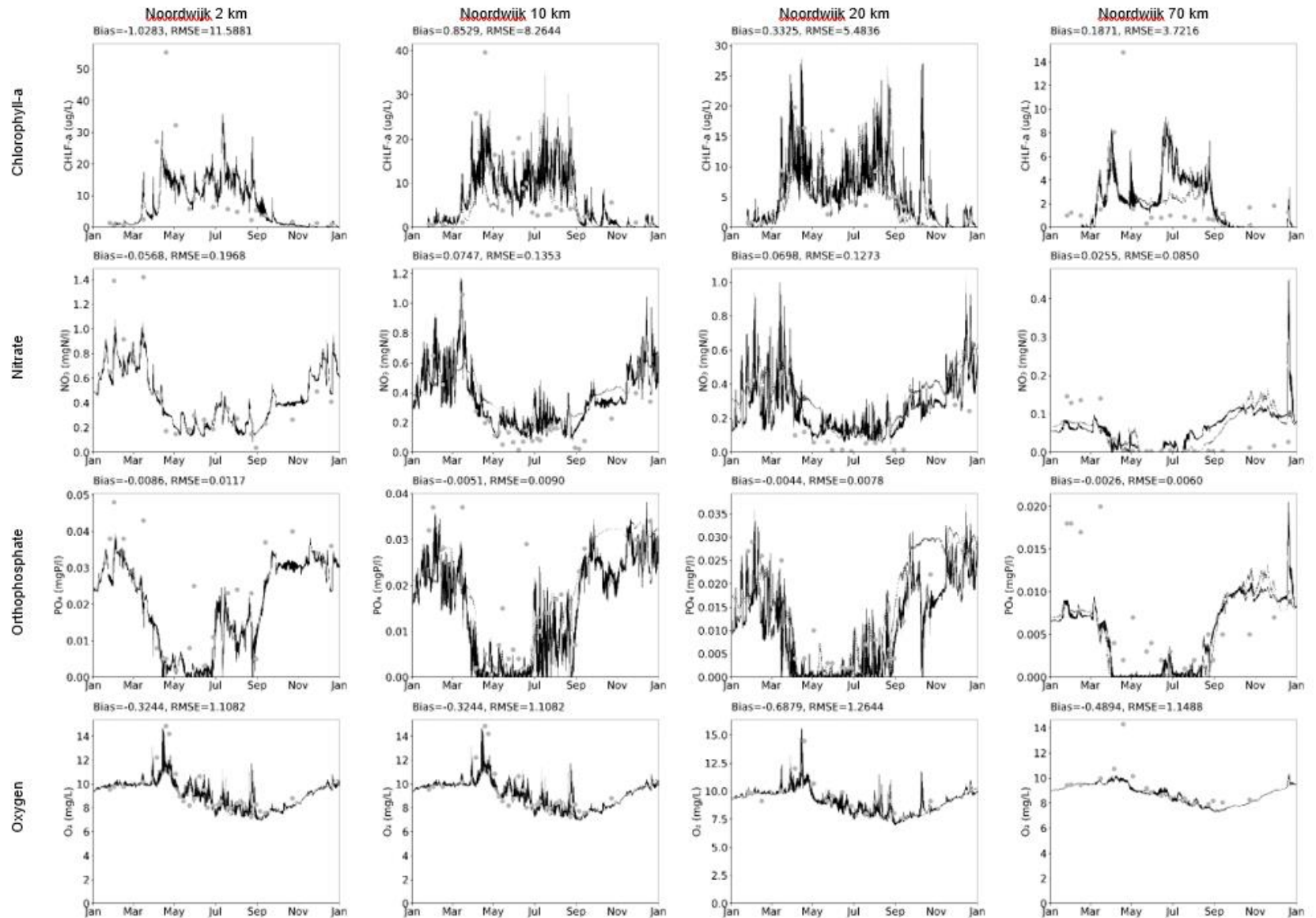


Figure 6.5 : Comparison of simulated (black lines) and observed (gray dots) chlorophyll-a, NO₃, PO₄ and O₂ time series along the Noordwijk transect for the year 2007. The dotted line represents the results of the coarse grid model.

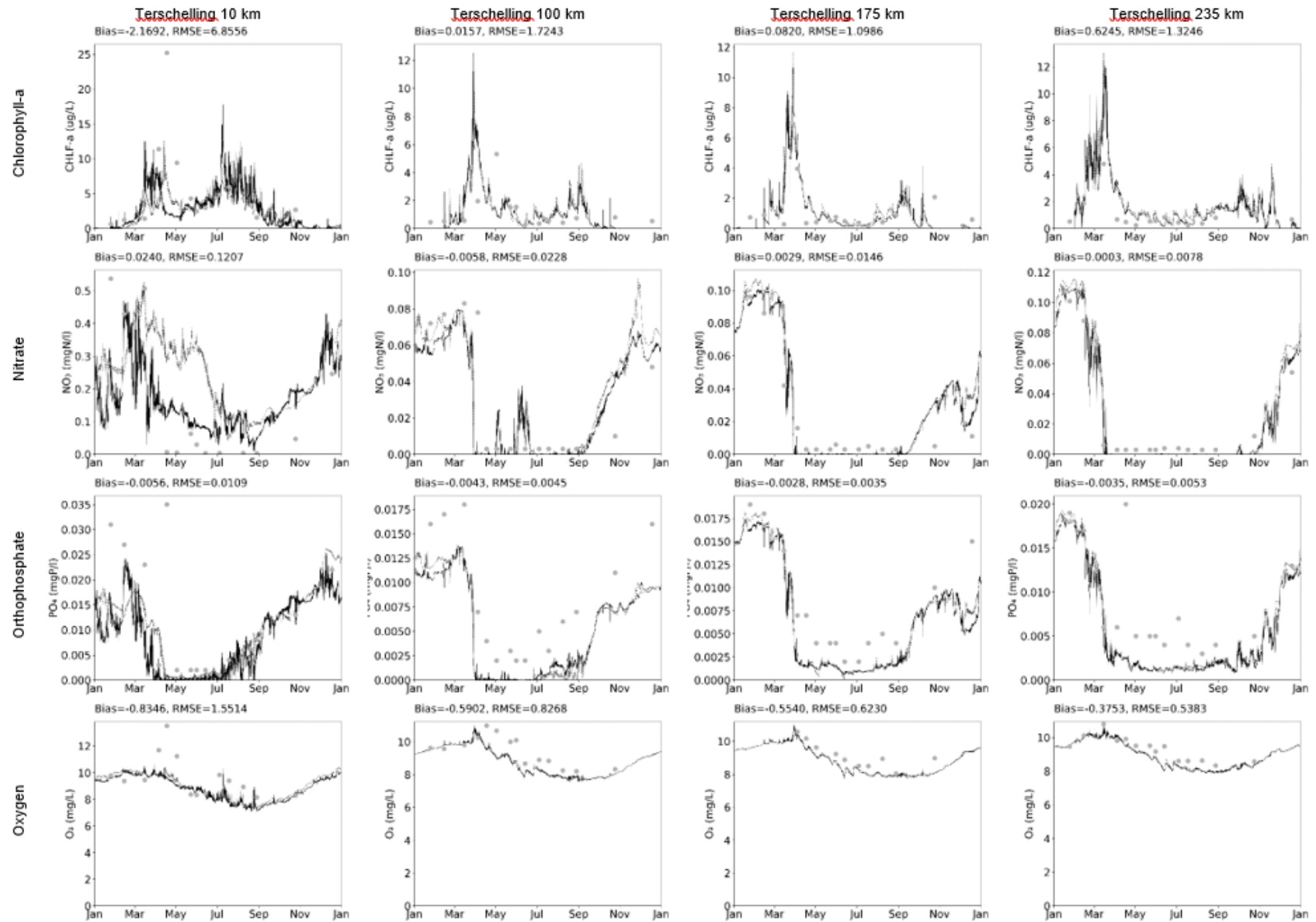


Figure 6.6 Comparison of simulated (black lines) and observed (gray dots) chlorophyll-a, NO₃, PO₄ and O₂ time series along the Terschelling transect for the year 2007. The dotted line represents the results of the coarse grid model.

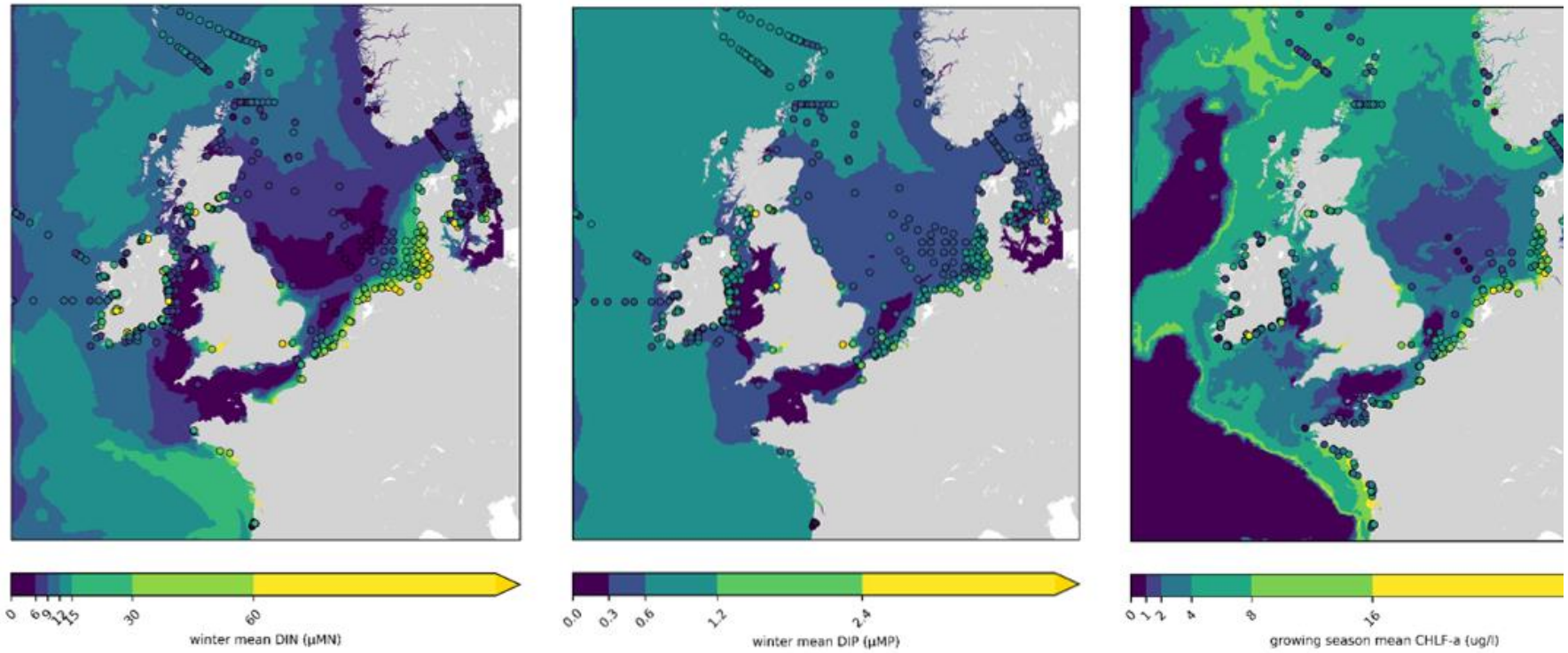


Figure 6.7 Comparison of simulated (2007) winter-mean DIN and DIP and growing season-mean chlorophyll-a to ICES data statistics (2006-2014). Mean reported values at ICES monitoring locations are indicated by colored dots. Growing season = March-September.

Overall, the model reproduces the temporal patterns of major nutrients, chlorophyll-a and O₂ well at the monitoring locations.

Along the most southern transects (e.g., Noordwijk, Figure 6.5), at the most offshore stations, the increase of NO₃ concentrations at the end of the summer starts too early in the season in the model, leading to an overestimation of summer phytoplankton biomass as well. It is not clear yet where this early increase comes from. This could be linked to overestimated nutrient inflows from the South, or to an underestimation of nitrogen retention in bottom sediments. This should be further investigated in the next stage of the project. Along the Terschelling transect (Figure 6.6), the timing of the spring drop in nutrients and their autumn increase in the model is well synchronized the observations.

Along the Noordwijk transect, the model reaches P limitation in the summer, while this is not observed in the field, and overestimates NO₃ concentrations (close to depletion in the observations). Similarly, along the Terschelling transect, NO₃ depletion is well reproduced by the model, but summer PO₄ concentrations are consistently underestimated. The simulated phytoplankton biomass being very consistent with measurements, and winter nutrient levels well reproduced by the model, it seems that the N:P ratio of nutrient uptake by phytoplankton may be underestimated. Sensitivity of the model to this parameter should be carried out.

Simulated O₂ concentrations match observations. The O₂ peak linked to the spring bloom is well represented. However, the model slightly underestimates O₂ concentrations over the summer period at all stations. The reason for these discrepancies should also be investigated in the next calibration/validation step.

The coarse-grid model provides very similar results to the fine-grid model for all water quality variables in this reference-scenario, except for locations close to complex shorelines (e.g., see NO₃ time series at Terschelling 10 km station in Figure 6.6). The coarse-grid model therefore is an adequate tool to test new model developments and get first estimates of the effects of changes in forcing conditions at offshore locations.

6.2.2 Seasonal means of inorganic nutrients and chlorophyll a

Ability of the model to reproduce spatial variability of nutrients and phytoplankton biomass is assessed using ICES data for 2006-2014 (accessed through the COMPEAT tool, developed for automate OSPAR assessments:

https://ocean.ices.dk/core/compeat?assessmentperiod=20062014_Test). Comparison of model maps to winter means of dissolved inorganic nutrient measurements and growing-season (March-September) means of chlorophyll-a show that 3D DCSM-FM Water Quality performs well in representing the spatial variability of these variables in the central North Sea (Figure 6.7). Gradients in concentrations from the coast towards the open sea are well represented. DIN is slightly overestimated in the Kattegat Bay, while DIP is slightly underestimated. Chlorophyll-a levels during the growing season match the assessment data well. These are however overestimated by the model near the Northern open boundary and the French coast. This is most likely due to an overestimation of the mixing during the growing season in the deep areas.

6.3 Results

We present in this section results of simulated primary production, as well as other relevant water quality parameters, such as chlorophyll-a and dissolved inorganic nutrients. The modelled primary production results are calculated for the entire water column. For other water quality variables, results are plotted for one specific vertical layer.

6.3.1 Effect of changes in hydrodynamics

Spatial changes in water quality variables

Changes in wind and water flows due to OWFs overall lead to an increase in yearly average primary production in the farm areas. This is visible for the scenario OWF2020 hydro especially North from the Dutch coast and is striking in the upscaling scenario (Figure 6.8 and Figure 6.9). In the latter, the yearly average primary production increases up to 0.25 gC/m²/day in the large windfarm areas off the British coast and in the central North Sea (note that the average primary production for 2007 over the plotted domain is 0.58 gC/m²/day). As expected, the increase in these areas is even stronger in spring, when the phytoplankton bloom occurs. The increase in spring primary production reaches ~50% in the large OWF areas from the upscaling scenario, due to changes in hydrodynamics (i.e., extra vertical mixing).

The effects on surface chlorophyll-a are not plotted here but show similar patterns as for primary production. Surface chlorophyll-a overall increases in OWF areas as a consequence of changes in hydrodynamics, especially in the central North Sea. Difference in simulated concentrations between the OWF2050 hydro scenario and the reference run reach ~+1 µg/L for the spring season.

The local effect of the OWFs on primary production is however very patchy. Along the Dutch coast, and in the northern part of the model domain (latitude > 55), the changes induced in hydrodynamics can lead locally to a decrease in primary production. This patchiness is also visible in the stratification maps (subsections 3.3.3 and 3.3.4).

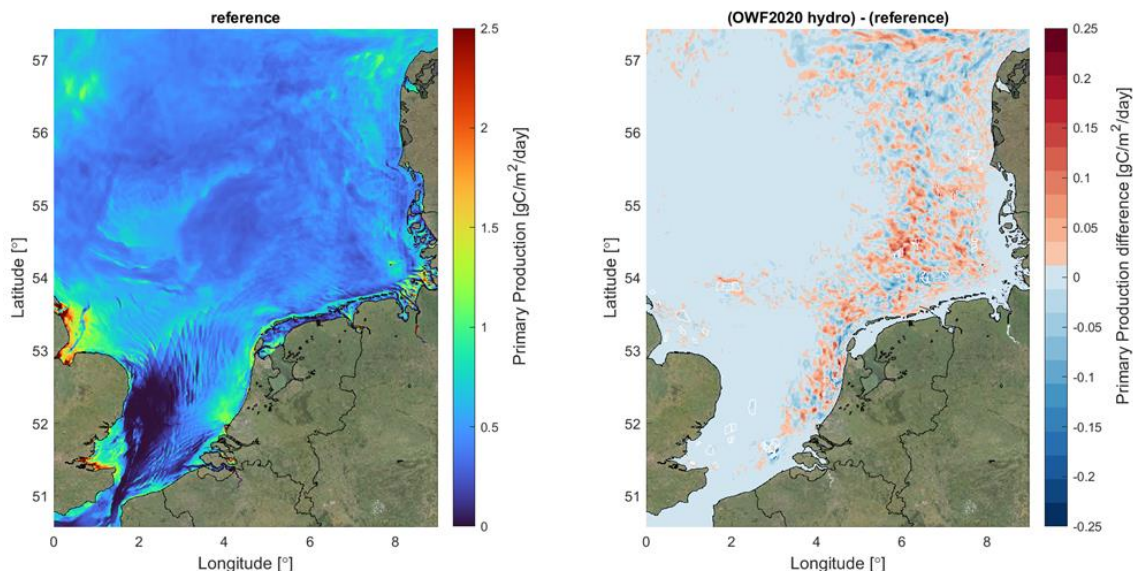


Figure 6.8 Left: average primary production over 2007 in the reference run. Right: difference between average primary production simulated in the OWF2020 hydro scenario and in the reference run for 2007.

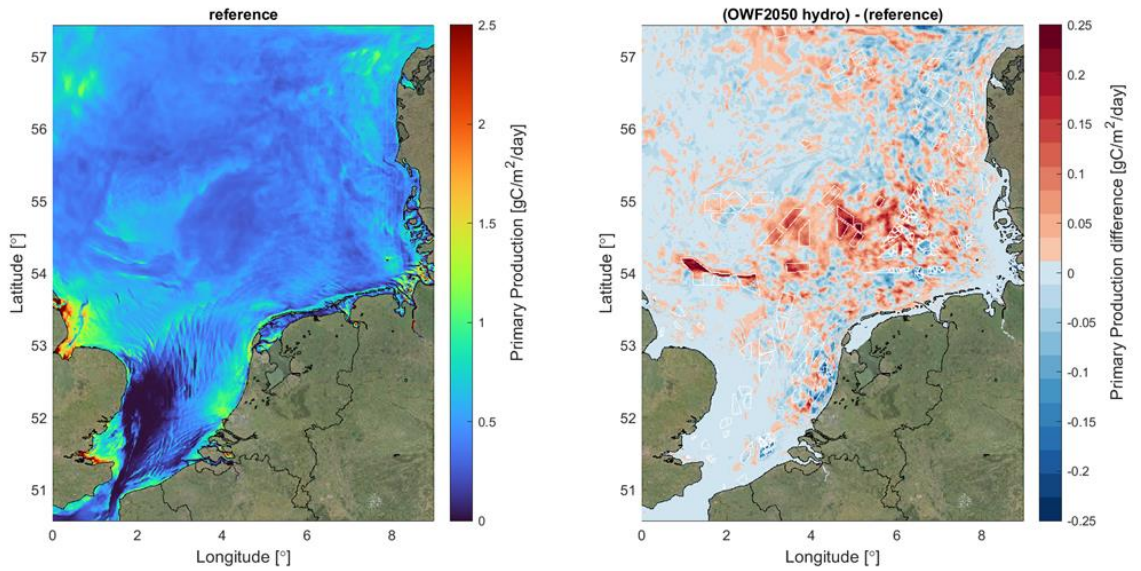


Figure 6.9 Left: average primary production over 2007 in the reference run. Right: difference between average primary production simulated in the OWF2050 hydro scenario and in the reference run for 2007.

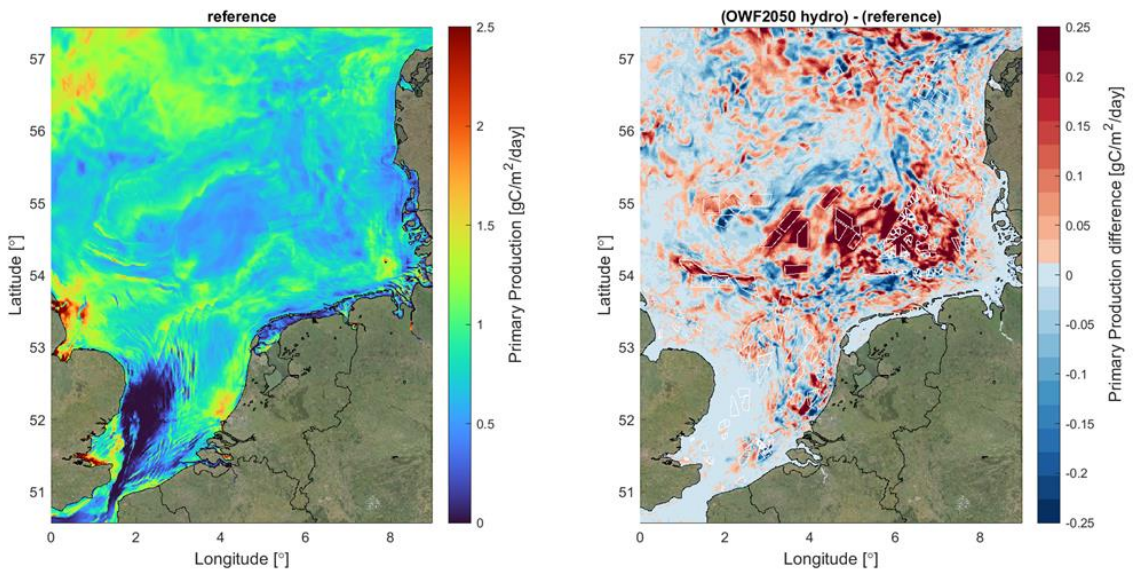


Figure 6.10 Left: average primary production for spring 2007 (March, April, May) in the reference run. Right: difference between average primary production simulated in the OWF2050 hydro scenario and in the reference run for spring 2007.

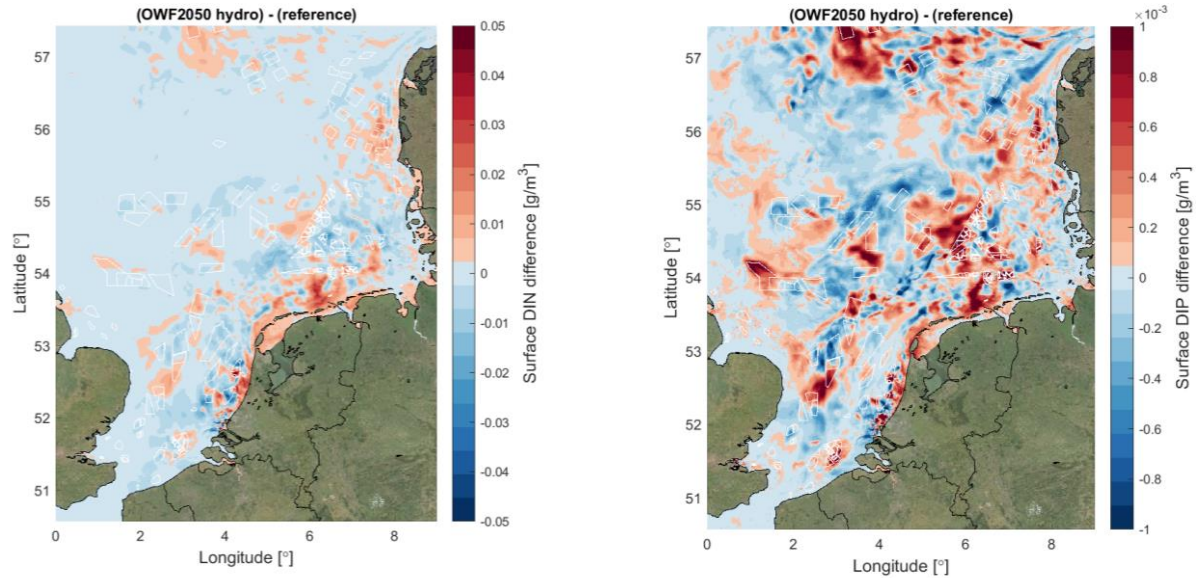


Figure 6.11 Left: difference between average DIN simulated in the OWF2050 hydro scenario and in the reference run for spring 2007. Right: difference between average DIP simulated in the OWF2050 hydro scenario and in the reference run for spring 2007.

The effect of changes in hydrodynamics on surface DIN is not evident. The changes in concentrations are very limited, since it is the limiting nutrient in most of the model domain (Figure 6.11 – left). Therefore, the additional available DIN due to increased vertical mixing is directly taken up for primary production. Surface DIN concentrations however increase along the northern Dutch coast.

Increased vertical mixing by OWFs lead to a clear increase in surface DIP concentrations (see Figure 6.11 – right for differences between OWF2050 hydro scenario and reference run for the spring period). This increase is moreover most likely underestimated, since P uptake for primary production seems to be systematically overestimated in the model.

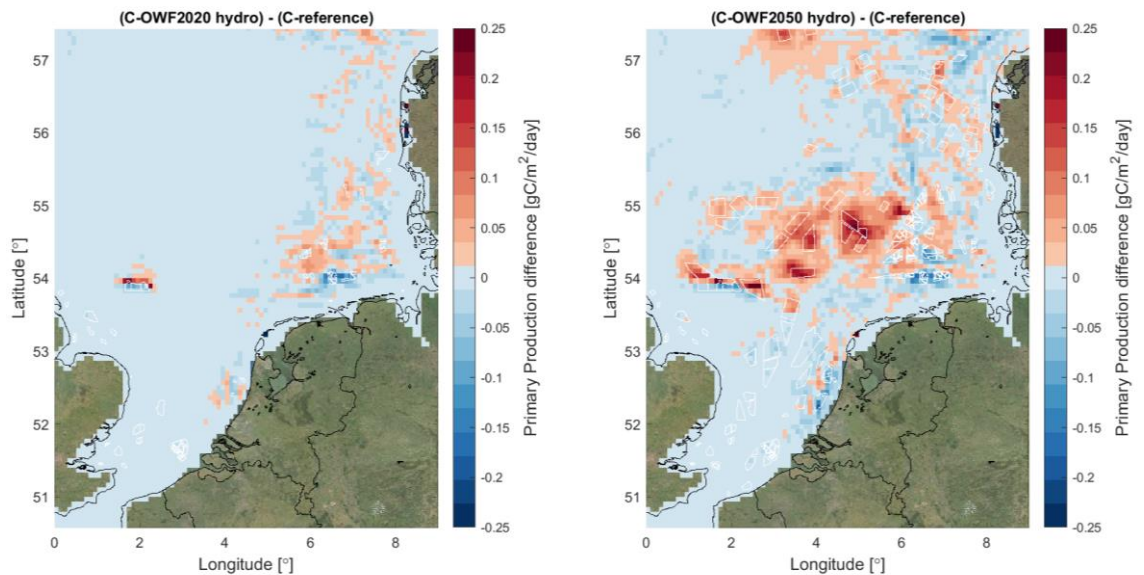


Figure 6.12 Difference in the yearly average primary production simulated in scenarios OWF2020 hydro (left) and OWF2050 hydro (right) in comparison to the reference run. For comparison with fine-grid results, see right frames in Figure 6.8 and Figure 6.9.

The coarse grid model gives similar effects as with the fine grid (Figure 6.12). As this is also the case for sediment dynamics, it provides a good base for a first assessment of the effects of combined changes in hydrodynamics and sediment dynamics on primary production.

Changes in temporal patterns

Chlorophyll-a time series simulated in the reference run and the OWF2050 hydro scenario are compared within two OWF areas (Figure 6.13). These areas are chosen for their contrasting ecological functioning:

- OWF-1 is located close to the Dutch coast in a relatively shallow area (~25 m deep). The water column is well mixed;
- OWF-2 is located far offshore, in an area where the water column is ~45 m deep. The water column is strongly stratified, with an average temperature difference of 3.5°C between the surface and the bottom in the spring and summer months (March-August).

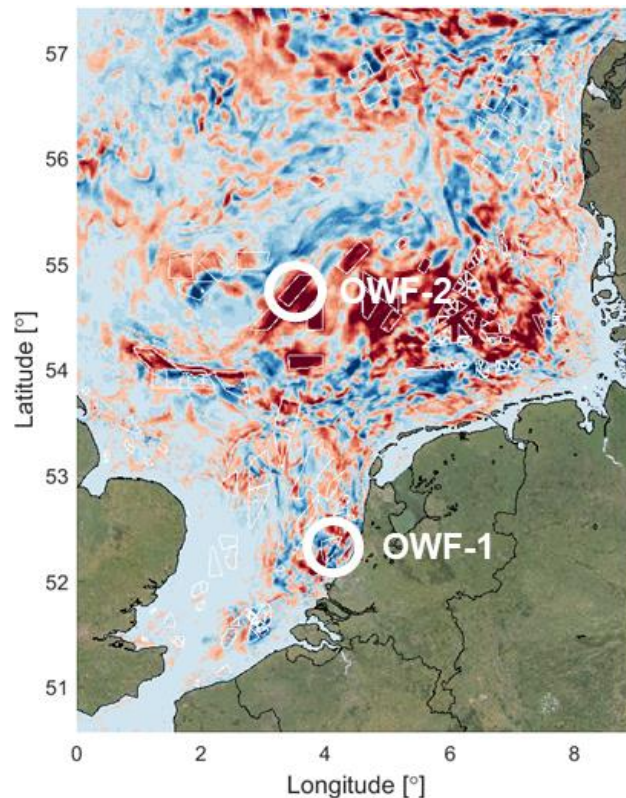
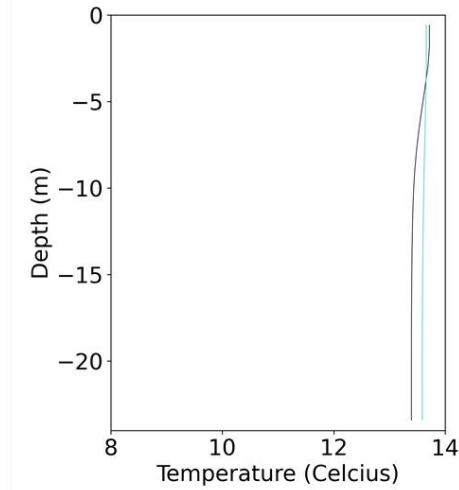


Figure 6.13 Locations where temporal patterns are compared.

Results show that in the more stratified OWF area (OWF-2), where there is a clear change in the temperature vertical profile, the spring bloom occurs later than in the reference run (Figure 6.14 – right). The peak in chlorophyll-a concentration is reached about 2 weeks later in the upscaling scenario run than in the reference run, both at the surface and at the thermocline. No clear pattern is visible at the coastal well-mixed location (OWF-1, see Figure 6.14 – left).

OWF-1



OWF-2

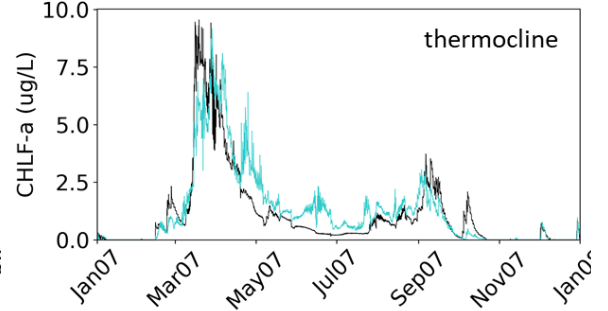
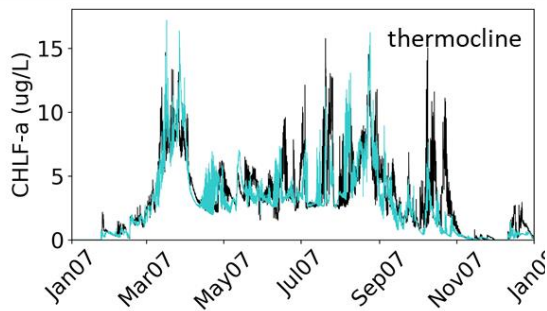
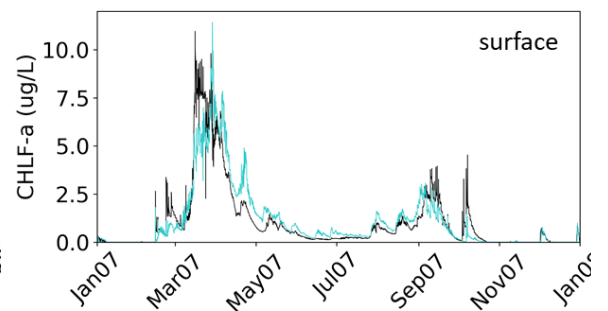
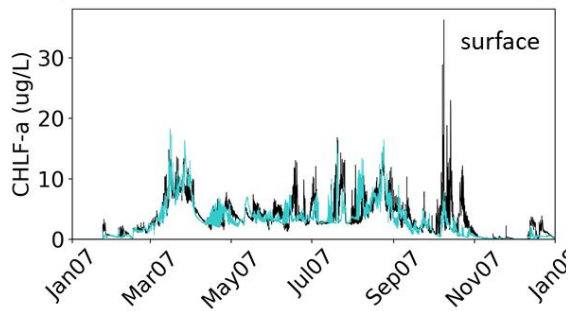
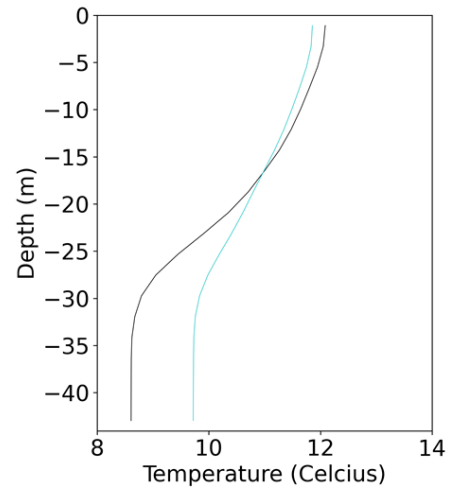


Figure 6.14 Average spring-summer temperature depth profiles (top) and time series of simulated chlorophyll-a concentrations at the surface (middle) and at the thermocline (bottom) in OWF areas OWF-1 (left) and OWF-2 (right). The black lines represent the results for the reference scenario and the blue line for the OWF2050 hydro scenario.

6.3.2 Effect of mussel growth on pillars

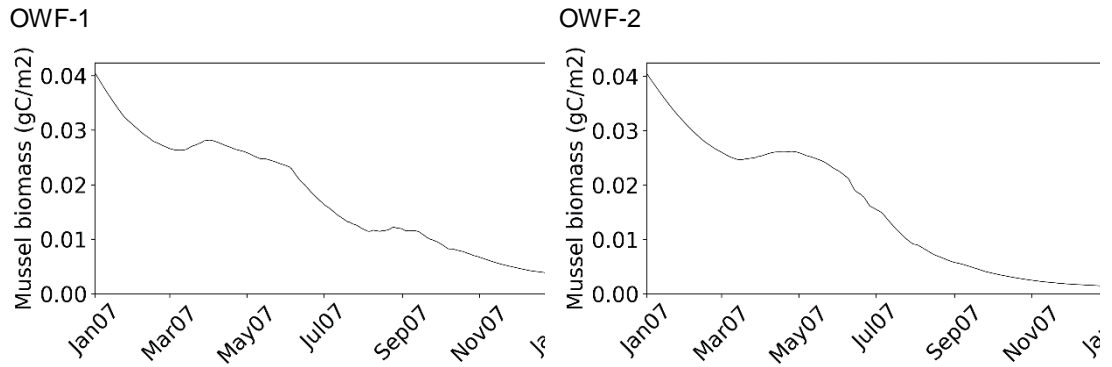


Figure 6.15 Simulated mussel biomass on wind turbine pillars relative to total seabed area for scenario OWF2050 hydro+mussels.

With the current implementation of DEBGRZ and using the same parameterization for blue mussel dynamics as for the Wadden Sea bed, the mussel biomass on pillars declines throughout the year. Simulated grazing by mussels is negligible compared to mussel death and primary production. There is therefore no clear difference in simulated chlorophyll-a concentrations or primary production between scenarios with changes in hydrodynamics only and those including mussel biomass on pillars close to the water surface.

At this stage, no conclusions can therefore be derived on the effect of mussel growth on wind turbine pillars. Further developments and testing of the DEBGRZ module are needed to be able to represent the effect of mussel growth on wind turbine pillars.

6.3.3 Combined effects of changes in hydrodynamics and sediment dynamics

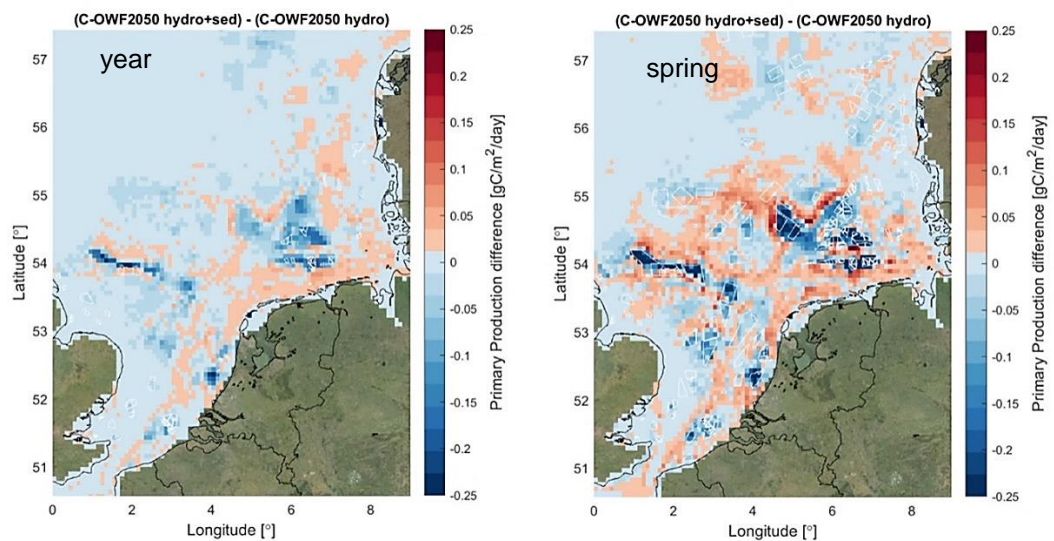


Figure 6.16 Difference in the yearly average (left) and spring average (right) primary production simulated in scenario OWF2050 hydro+sed in comparison to the reference run.

Overall, changes in sediment dynamics due to the presence of OWFs result in a decrease in primary production, especially in the large farm areas at latitudes 54-55 (Figure 6.16). This was to be expected, since increase in turbulence within these OWF areas lead to an increase in the simulated suspended sediment in this zone (see perturbation field in Figure 6.3), in turn leading to a less favourable light climate for primary producers.

In the shallower areas along the Dutch coast, where surface sediment concentrations decrease as a result of OWFs, primary production is higher than in the scenarios including changes in hydrodynamics only. These patterns show even stronger contrasts over the spring period. Considering the combined changes of hydrodynamics and sediment dynamics due to OWFs, the most visible effects on primary production are in the most offshore wind farm areas, at latitudes 54-55 (Figure 6.17). The wind farm areas located in the central part of the simulated domain (longitudes 2-6) still show a significantly higher primary production than in the reference run. On the contrary, the loss of primary production due to the decrease of light availability in the German wind farm areas exceeds its increase due to higher vertical mixing of the water column (and its inorganic nutrient concentrations).

Therefore, when considering both changes in hydro- and sediment dynamics, primary production in these OWF areas is lower than in the reference run.

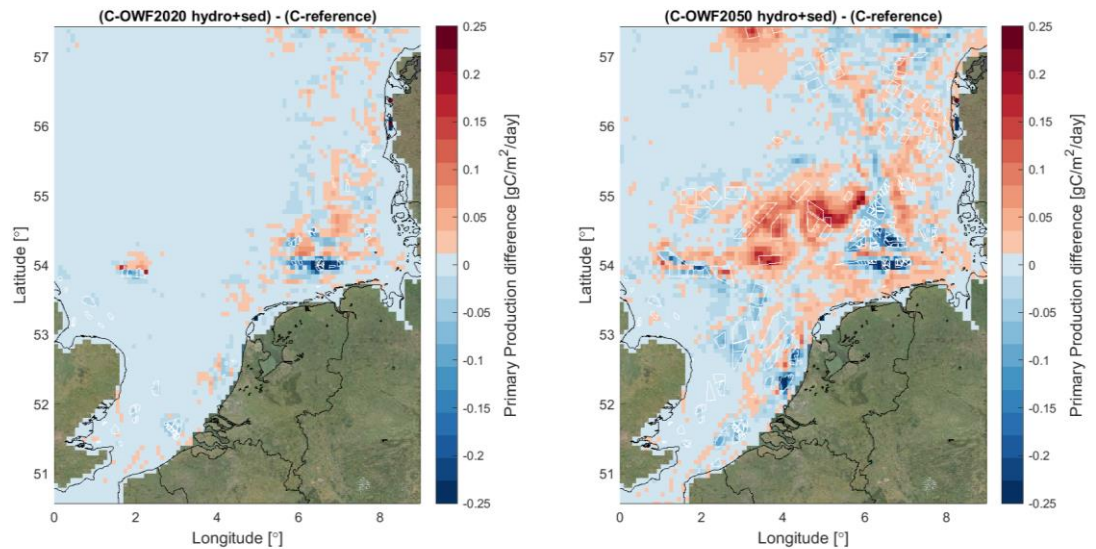


Figure 6.17 Difference in the yearly average primary production simulated in scenarios OWF2020 hydro+sed (left) and OWF2050 hydro+sed (right) in comparison to the reference run.

6.4 Discussion

6.4.1 First results on the ecological effects of OWFs

Our results show that OWFs can have a significant effect on primary production. Their net effect is highly heterogeneous over space. Increased vertical mixing leads to an increase in nutrient availability at the surface and therefore to increased primary production and chlorophyll-a concentrations.

Overall, changes in sediment dynamics due to the presence of OWFs lead to an increase in pelagic inorganic matter concentrations as a result of higher mixing, with the exception of areas closer to the coast, where sediment concentrations decrease as a result of lower bottom shear stress. As a consequence, in large OWFs from the central North Sea (mainly from the upscaling scenario), primary production decreases due to the deterioration of the light climate. The net combined effect of changes in hydrodynamics and sediment dynamics is extremely variable over space, with a significant increase of primary production in some OWFs, and a significant decrease in others (e.g. German OWFs). These are however, preliminary estimates. The model will need further refinement to provide reliable quantitative estimates of this net effect. This will require fully coupling the sediment and ecological components of 3D DCSM-FM, and thoroughly validating the simulated light climate.

On top of this, the growth of mussels on wind turbine pillars may also have a significant effect on phytoplankton biomass and primary production. Slavik et al. (2019) estimated that the construction of all OWFs, currently under construction, planned and consented, in addition to those already in operation, might lead to an increase in the overall abundance of blue mussels in the southern North Sea by more than 40%, in turn leading to a decrease in primary production. At the moment, the parameterization used for the dynamics of filter-feeders on pillars still needs to be adapted to be able to represent this effect. If we assume that the estimates from Slavik et al. (2019) are correct, it is difficult to determine what the total effect of OWFs will be, since changes linked to hydrodynamics and sediment dynamics are of the same order of magnitude.

In places, where the combined effect of hydro- and sediment dynamics led to a decrease in primary production, the growth of mussels on wind turbine pillars might lead to drastic changes in ecosystem functioning. Refining our estimates of the individual effects of changes in hydrodynamics, sediment dynamics, and filter-feeder growth on pillars will constitute the next step of this work.

Our results show that OWFs can also have a significant effect on the timing of the spring bloom in highly stratified areas, which might affect the life cycles of higher trophic levels.

6.4.2 Future model improvements

Coupling with sediment dynamics

The full coupling of the sediment and ecological components of 3D DCSM-FM will allow for a refined assessment of the effects of changes in light climate. The ability of the model to represent light climate (e.g., extinction) should therefore be thoroughly validated.

Once the sediment dynamics are fully calibrated, accumulation dynamics of nutrients on the seabed can be refined (now modelled as net sedimentation) to better represent seasonal dynamics and spatial variability in retention and re-mobilization.

Improvement of biogeochemical processes

The validation of the 3D DCSM-FM ecological model for 2007 showed that the N:P ratios of nutrient uptake for primary production is most likely underestimated. A sensitivity to these parameters should be carried out to investigate ways to better represent nutrient limitation and summer nutrient concentrations.

In deep areas, the interpolation of the 3D open boundary at the 20 equidistant vertical layers might lead to an overestimation of surface nutrient concentrations. For example, along the southern boundary, the surface layer has a thickness of ~200 m, which is much deeper than the thermocline. Using a z-sigma approach for the vertical layering of the model will most likely improve the representation of vertical gradients in nutrient concentrations in deep areas, which can have an important effect on lateral transport as well.

Representation of mussels on pillars

The DEBGRZ module should be further tested and calibrated to represent the growth of blue mussels on wind turbine pillars. This will require gathering more data on biomass dynamics in OWFs from the literature for validation.

Model validation and analysis

Once these points are addressed, the fully coupled model should be validated for the 2007-2008 period, to assess its ability to reproduce interannual variations, and for the year 2017, when the first OWFs were already constructed. Comparison with existing data within OWF areas in 2017 will allow for validating the estimated ecological effects. Comparison of model results to primary production measurements would be extremely beneficial to the study.

Mass balances should be calculated within OWF areas to fully grasp how rates of biogeochemical processes are affected over time. At this stage, it is not possible to calculate mass balances for overlapping areas. These were only calculated for a larger domain to check model consistency.

7 Conclusions

7.1 Model performance

7.1.1 Coupling

Due to various technical problems it was not possible (given the available time) to perform fully coupled model runs with the fine sediment model and the water quality and ecology processes. The technical issues are solved and fully coupled model runs should be possible. This will greatly increase our ability to assess the cumulative effects of changes in hydrodynamics and in SPM concentrations caused by the wind farms.

7.1.2 Resolution and calculation times

The full resolution model with all the DELWAQ processes included takes on the Deltares calculation cluster about two weeks to run. This is a serious impairment. For some of the full resolution model runs of the ecological model we were fortunate enough to be able to make use of the Cartesius cluster at SurfSARA. This reduced calculation times to about 3 days. The differences between the full-scale model and the coarser resolution model appear to be relatively limited and for many applications the coarser grid model (which also runs in about 3 days) will be sufficient. At regional scales it may still be important to use the finer scale model; this needs further assessment.

7.1.3 Validation

The current validation of all three modules has been carried out on easily available datasets, such as MWTL and already processed satellite imagery. There are more data available, particularly abroad and more data are currently becoming available from a variety of sources, including ADCP (Acoustic Doppler Current Profile) measurements from the North Sea farms (an aquaculture site) and measurements from wind farm locations. The current validation really lacks data from near the bed and near the pycnocline.

Another recurring problem for validating ecological models is that the available parameters are generally state variables, not processes. Many variables are the eventual results of sources and sinks. E.g. a local nutrient concentration is the result of inputs into the system and subsequent transports on one hand and uptake of nutrients by phytoplankton on the other. Often measured chlorophyll-a is used as a proxy for algal biomass. That is already a source of uncertainty, as chlorophyll content per gram biomass can vary (often algae that are adapted to low light conditions have higher chlorophyll contents than algae that are adapted to low nutrient concentrations). Also, biomass is a resultant of primary production on one hand and mortality (mostly due to grazing) on the other hand. Earlier projects have taught us that it is entirely possible that major effects can be seen in primary production with significant consequences for shellfish, while the net result in chlorophyll measurements yields very little effect. More process measurements would be very useful for model validation.

However, our overall impression is that with such a complex project and a first application of a totally new, also complex modelling system, the first results are remarkably good. Some processes need further calibration (e.g. the bias in the SPM models, that currently give values that are too low) but the fact that general patterns in physical and ecological parameters seem to be reproduced with remarkable accuracy, indicates that this modelling suite is eminently suitable for such scenario explorations. At present, clearly the model results should not be taken at face value. In this stage the models are primarily a research tool. However, they certainly have the potential to be developed into policy support tools.

7.1.4 Missing processes

One of the things we could not yet include in this study is the effect of wind wakes from the wind farms. There is visible reduction of wind speeds in wakes of farms, but this is much less than within the farms (Boon et al. 2018 and pers. comm. Sofia Caires). However, the wakes of multiple farms can certainly cover a large surface area. So, although the effects on waves and wave mixing might be relatively small, this is something to be addressed in the near future.

The implementation of mussels in the upper layers of wind farms (on the turbine monopiles) does need better calibration. The dynamic energy budget (DEB) model to simulate growth of shellfish requires certain model parameters that are specific for the species as well as for the location. In the first attempt at incorporating mussels in the upper water layers we used the standard parameter set that is used for the Wadden Sea, an area that has average SPM concentrations orders of magnitude higher than the upper layers of the North Sea. In the model the mussels died off, which is clearly not the case in the field, where mussels grow very well in the upper 5 meters of the water column on the turbine monopiles (Degraer et al. 2013). This clearly requires further calibration of mussel parameters suitable for this environment.

7.2 Effects of wind farms

The 2020 scenarios showed effects in stratification, currents, SPM dynamics and ecological processes, but these were restricted to the wind farm areas and the immediate vicinity. The ecosystem modelling results have given clear indications that ecosystem-scale changes in stratification, currents, fine sediment and productivity of different trophic levels are likely with large upscaling of offshore wind. These are likely to have knock-on effects on higher trophic levels through various pathways. These pathways are directly linked to the energy budgets of these apex species.

7.2.1 Effects through changes in benthic – pelagic transport

The most clear-cut and also likely the most important pathway by which effects at lower trophic levels are going to influence higher trophic levels is the effect of increased water column mixing. This has a direct and significant impact on primary production. The first model results indicate that in certain areas increases or decreases in the order of magnitude of 0.25 gC/m²/day are possible. These larger changes occur in areas in the central southern North Sea, where normal annual averages range around 0.5 gC/m²/day. So, such effects are certainly significant. In a few limited areas the models also predict decreases, of a similar magnitude. These decreases are 1) limited to the wind farm locations and immediate vicinity and 2) these areas are closer to the coast, with generally higher rates of primary production. Hence the absolute decrease is similar, but proportionally the effects are less.

The increased mixing will also mean that more food and oxygen is transported towards the bed. The Oyster Grounds in the central southern North Sea is typically an area with stable summer stratification that often coincides with low oxygen levels (Peeters et al., 1995). This can be limiting for benthic communities. This clearly needs further investigation and quantification, but it seems likely that benthic communities are likely to benefit proportionally more from the increased production than pelagic grazers such as zooplankton. This means that predators that predominantly feed on benthic prey will be affected differently than species (e.g. bird species such as terns) that feed relatively close to the surface and feed on fish that tend to feed on zooplankton rather than benthos.

7.2.2 Effects through changes in temperature and / or habitat

Temperature is one of the main ecological drivers. It affects oxygen uptake due to changes in metabolism (Varó et al., 1991), species distribution (Neumann et al., 2009), swimming in fish (Batty et al., 1991) and plankton (Gill and Crisp, 1985) and many other ecologically important processes. The hydrodynamics model showed that in the upscaling scenarios surface temperatures were affected between 0.2 – 0.5 °C. The figures shown in section 3.3.4 are annual averages. As stratification occurs here in summer and is broken up in winter, the differences in summer are higher (can be up to 1 °C). Such changes may have an effect on the distribution of certain species and need further investigation in future.

Future changes in temperature are also expected due to climate change (Harley et al., 2006). The fundamental causes of temperature changes and their spatial extent between climate change and effects by offshore wind farms is different. OWF-effects are far more localised and due to mixing, while climate change acts on much larger spatial scales and is due to increased air temperatures. Models such as these, can be used to assess the interactive effects.

The presence of turbines and scour protection offers different settlement habitat. This has not been incorporated yet. Physical habitat formation and changes in biodiversity have not been specifically addressed in this study but are the subject of various other projects (Degraer et al., 2013; Lengkeek et al., 2017; Raoux et al., 2017). Future work needs to address these effects in conjunction with the ecosystem effects, such as the changes in primary production patterns in the North Sea. Specifically, the fact that offshore wind turbines offer substantial 'alien' settlement habitat for normally benthic species in the upper part of the water column, which will locally affect nutrient recycling and particle dynamics, is something that will need future attention.

7.2.3 Effects through changes in competition in lower trophic levels

The whole complex of new hard substrate being available at the bed and in the water column, as well as changes in near-bed oxygen levels and food supply towards the bed is likely to change the relative importance of various carbon pathways through the marine food web (Duffill Telsnig et al., 2019; Ehrnsten et al., 2019). Such changes can fundamentally alter the functioning of a system. Even though not all these changes will be detrimental e.g. for species of high conservation interest or for ecosystem services, such as fisheries, there are likely to be winners and losers. Although the implementation of a dynamic energy budget model of blue mussels was not immediately successful within this research, investigating trophic relationships with such models is likely to yield more insight into these pathways and therefore into ultimate effects.

7.3 Locations sensitive to ecosystem effects

A clear result of this first study is that offshore wind affects the different areas in the North Sea physically in different ways, which ultimately results in different ecological effects. Based on this first study, we can differentiate roughly 5 different areas where physical and ecological effects differ (Figure 7.1).

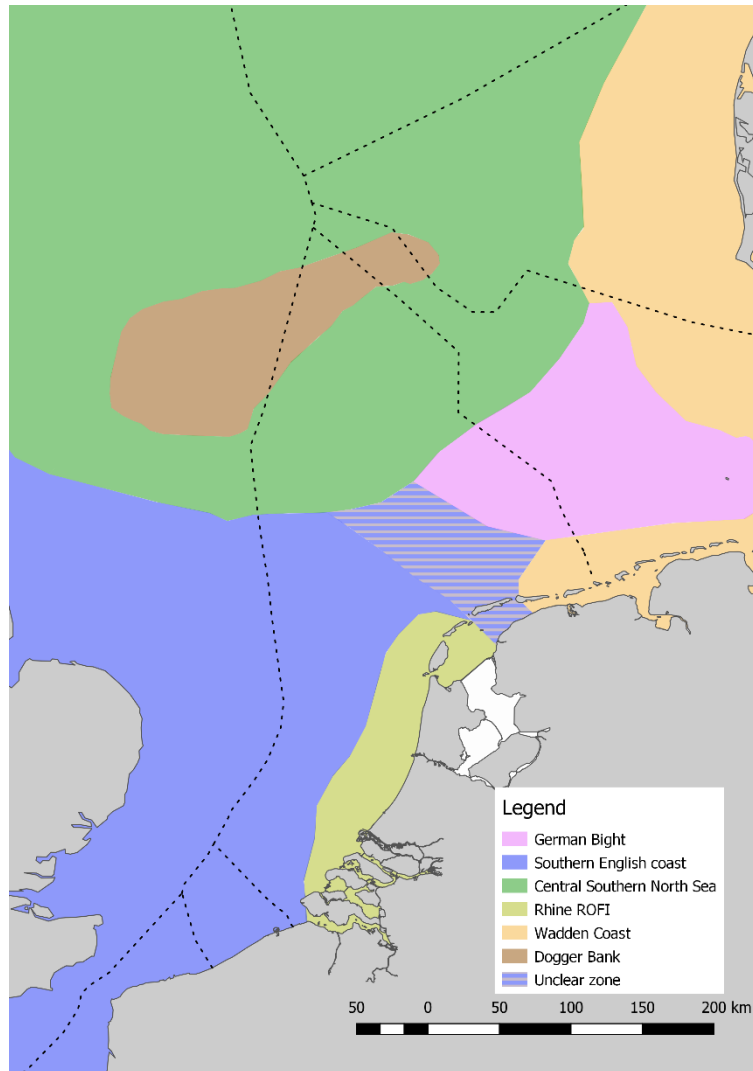


Figure 7.1: Areas with different ecosystem effects in the North Sea.

7.3.1

Central German Bight

This area is characterised by regular but not very strong stratification. Temperature stratification is dominant, but also salinity plays a role here. This is an area where there are strongly opposing effects of wind farms. On one hand, increased availability of nutrients can boost primary production, however, increased SPM levels in the upper layers can also reduce this. The model runs with the adapted SPM fields suggest that SPM effects are significant and in some sub-areas dominant. This clearly needs further quantification with the fully coupled model system and well calibrated SPM fields.

7.3.2

UK Coast and western most areas of the Dutch continental shelf

These are the areas that are fully mixed. Changes in stratification do not occur here. Particularly close to the Thames estuary, the system is extremely turbid and hence very low in productivity. Certainly, in absolute terms, any increase in SPM in the top layers does not decrease productivity much further. Further away from the Thames estuary, increased turbidity does reduce production.

7.3.3 Central Southern North Sea

This area is regularly stratified and some areas always seasonally stratified due to temperature. Even the areas with relatively strong seasonal stratification see clear effects from wind farms. This area is most strongly impacted by wind farm effects and the effects reach well beyond the immediate wind farm areas. The area is low in SPM concentrations in the upper layers. Wind farms appear to increase the concentration, but this does not cancel out the effects of increased nutrient availability in the upper layers.

In this area the net effect is an increase in primary production. Although there is an overall increase in the primary production, onset of phytoplankton growth in spring appears to be a bit later in these areas.

7.3.4 Holland coast and Rhine ROFI

This is an area with high nutrient availability and without temperature stratification, but some salinity stratification. It is a highly dynamic area with strong residual currents. In this area primary production is more light-limited than nutrient-limited. Nutrient availability in upper layers is high due to riverine input. The net effect is that higher fine sediment concentrations in the upper layers decrease primary production.

7.3.5 German and Danish Wadden coast

This area is in most ways similar to the UK coastal area. It is generally not stratified, or only very occasionally. It is high in nutrients but due to high SPM concentrations it is light limited and not very productive. Effects of wind farms on SPM concentrations in the upper layers and on productivity are minimal. There is no clear delineation between this zone and the UK Coastal zone, hence the blue/orange hatched area is indicated as “unclear zone”.

7.3.6 The Dogger Bank

This is a relatively isolated shallow area surrounded by the seasonally stratified area. It has a unique composition of ecological communities. Sufficient light penetrates to the bed for primary production, hence this is one of the few areas in The North Sea where microphytobenthos occurs. The stratification regime of the Dogger Bank is unclear, some areas occasionally have some (not very strong) temperature stratification. The bed consists predominantly of medium sand and coarse-grained material, so even though waves easily reach the bed, resuspension of fine sediment from the bed is limited. The resulting effects of offshore wind farms on the Dogger Bank on primary production are limited and spatially varying. In some areas there is a small net increase in other areas a small net decrease.

8 References

- Battjes, J. A., and Janssen, J. (1978). Energy loss and set-up due to breaking of random waves. In "Coastal Engineering 1978", pp. 569-587.
- Batty, R. S., Blaxter, J. H. S., and Bone, Q. (1991). The effect of temperature on the swimming of a teleost (*Clupea harengus*) and an ascidian larva (*Dendrodoa grossularia*). *Comp.Biochem.Physiol.* **100A**, 297-300.
- Boon, A. R., Caires, S., Wijnant, I. L., Zijl, F., Schouten, J. J., Muis, S., Van Kessel, T., Van Duren, L. A., and Van Kooten, T. (2018). "Assessment of system effects of large-scale implementation of offshore wind in the southern North Sea," Rep. No. 11202792-002-ZKS-0006. Deltares, Delft.
- Degraer, S., Brabant, R., and Rumes, B. (2013). "Environmental impacts of offshore wind farms in the Belgian part of the North Sea: Learning from the past to optimise future monitoring programmes.." Royal Belgian Institute of Natural Sciences, Brussels.
- Deutsche WindGuard, G. (2018). "Capacity density of European offshore windfarms ". INTERREG project Baltic Lines.
- Duffill Telsnig, J. I., Jennings, S., Mill, A. C., Walker, N. D., Parnell, A. C., and Polunin, N. V. C. (2019). Estimating contributions of pelagic and benthic pathways to consumer production in coupled marine food webs. *J Anim Ecol* **88**, 405-415.
- Ehrnsten, E., Norkko, A., Timmermann, K., and Gustafsson, B. G. (2019). Benthic-pelagic coupling in coastal seas – Modelling macrofaunal biomass and carbon processing in response to organic matter supply. *Journal of Marine Systems* **196**, 36-47.
- Floeter, J., van Beusekom, J. E. E., Auch, D., Callies, U., Carpenter, J., Dudeck, T., Eberle, S., Eckhardt, A., Gloe, D., Hänselmann, K., Hufnagl, M., Janßen, S., Lenhart, H., Möller, K. O., North, R. P., Pohlmann, T., Riethmüller, R., Schulz, S., Spreizenbarth, S., Temming, A., Walter, B., Zielinski, O., and Möllmann, C. (2017). Pelagic effects of offshore wind farm foundations in the stratified North Sea. *Progress in Oceanography* **156**, 154-173.
- Gill, C. W., and Crisp, D. J. (1985). The effect of size and temperature on the frequency of limb beat of *Temora longicornis* Müller (Crustacea: Copepoda). *Journal of experimental marine Biology and Ecology* **86**, 185-196.
- Hasselmann, K., Barnett, T., Bouws, E., Carlson, H., Cartwright, D., Enke, K., Ewing, J., Gienapp, H., Hasselmann, D., and Kruseman, P. (1973). "Measurements of wind-wave growth and swell decay during the Joint North Sea Wave Project (JONSWAP)." Deutsches Hydrographisches Institut.
- Herman, P. M. J., Asjes, J., Hummel, H., Jak, R., Kromkamp, J. C., Lindeboom, H. J., Soetaert, K., Troost, T. A., Van der Meer, J., Van der Molen, J., Van de Wolfshaar, K., Van Duren, L. A., and Van Kooten, T. (2019). "Understanding the North Sea Ecosystem," Rep. No. I1000486-000-OA-005. Deltares, Delft.
- Lengkeek, W., Didderen, K., Teunis, M., Driessen, F., Coolen, J. W. P., Bos, O. G., Vergouwen, S. A., Raaijmakers, T. C., de Vries, M. B., and Van Koningsveld, M. (2017). "Eco-friendly design of scour protection: potential enhancement of ecological functioning in offshore wind farms." Bureau Waardenburg; Wageningen Marine Research; Deltares, Culemborg.

- Neumann, H., Ehrich, S., and Kröncke, I. (2009). Variability of epifauna and temperature in the northern North Sea. *Marine Biology* **156**, 1817-1826.
- Peeters, J. C. H., Los, F. J., Jansen, R., Haas, H. A., Peperzak, L., and de Vries, I. (1995). The oxygen dynamics of the oyster ground, north sea. Impact of eutrophication and environmental conditions. *Ophelia* **42**, 257-288.
- Raoux, A., Tecchio, S., Pezy, J. P., Lassalle, G., Degraer, S., Wilhelmsson, D., Cachera, M., Ernande, B., Le Guen, C., Haraldsson, M., Grangeré, K., Le Loc'h, F., Dauvin, J. C., and Niquil, N. (2017). Benthic and fish aggregation inside an offshore wind farm: Which effects on the trophic web functioning? *Ecological Indicators* **72**, 33-46.
- Rogers, W. E., Hwang, P. A., and Wang, D. W. J. J. o. P. O. (2003). Investigation of wave growth and decay in the SWAN model: three regional-scale applications. **33**, 366-389.
- Van Leeuwen, S., Tett, P., Mills, D., and van der Molen, J. (2015). Stratified and nonstratified areas in the North Sea: Long-term variability and biological and policy implications. *J. Geophys. Res.* **120**, 4670-4686.
- Varó, I., Taylor, A. C., Navarro, J. C., and Amat, F. (1991). Effects of temperature and oxygen tension on oxygen consumption rates of nauplii of different *Artemia* strains. *Marine Ecology Progress Series* **76**, 25-31.
- Zijl, F., Groenenboom, J., and Laan, S. C. (2020). "Development of a 3D model for the NW European Shelf (3D DCSM-FM)," Rep. No. report 11205259-015-ZKS-0001 (draft). Deltares, Delft.
- Zijlema, M., Van Vledder, G. P., and Holthuijsen, L. J. C. E. (2012). Bottom friction and wind drag for wave models. **65**, 19-26.

9 Acknowledgements

We acknowledge that parts of the results of this research have been achieved using the DECI resource Cartesius based in The Netherlands at SURFsara with support from PRACE. The support of Maxime Mogé from SURFsara (The Netherlands) to the technical work is gratefully acknowledged.

A Memo regarding scenario choice

A.1 Background

Based on the discussion during the project meeting on the 24th of February 2020, as well as internal discussions and feedback from our reviewer, Peter Herman, we have come up with a design for the large upscaling scenario. The scenario is regularly referred to as a 2050 scenario, although we want to stress that this is not a realistic expectation for 2050. It is a scenario based on currently available targets of the offshore wind industry distributed over available space in such a way that we can learn as much as possible from it. Below follows a description and the underlying arguments how we got to our choice.

This document is an update of an earlier version, where we assumed an average energy production off 5 MW/km² for wind farms. This leads to a very large spatial claim. We have subsequently decided to increase this yield to 8 MW/km². In section 2.2.1. the reasoning for this is explained.

A.2 Scenario context

The aim is to design a scenario from which we can learn as much as possible of the behaviour of the system. A few other user factors have been taken into account (locations of N2000 areas and shipping routes), but only because it was possible to do this, without compromising the primary goal. ***This is a purely theoretical scenario for research purposes, not a proposal for a realistic future scenario.***

A.3 Arguments used to get to this design

A.3.1 Power generation.

We have used the national targets for 2050 obtained from “WindEurope” as a basis. These were presented during a special session regarding the future of fisheries in conjunction with offshore wind on the 22nd of January 2020.

This amounts to:

We can do it together



Source: BVG Associates for WindEurope

Figure A.1 Slide from the presentation by Giles Dickson (CEO WindEurope). Note these are the approximate targets per country, not specifically for the North Sea. This also covers areas in the Atlantic, the Baltic and the Mediterranean.

A.3.2 Distribution

Space requirements

Based on information from Remco Verzijlbergh (Whiffle) given during the meeting, we initially assumed an average yield of 5 Megawatt per km². I.e. for the Netherlands this would equate to a total area for offshore wind of 12.000 km² for a requirement of 60 GW. This yield is based on calculations by the industry assuming no restrictions on space availability; i.e. optimised for “Levelized Cost of Energy” (LCOE). This LCOE is determined by the number of turbines required to generate the target amount of power, cost for cables and other infrastructure. It is technically possible to reach yields of 8-10 MW/km², however, this means a poorer business case for the industry, as more and / or larger turbines are required to yield the same amount of energy per km². In our scenario we have opted for 8 MW/km², requiring a total of 7500 km² in the Dutch EEZ. Whether will be achievable in reality, still remains to be seen and will be the subject to further investigation by Whiffle, KNMI and TU Delft.

Minimum and maximum cluster size

Most of the currently designated wind farm areas appear to have a ballpark size of around 600 km². We do not know all the arguments why development areas were chosen as they were, but we

assume that making contiguous windfarm areas too large would diminish their energy yield (Deutsche WindGuard, 2018). It is clear that wind and hydrodynamic effects will differ in a patchy configuration, compared to large continuous areas.

If we look at the yield of a number of currently existing windfarms, it seems true that the larger the wind farm size the lower the capacity density (yield per surface area) (Table A.1).

Table A.1 Sizes and capacity densities (C.D.) of several operational and under construction windfarms

Wind farm	Production (MW)	Surface area (km ²)	C.D. (MW/km ²)
Prinses Amalia	120	14	9
Luchterduinen	129	18	7
OWEZ	108	27	4
Westernmost Rough	210	32	7
Gemini	600	70	9
London Array	630	120	5
Norfolk Boreas	1800	725	2

OWEZ is of course an older wind farm that is due to be decommissioned in the next few years, which may explain its relatively low yield. This farm has relatively small turbines sizes. The newer wind farms appear to have a larger yield, although the new Norfolk Boreas farm, covering about 725 km² will only yield 2 MW/km² (<https://group.vattenfall.com/uk/what-we-do/our-projects/vattenfallinnorfolk/norfolk-boreas>).

We have therefore chosen to opt for maximum cluster sizes in the order of magnitude of 400 km². With larger cluster sizes we assume the high yields of 8 MW/km² are physically not achievable. In order to reduce complexity and create a large number of clusters we have also opted for cluster sizes that are not much smaller than this.

North Sea and adjacent waters

Many countries have already defined search areas for wind energy. For the UK, Ireland, Denmark and Norway these search areas exceed the requirement. Wind farm clusters have been located in those search areas.

For countries such as the UK, France and Denmark with search areas in the North Sea as well as in other waters we have divided the wind farm clusters according to the ratios of designated search areas in the various waters.

For Germany we had to make a choice for areas as the currently available search areas are insufficient to achieve 36 GW. We have opted for a northern location. This was a previous search areas (Nordschillgrund) which has disappeared from the most recent maps. However, in the German EEZ there are not many alternatives.

Physically diverse environments

As within this project, a great deal of focus will be on wind farm effects on stratification and destratification, we have taken care to distribute hypothetical wind farms over the various stratification regimes, based on the well-known map (Van Leeuwen et al., 2015). We need to bear in mind though, that these regimes are based on models as well and may differ from reality. They also may differ from our model.

We have furthermore deliberately placed some wind farms on known 'frontal' areas, such as the Frisian front system.

International shipping lanes

We have taken into account the location of the international shipping lanes and the traffic separation system (TTS) as defined by the International Maritime Organisation (IMO). These routes are based on international agreements and are unlikely to change drastically in the next few decades. However potential new shipping lanes catering for routes via the Arctic area have not been taken into account.

The existing shipping lanes are predominantly located south of the Gemini wind farms. As future farms are likely to be planned in the northern section of the Dutch EEZ, the impact on the layout of the scaled-up scenario is limited.

A.3.3 Specific for the Dutch wind farms

N2000 areas

Based on policies and the current draft of the North Sea agreement, we have decided to avoid The N2000 areas as well as the two additional areas "Centrale Oestergronden" and "Bruine Bank". These are likely to get some level of protected status and are unlikely to be re-designated for windfarms. Excluding these areas does not compromise our options for choosing hydrodynamically diverse areas. By not using these areas we hope to avoid misinterpretations of these maps, when the results of our study are made public.

IJmuiden Ver

In keeping with not building on the Brown Bank area, we have shifted the current lay-out of "IJmuiden Ver" Northward to fall outside the Brown Bank area. Verbal comments from EZK and LNV indicated that this was likely. The shape of this area may change in future, with this shift, but as we have no clear idea how, we have left as was. Also, the delineation of the future Brown Ridge area may differ from Figure A.4. It is possible that the locations we used in the upscaling scenario overlap with the future delineation of the Brown Ridge and will therefore be not realistic.

A.4 Within farm lay-out

We also need to make a choice regarding the size and distance between turbines within a farm. Our current estimate is that this will have some effect, particularly on the water movement, but the effect is less than the effect of the positioning of the farms.

From the offshore wind industry (pers. comm. Giles Dickson) we know that future turbines will not be less than 8 MW. However, we have currently no idea how far the growth of turbine size will increase in the coming decades. Other information picked up from collaborating with the industry, is that they want to curb the strong growth in turbine size, in order to concentrate on optimising their installation vessels and equipment. We therefore intend to keep the turbine size (and the related distance between the turbines) at 12 MW for all future farms. The farms already under construction or in an advanced planning phase we use the planned lay-out. Our current in-farm lay-out for present, planned and future farms is shown in Table A.2.

Table A.2: Proposed lay-out for operational, planned and future wind farms.

	Stem density (piles/km ²)	Stem diameter (m)
Operational	3.15	5
Under construction	0.85	8
Future	0.67	12

A.5 Scenario choice

Figure 2.1: Current proposed layout for the large upscaling scenario. Figure 2.1 shows the currently proposed lay-out, based on the arguments set out above. The focus of this project is on the Dutch EEZ, but we have included a number of farms in the Baltic, the Northern North Sea, around Ireland and the Atlantic. We have the targets for these countries available and we currently do not know how far effects of the installation of offshore wind farms extends.

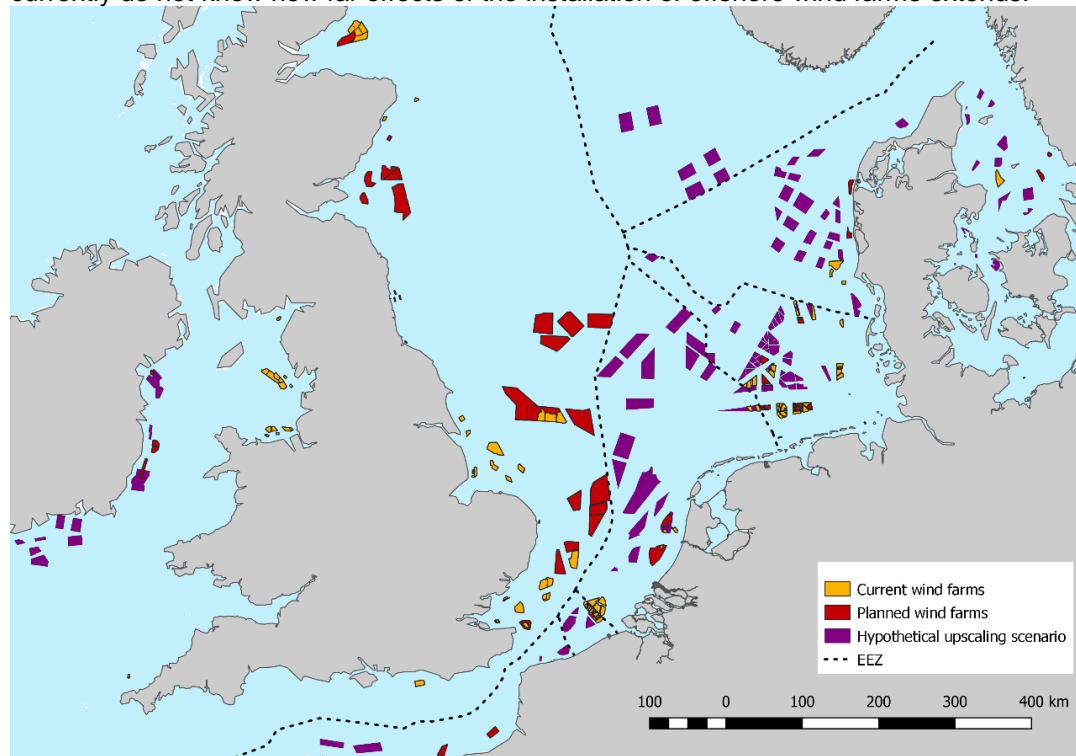


Figure A.2 Current proposed layout for the large upscaling scenario.

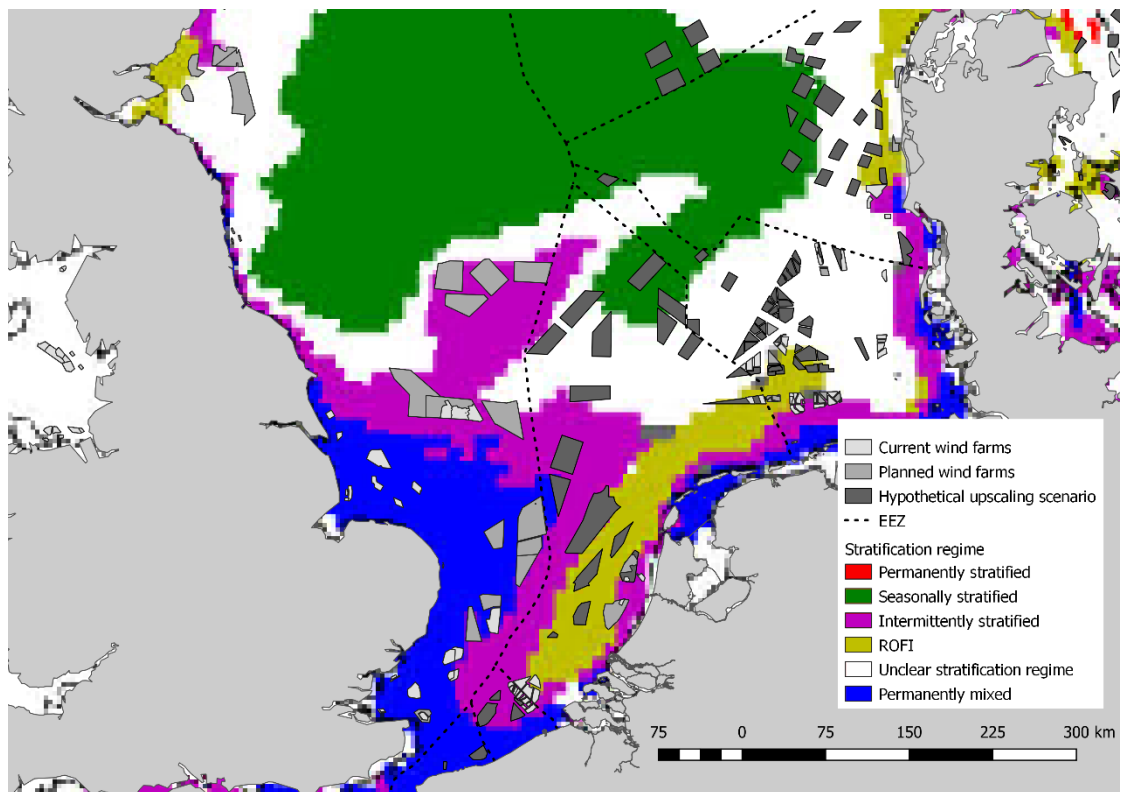


Figure A.3 Future scenario superimposed on the stratification regimes identified in (Van Leeuwen et al., 2015).

Figure A.3 shows the distribution of the farms in the proposed scenario superimposed on the stratification regimes. According to the model by Van Leeuwen et al. (2015), the Dutch EEZ has relatively little surface area that is permanently mixed. However, some of the planned farms in the UK zone are in such areas.

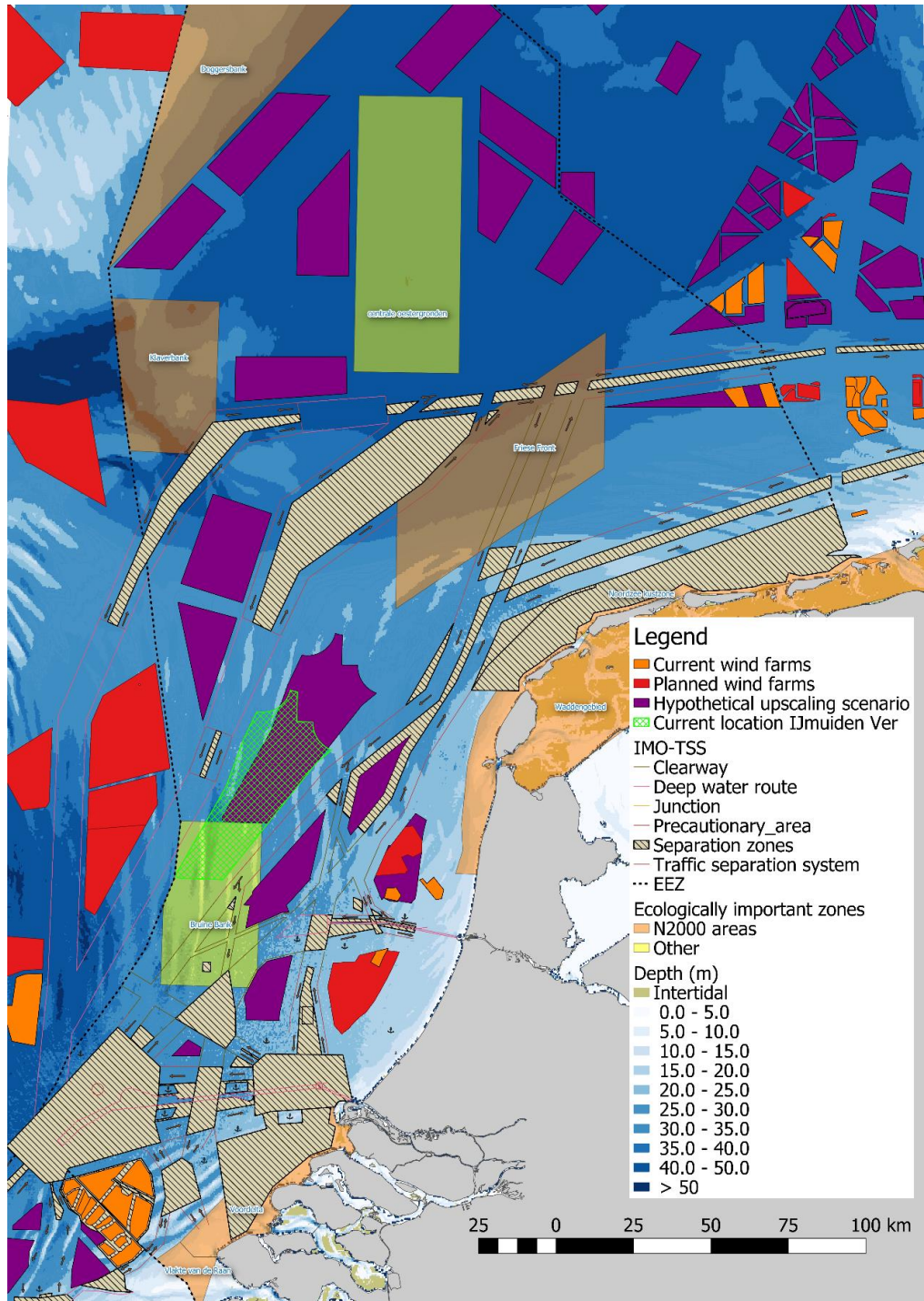


Figure A.4 Detail of the Dutch EEZ of the proposed scenario, including the current official location of IJmuiden Ver (green hatched area) as well as the important ecological zones that at present will not be developed for offshore wind and the IMO shipping lanes. Note: at the time of constructing this scenario the future delineation of IJmuiden-Ver and the Brown Ridge were unknown. The current delineations differ from this map.

Figure A.4 shows the same scenario, now zoomed in on the Dutch EEZ. This figure shows the depth. In the proposed scenario we have a wind farm adjacent to the “Frisian Front” N2000 area, which straddles part of the actual front area (delineated by the depth contours).

A.5.1 Factors not taken into account

There are many other functions that will influence the future choices of farm locations. We have in our current lay-out ignored the demands of

- Military zones
- Sand mining areas
- Important fishing grounds that in future may be kept free from wind farm development
- Important fly-ways for migrating birds
- Important areas for seals

We are aware that these issues may all play a role in future scenarios. It is therefore imperative that these scenario maps are not taken as realistic scenarios.

The other issue that has not been taken into account but should be addressed in future is the presence of land-based wind farms. On the large North Sea scale, wind extraction on land will ultimately affect processes at sea and vice versa.

A.6 References

Deutsche WindGuard, GmbH. 2018. "Capacity density of European offshore windfarms " In.: INTERREG project Baltic Lines.

Van Leeuwen, S., P. Tett, D. Mills, and J. van der Molen. 2015. 'Stratified and nonstratified areas in the North Sea: Long-term variability and biological and policy implications', J. Geophys. Res., 120: 4670-86.

B Fine sediment model (appendix)

B.1 Sedimentation and erosion parameters

Table B.3 Sedimentation and erosion model parameters.

Characteristics	IM1	IM2	IM3
Settling velocity [mm s ⁻¹]	0.125	1	0.001
Deposition efficiency [-]	0.2	0.2	0.1
Percentage of sedimentation flux towards S2 [-]	0.05		
Critical shear stress for erosion from S1 [Pa]	0.2		
0 th order resuspension flux S1 [g m ⁻² d ⁻¹]	8.640*10 ³		
1 st order resuspension velocity S1 [d ⁻¹]	0.3	0.1	0.1
Critical shear stress for erosion from S2 [Pa]	1.5		
Factor resuspension pick-up [-]	3.0*10 ⁻⁸		
Maximum resuspension pick-up [g/m ² /d]	3.6*10 ³		
Porosity [-]	0.4		
Layer thickness S2 [m]	0.1		

B.2 Location of CEFAS smart buoys



Figure B.5 Location of CEFAS smart buoys.

B.3 Location of transects



Figure B.6 Location of transects used for calculating sediment fluxes

B.4 Spatial distribution SPM

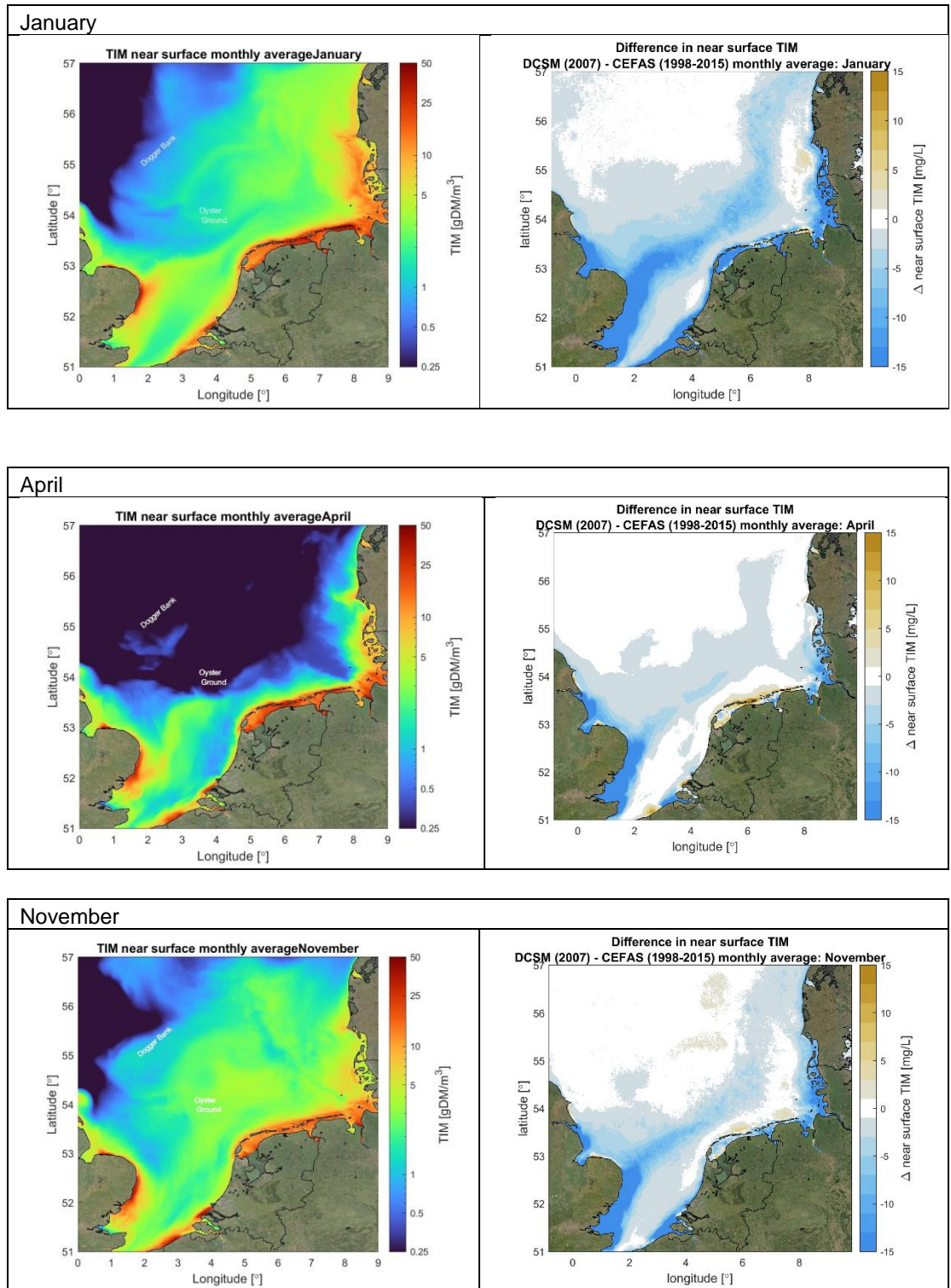


Figure B.7 Left: spatial distribution of SPM in different months. Right: deviation of surface concentrations with CEFAS remote sensing data.

B.5 References

- Bockelmann, F. D., Puls, W., Kleeberg, U., Müller, D., & Emeis, K. C. (2018). Mapping mud content and median grain-size of North Sea sediments—A geostatistical approach. *Marine geology*, 397, 60-71.
- Boon, A.R., S. Caires, I.L. Wijnant, R. Verzijlbergh, F. Zijl, J.J. Schouten, S. Muis, T. van Kessel, L. van Duren, T. van Kooten (2018). Assessment of system effects of large-scale implementation of offshore wind in the southern North Sea. Report 11202792-002-ZKS-0006 of Deltares in collaboration with KNMI, WUR and Whiffle. Delft, The Netherlands.
- Silva (2016). Monthly average non-algal Suspended Particulate Matter concentrations. Cefas, UK. V1. doi: <https://doi.org/10.14466/CefasDataHub.31>
- Swart, 1974. Offshore sediment transport and equilibrium beach profiles. Ph.D. thesis, Delft University of Technology, Delft, The Netherlands. Delft

Deltares is an independent institute for applied research in the field of water and subsurface. Throughout the world, we work on smart solutions for people, environment and society.

Deltares

www.deltares.nl